UNIVERSITY OF CALIFORNIA, SAN DIEGO

The Role of MicroRNAs in Flow Regulation of Endothelial Functions

A dissertation submitted in partial satisfaction of

the requirements for the Doctor of Philosophy

in

Bioengineering

by

Kuei-Chun Wang

Committee in Charge:

Professor Shu Chien, Chair
Professor Steve Briggs
Professor Shankar Subramaniam
Professor Gene Yeo
Professor Kun Zhang

2012

The Dissertation of Kuei-Chun Wang is approved, and it is acceptable in quality and form for publication on microfilm and electronically:

_____

_____

_____

_____

_____

Chair

University of California, San Diego

2012

DEDICATION

This dissertation is dedicated to my parents, Fu-Jung Wang (王富榮) and Ken-Ming Li (李根明), for their love, guidance, and support throughout my life.

TABLE OF CONTENTS

LIST OF FIGURES

LIST OF TABLES

ACKNOWLEDGEMENTS

I would like to give my deepest gratitude to my advisor, Dr. Shu Chien. His constant support, encouragement, and guidance not only inspire me completing this dissertation but also help me through the difficulties within the past few years. The completion of this thesis would not have been possible without the thoughtful and detailed comments from my thesis committee members, Dr. Shankar Subramaniam, Dr. Kun Zhang, Dr. Gene Yeo, and Dr. Steve Briggs. I also would like to extend thanks to our collaborators, Dr. John Shyy for his constructive input, Dr. Lana Garmire for the data analysis, and Dr. Clark Wu for the Doppler study.

Special thanks go to Dr. Julie Li for her mentorship, patience and inspiration to help me complete my dissertation. The current and past members in Chien lab also deserve my sincere thanks. I would like to acknowledge Drs. Leona Flores, Daniel Fero, Joann Chang, Angela Young, Ian Lian, Jing Zhou, Sung Sik Hur, Jason Haga, and Vernon Shih for their stimulating discussions, Jerry Norwich, Phu Nguyen, and Suli Yuan for the technical assistance, Drs. Anna Weiss and Dayu Teng for helping me with animal experiments, and my fellow graduate students Yi-Ting Yeh, Carol Kuo, Ruyue Xue, Min-Shu Chan, and Kadir Tung for their assistance and friendship.

Most importantly, I would like to thank my parents, Fu-Jung Wang and Ken-Ming Li, and my girl friend Wen-Ching Chuang for their support, encouragement, and unwavering love throughout my life. Without them, any accomplishment I have achieved would not have been possible.

Chapter II, in part, has been submitted for publication of the material as it appears in *Proc Natl Acad Sci U S A*, Wang, K.C., Garmire, L., Young, A., Nguyen, P., Trinh, A., Subramaniam, S., Wang, N., Shyy, J., Li, Y.S., Chien, S, 2010. The

dissertation author Kuei-Chun Wang was the primary investigator and author of the paper.

VITA

Education

2001	B.S. in Chemical Engineering
	Minor in Life Science
	National Tsing Hua University, Taiwan
2004	M.S. in Cellular and Molecular Biology
	National Tsing Hua University, Taiwan
2012	Ph.D. in Bioengineering
	University of California, San Diego

List of Publications

1. **Wang, K.-C.**, Li, Y.-S., Subramaniam, S., Chien, S. 2012. MicroRNA-23b mediates anti-proliferative effect of pulsatile flow on endothelial cells by targeting cyclin H. *Manuscript in preparation*.
2. Hur, S.S., Del Álamo, J.C., Park, J.S., Li, Y.-S., Nguyen, H.A., Teng, D., **Wang, K.-C.**, Flores, L., Alonso-Latorre, B., Lasheras, J.C., Chien, S. 2012. Roles of cell confluency and fluid shear in 3-dimensional intracellular forces in endothelial cells. *Proc Natl Acad Sci U S A*. 109(28):11110-5.
3. Fero, D., **Wang, K.-C.**, Nguyen, P., Hur S.S., Hu, Y., Li, Y.-S. Ephrin-A1 regulates cell remodeling and migration. 2011. *Cellular and Molecular Bioengineering*. 4(4): 648-655.
4. Wu, W., Xiao, H., Laguna-Fernandez, A., Villarreal Jr., G., **Wang, K.-C.**, Geary, G., Zhang, Y., Wang, W.-C., Huang, H.-D., Zhou, J., Li, Y.-S., Chien, S., Garcia-Cardena, G., Shyy, J. 2011. Flow-Dependent Regulation of Krüppel-Like Factor 2 Is Mediated by MicroRNA-92a. *Circulation.124(5): 633-641.*
5. Zhou, J., **Wang, K.-C.**, Wu, W., Subramaniam, S., Shyy, J., Chiu, J.-J., Li, Y.-S., Chien, S. 2011. MicroRNA-21 targets peroxisome proliferators-activated receptor-α in an autoregulatory loop to modulate flow-induced endothelial inflammation. *Proc Natl Acad Sci U S A*. 108(25):10355-60.
6. **Wang, K.-C.**, Garmire, L., Young, A., Nguyen, P., Trinh, A., Subramaniam, S., Wang, N., Shyy, J.YJ, Li,Y.-S., Chien, S. 2010. Role of MicroRNA-23b in Flow-Regulation of Rb Phosphorylation and Endothelial Cell Growth. *Proc Natl Acad Sci U S A*. 107(7):3234-9.
7. Chiang, Y.-W., Wu, J.-C., **Wang, K.-C.**, Lai, C.-W., Chung, Y.-C., Hu, Y.-C. 2006. Efficient expression of histidine-tagged large hepatitis delta antigen in baculovirus-transduced baby hamster kidney cells. *World J Gastroenterol*. 12(10):1551-1557.
8. Ho, Y.-C., Huang, S.-M., Chung, Y.-C., **Wang, K.-C.**, Hu, Y.-C.2005. Transgene expression and differentiation of baculovirus-transduced human mesenchymal stem cells. *J. Gene. Med*. 7:860-8.

9. Chen, Y.-H., Wu, J.-C., **Wang, K.-C.**, Chiang, Y.-W., Lai, C.-W., Chung, Y.-C., Hu, Y.-C.2005. Baculovirus-mediated production of HDV-like particles in mammalian cells using a novel oscillating bioreactor. *J. Biotechnol*. 118 (2): 135-47.
10. **Wang, K.-C.**, Wu, J.-C., Chung, Y.-C., Ho, Y.-C., Chang, M. D.-T., Hu, Y.-C.2004. Baculovirus as a highly efficient gene delivery vector for the expression of hepatitis delta virus antigens in mammalian cells. *Biotechnol. Bioeng*. 89: 464-473.
11. Hsu, C.-S., Ho, Y.-C., **Wang, K.-C.**, Hu, Y.-C.2004. Investigation of optimal transduction conditions for baculovirus-mediated gene transfer into mammalian cells. *Biotechnol. Bioeng*. 88: 42-51.
12. Ho, Y.-C., Chen, H.-C., **Wang, K.-C.**, Hu, Y.-C.2004. Highly efficient baculovirus-mediated gene transfer into chondrocytes. *Biotechnol. Bioeng*. 88: 643-651.

Honors

1. 2005-2008 **Taiwan Merit Scholarship**, National Science Council, Taiwan.
2. 2010-2011 **Western States Affiliate Pre-doctoral Fellowship**, American Heart Association.

ABSTRACT OF THE DISSERTATION

The Role of McroiRNAs in Flow Regulation of Endothelial Functions

by

Kuei-Chun Wang

Doctor of Philosophy in Bioengineering

University of California, San Diego, 2012

Professor Shu Chien, Chair

The disparate effects of different flow patterns play important roles in regulating the functions of vascular endothelial cells (ECs). The focal nature of atherosclerotic plaque formation reveals that the pulsatile flow (PS) along the straight part of arterial tree exerts athero-protective effects on the ECs, while the disturbed flow characterized as the oscillatory flow (OS) found at the arterial bifurcation induces pro-atherogenic responses. MicroRNAs (miRNAs) can regulate many vascular functions, but their roles in regulating endothelial responses to different types of fluid shear stresses remain unexplored. Using a genome-wide microarray approach, I profiled miRNA and mRNA expression levels in human ECs under 24-h PS and OS flows, as well as static control. Bioinformatics analyses of mRNA profiles indicate that PS flow predominantly regulates EC growth arrest genes, while OS flow primarily modulates EC inflammatory genes. Functional and miRNA studies show that PS flow suppresses EC proliferation through the effects of

miR-23b on cell cycle machinery, and that OS causes sustained expression of miR-21 to contribute to pro-inflammatory responses. Further mechanistic studies indicate that the PS flow-induced miR-23b modulates the integrity and activity of CDK-activating kinase (CAK) by directly targeting the cyclin H (CCNH) expression post-transcriptionally, which in turn suppresses the transcriptions and activities of CDK2, CDK4, as well as RNA polymerase II (Pol II). The reductions in basal transcriptions and cell cycle regulatory proteins result in the hypo-phosphorylation state of retinoblastoma (Rb) gene and protein, and hence EC growth arrest. These results reveal that the miR-23b/CAK/Pol II pathway is differentially regulated by PS and OS flows to result in their opposite effects on EC proliferation. Such a flow pattern-dependent correlation is validated in studies in vivo on rat carotid artery stenosis and ligation: the flow disturbance/reduction induced in the carotid artery *in vivo* led to a lower expression of miR-23b and a higher EC proliferation, in agreement with the studies on cultured ECs *in vitro*. These findings provide the functional understanding of the role of miRNAs in vascular biology, and also provide directions for the development of novel approaches for the diagnosis, treatment, and prevention of atherosclerotic diseases.

CHAPTER 1 INTRODUCTION

1.1 Basics in vascular physiology

The cardiovascular system is composed of the heart and blood vessels. The cardiac cycles generate the arterial blood pressure, which drives the blood flow through the blood vessels in the circulation. The blood flow not only serves as a transport system carrying oxygen and nutrients to the cells and removing waste products from the cells, but also provides the a wide range of functional communications between tissues and organs. Aside from the biochemical capability of blood flow, the physical factors (e.g., pressure gradient and resistance) in the cardiovascular system, that govern blood flow is referred to as “hemodynamics”. The hemodynamic conditions inside blood vessels lead to the development of stresses acting on the vessel walls, including the circumferential and tangential stress [1, 2]. As illustrated in figure 1.1, pulse pressure changes during the cardiac cycle cause the periodic stretch of arterial wall, resulting in cyclic circumferential stress on the vessel wall. The circumferential stress in vessel wall is non-uniform, with a high value at the inner layer and a low value at the outer layer. The blood flow passing along the vessel produces the tangential shear stress on the luminal surface of endothelium. The magnitude of the shear stress in the vascular tree is dependent on the characteristics of blood vessels. The shear stress has been reported to range from 10 to 70 dyn/cm^2 in arteries, whereas the corresponding values for veins are considerably lower, from 1 to 6 dyn/cm^2 [3, 4]. The stretch and shear stress are functions of the material properties of vessel wall, and can alter in vascular diseases such as hypertension, to lead to vascular remodeling to adapt to the new conditions [2].

The blood vessels are the conduits carrying blood from heart to tissues and from tissues to heart. Blood vessels vary not only with respect to size but also their anatomical structure, and these variations have profound effects on their functions in the

surrounding tissues. The arteries are mainly composed of three layers: the intima, the media, and the adventitia. The intima lining the lumen of the blood vessel is a single layer of endothelial cells (ECs) and elastic membrane, forming the interface between the circulating blood and the rest of vessel wall. The media layer surrounding the intima is composed of smooth muscle cells (SMCs) and elastic fibers composed of mainly collagen and elastin, and provide the high elasticity of vessel wall. The SMCs in resistance vessels contract and dilate to control blood flow and regulate blood pressure. The thickness of the media layer is the significant feature of artery. The adventitia is the outermost layer made of connective tissue, elastin, and collagen and forms a tough and protective covering. The function of the vessel wall depending on the interaction between layers in response to alterations of hemodynamic environments.

1.2 Atherosclerosis and vascular mechanics

Cardiovascular disease (CVD) is not only a major health problem worldwide but also results in severe economic burden to the society. World Health Organization (WHO) estimates that CVD will be responsible for 20 million deaths worldwide in 2015, accounting for at least one CVD-related complications in every three deaths. This burden is currently dominant and expected to aggravate in the near future, as other risk factors, such as diabetes and obesity, are reaching epidemic levels. Despite the immense efforts made over the past few decades toward the surgical interventions and management of advanced CVD, prevention of the disease is clearly a better option than cure. To enlighten the future therapeutics and prevention strategies of CVD, understanding the pathophysiology at cellular and molecular levels is of critical importance and offers new opportunities.

Cardiovascular diseases are diverse, but many of which, such as myocardial infarction, acute coronary syndrome, and stroke, are associated with “atherosclerosis”,

which is a hardening and narrowing process in medium- and large-sized arteries. While atherosclerosis is usually accompanied by other risk factors such as hypercholesterolemia, smoking, hypertension, etc., the main cause and progression of the disease are not yet fully understood. In brief, atherosclerosis is characterized as a chronic inflammatory disorder that usually results from the gradual plaque buildup within the arteries [5]. In the presence of single or multiple risk factors, atherosclerotic plaque formation initiated from endothelial damage and activation, which allow the accumulation of circulating lipids in the intima layer and the adhesion of macrophages to the vessel wall. The accumulated lipid, particularly low-density lipoprotein (LDL), is oxidized by oxygen free radical and becomes toxic to surrounding cells. The recruited macrophages uptake oxidized LDL to form foam cells and stimulate smooth muscle cells (SMCs) to de-differentiate into synthetic phenotype. Necrotic foam cells form the lipid core of the plaque, aggravate the inflamed state, and culminate the plaque deposits. SMCs proliferation and migration, with extracellular matrix secretion, lead to further progress of soft plaques and eventually lead to wall thickening and luminal narrowing, making it difficult for blood to flow through. Over time, the plaques become vulnerable and unstable, and the rupture of the plaque allows blood contact and results in the formation of intraluminal thrombus. Rapid formation and expansion of thrombus can lead to abrupt luminal occlusion, causing acute coronary syndrome, myocardial infarction, as well as stroke, leads to CVD fatalities.

Hemodynamic forces due to the blood flow and pulsatile pressure constantly act on the compliant vessel wall in the form of fluid shear stress and cyclic circumferential stretch. Hemodynamic forces are important features for maintaining vascular homeostasis under physiological conditions, while alterations of the forces are associated with the development and progression of atherosclerotic lesions. Many of the

biochemical risk factors for atherosclerosis are systemically imposed to the vessel wall, but the lesions are preferentially found at arterial branches and curvatures, where the blood flow patterned is not streamlined are referred to as disturbed flow. The characteristics of disturbed flow include low shear, flow separation and reattachment, reciprocating flow, as well as turbulence in some regions. On the other hand, the straight part of arterial tree, such as abdominal aorta and common carotid arteries, where the blood imposes forwarding pulsatile laminar flow with a high shear stress, is usually spared of atherosclerotic lesion [6]. As illustrated in figure 1.2, these local rheological factors have been correlated to the physiological and patho-physiological responses of the endothelium that lines the vessel, leading to a widely accepted hypothesis that unidirectional laminar pulsatile flow with high shear stress is athero-protecive, while the disturbed flow is atherogenic [3, 7-9] The luminal narrowing or “stenosis” caused by the atherosclerotic lesion plaques induces an accelerated flow in the stenotic throat, followed by disturbed flow at the post-stenotic dilatation region, and hence may further aggravate the development of atherosclerotic lesion.

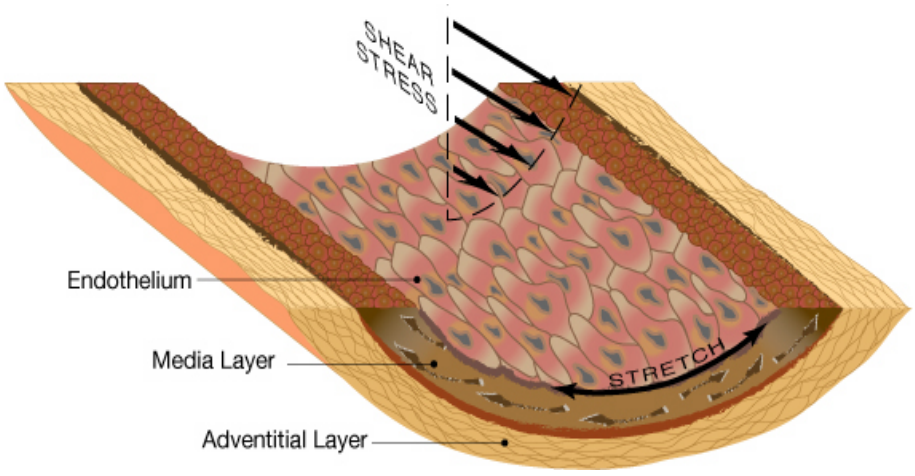

Figure 1.1 Schematic diagram of forces acting on arterial wall. The blood pressure and flow result in cyclic circumferential stretch and fluid shear stress on the elastic vessel wall. (Adapted from J. Chiu and S. Chien, 2011)

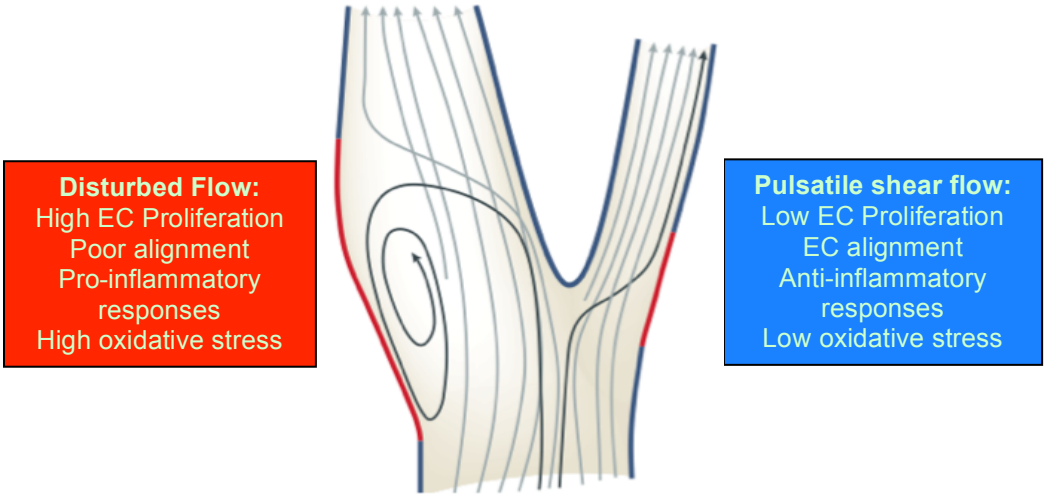

Figure 1.2 Vascular bifurcation, flow patterns, and EC phenotypes. The pulsatile laminar shear flow in the straight part of arterial tree decreases EC turnover, suppresses the expression of inflammatory genes, and maintains low oxidative stress, and hence is athero-protective. Conversely, the disturbed flow at branch points and curvatures is associated with high EC turnover, upregulation of inflammatory molecules, and high oxidative stress, and hence is athero-genic. (Adapted from Cornelia Hahn and Martin A. Schwartz, 2009)

1.3 Endothelial cells responses to shear stress

Vascular endothelial cells (ECs), forming the interface between circulating blood and vessel wall, are exposed to mechanical stimuli of fluid shear stress and cyclic circumferential stretch. Shear stress acting primarily on the EC to modulate its homeostasis [2, 10, 11]. Vascular smooth muscle cells (SMCs) are primarily subjected to cyclic stretch of the vessel wall [11, 12]. *In vitro* co-culture studies have revealed that shear stress can modulate the communications between SMCs and ECs. Thus, shear stress not only regulates ECs but also has significant effects on the underlying SMC layers. Thus, EC-SMC co-culture has been often used as *in vitro* models to study mechano-transduction in various physiological and pathophysiological processes [13, 14].

Vascular ECs not only function as a selective barrier between the circulating blood and vessel wall, but also play crucial roles in regulating vascular homeostasis [2].

ECs modulate vascular tone through SMCs by releasing vasoconstrictor and vasodilators, such as endothelins and nitrite oxide (NO), respectively [15]. The EC monolayer also presents an anti-thrombotic surface by expressing the membrane protein thrombomodulin (TM), which inactivates the pro-coagulant thrombin and activates the anti-coagulant protein C [16, 17]. The production of cytokines and growth factors such as platelet-derived growth factor (PDGF) from ECs mediates the vascular remodeling under normal and pathological conditions [18-20]. In addition, ECs induce white blood cell adhesion by presenting chemotactic and adhesion molecules on their membrane in response to local inflammatory stimuli [21]. Accumulating evidence suggests that endothelial damage or dysfunction might be the starting point of vascular diseases [22]. Many of the EC functions and dysfunction have been shown to associate with different types of shear stress. Studies of the underlying molecular mechanisms may help us further understand the pathogenesis of vascular diseases.

In the past few decades, a number of *in vitro* models have been developed to reproduce important features of the flow environment in blood vessel and to study the effects of fluid shear stress on EC functions. The two major shear systems widely used to mimic flow conditions are the parallel-plate flow chambers and cone-plate viscometers [3, 23]. In the parallel-plate chamber system, the fluid flow is driven by the pressure difference (ΔP) across the rectangular chambers, and the shear force generated is uniform across the chamber; changes of ΔP governor the magnitude of shear stress. In the cone-plate viscometer, a cone submerged in medium over cultured EC monolayer is rotated at controlled velocities to generate different magnitudes of shear stress, even to the turbulent flow level. In the present study, the parallel-plate chamber (figure 1.3) was used to generate pulsatile shear stress (PS) to mimic the flow pattern in the straight parts of arteries at a mean magnitude of 12 dyn/cm^2 and a sinusoidal pulsatility of ±4

dyn/cm^2 at 1 Hz; the flow is laminar for the Newtonian perfusing fluid. In addition, oscillatory shear stress (OS), which is the important feature of disturbed flow, was generated using this system at 0.5±4 dyn/cm^2. The mean flow rates (Q) were calculated based on the Hagen-Poiseulle equation:

$$Q = \frac{\tau b h^2}{6\mu}$$

Where t is the shear stress; μ is the fluid viscosity; *b* and *h* are the width and height of the chamber, respectively. The applications of these flow patterns allow the study of EC signaling, gene expression, phenotype, and function in response to pulsatile and oscillatory flows, which are the main features of the flow patterns at the athero-protective and athero-prone regions of arteries, respectively.

Fluid shear modulates EC functions through the activation of mechano-sensors and signaling pathways, alteration of cytoskeleton organization, and changes in gene and protein expressions. The mechano-sensing in ECs can be mediated by a variety of membrane-bound “sensors”, including integrins [24], G proteins and G-protein-coupled receptors (GPCRs) [25, 26], receptor tyrosine kinases (RTKs) [27], ion channels (such as Ca^{++} and K^{+} channels) [28], junctional proteins (such as PECAM1) [29], primary cilia [30], and specialized lipid rafts (such as caveolae) [31], which are coupled to the signaling networks. Numerous studies have shown that shear stress activates these mechano-sensors through protein-protein interactions, phosphorylation, and changes in membrane fluidity, and that these events transmit extracellular mechanical stimuli through intracellular and biochemical signaling cascades to the nucleus, resulting in alterations of gene expression and consequent structural and functional adaptations in ECs. Mechano-senstive pathways in ECs are diverse, including the mitogen-activated protein kinase (MAPK) family (such as ERK1/2, p38, and JNK), PI3K/AKT/mTOR

pathway, and others (such as FAK, Rho, PKC, and Src) [10]. Through these signaling molecules, flows with distinctive shear stress patterns can differentially modulate EC gene expressions and functions such as vasomotor tone, proliferation, survival, and remodeling. Blockade of these mechano-sensing and transduction pathways impairs the flow regulation of EC functions. Although there have been considerable progresses in the understanding of mechano-sensing and intracellular signaling, the interplays between sensors and pathways and their exact contributions remain uncertain.

The flow regulations of EC functions have been evaluated at molecular and cellular levels, both *in vitro* and *in vivo*. *In vitro* studies have demonstrated that the exposure of ECs to steady or pulsatile laminar high shear stress, mimicking the athero-protective flow, leads to the quiescent and anti-inflammatory phenotypes, including low EC turnover, low permeability, cell alignment to the flow direction, and up-regulation of anti-inflammatory genes [32-34]. Conversely, ECs subjected to long-term disturbed flow, mimicking the athero-prone oscillatory low shear, exibit proliferative and pro-inflammatory phenotypes, including high permeability, expressions of pro-inflammatory genes, and consequently a more active surface for monocytes to adhere [3]. Due to the advancement of high-throughput technology in the last decade, the potential mechanisms responsible for flow regulation of EC phenotypes have been further elucidated using cDNA microarray and proteomics approaches [35-38]. Despite the differences in platforms and cell sources, *in vitro* studies have identified cohorts of mechano-sensitive genes/proteins contributing to the EC athero-protective and athero-prone phenotypes. The use of *in vivo* animal model to analyze gene expression as a function of flow pattern has only partially confirmed the shear-modulations of these genes/proteins [39, 40]. The discrepancy of some of the *in vitro* and *in vivo* results are possibly attributed to the disease progression, complicated cell-environment and cell-cell

interactions, different section of arteries, and the presence of other risk factors in the in vivo studies, and the artificial experimental setting of the *in vitro* experiments.

Others and we have previously demonstrated that steady laminar and pulsatile shear stresses induced by flows with a definite direction inhibits EC proliferation [33, 34]. The molecular mechanism by which steady laminar shear stress causes EC growth arrest has been attributed to the sustained p53 and $p21^{cip}$ expressions and Rb hypo-phosphorylation. The Rb hypo-phosphorylation, probably resulted from the down-regulation of several cyclin-dependent kinases (CDKs), leads to the inhibition of EC proliferation. On the other hand, the disturbed flow patterns enhances EC turnover [32, 41]. Recent studies suggest that OS-induced EC proliferation is regulated through histone deacetylases (HDACs) [42] and the activation of SMAD1/5 [43].

In addition to the mechanisms outlined above for flow regulation of EC proliferation through protein signaling and expression, microRNAs (miRNAs) have recently been shown as key regulators modulating cellular functions in a variety of contexts. It is vital to examine the role of miRNAs in regulating EC phenotypes/functions under different flow patterns.

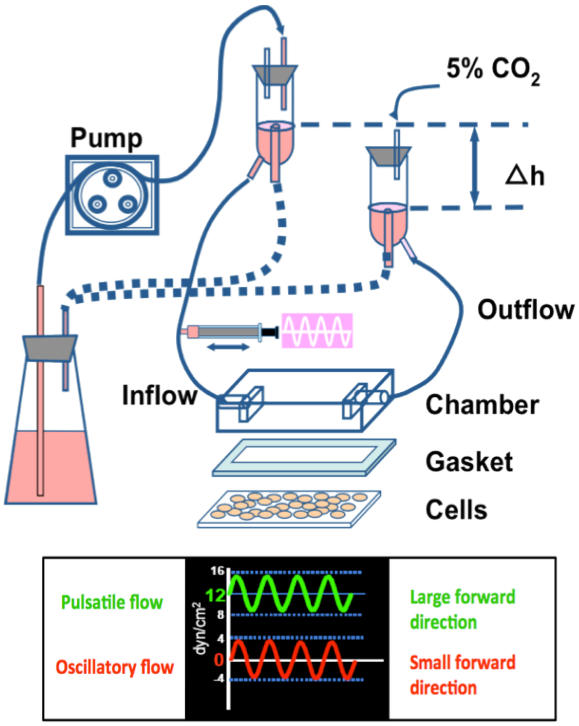

Figure 1.3 Scheme of the parallel-plate flow chamber system. Lower panel: the magnitudes and patterns of PS and OS flow used in this study.

1.4 MicroRNAs

MicroRNAs (miRNAs) are small noncoding RNAs (about 21-25 nucleotides) that regulate gene expression by binding to a target mRNA, thereby causing either its degradation or translational repression [44, 45]. It is estimated that miRNAs regulate at least 30% of the human genes through such post-transcriptional processes in various biological processes in health and disease, including cell proliferation and differentiation. MiRNAs either are encoded as independent genes that contain their own promoters and regulatory sequences, or exist in introns and even exons of host genes. As illustrated in figure 1.4, transcription of miRNAs is primarily carried out by RNA polymerase II, and the transcript from either intergenic or intronic miRNA is called pri-miRNA, which ranges from hundreds to thousands of nucleotides. In the nucleus, pri-miRNAs are processed into a short stem-loop pre-miRNAs by a complex consisting of RNase III enzyme Drosha

and DGCR8. Pre-miRNAs are then exported from the nucleus to the cytoplasm by the shuttle protein Exportin-5. In the cytoplasm, the hairpin loops are further cleaved by another RNase III enzyme, Dicer, to yield the 22-nt miRNA duplex. After unwinding by an unidentified helicase, one of the duplex is the mature miRNA that acts as the functional guide strand. The complementary strand, termed as the passenger strand or miRNA*, is rapidly degraded. The mature miRNAs usually target the complementary sequences of the 3'UTR of mRNAs with the help of a class of RNA binding proteins called Argonaute (Ago) and are packed into a miRNA-induced-silencing complex (miRISC). The gene expression is silenced by either degradation of the miRNA-mRNA complex or inhibition of translation. Although several hypotheses have been reported, the detail mechanisms that miRNAs repress gene expression remain uncertain.

A growing number of evidence suggests that miRNAs play critical roles in regulating vascular homeostasis and development [46-49]. Global reduction of miRNAs in ECs by dicer knockdown alters gene expressions, such as Tie-1, Tie-2, eNOS, VEGFR2 etc., that affect various endothelial functions, including the reduction of EC proliferation and angiogenesis *in vitro* [46, 48]. When both Dicer and Dorsha are knocked down in ECs, capillary sprouting and tube-forming activity are significantly reduced . *In vivo* studies have demonstrated that deletion of endothelial dicer resulted in the early embryonic lethality during mouse and zebrafish development [50, 51], suggesting that embryonic angiogenesis is highly dependent of miRNAs. Deletion of dicer in vascular SMCs also causes the embryonic lethality due to the loss of both contractile and synthetic phenotypic proteins [52]. MiRNA profiling studies suggest that miRNAs, particularly the ones that are abundant in vascular cells, are the key modulators of vascular functions. For example, miR-126, which is regarded as an EC-specific miRNA, has been shown to modulate basic endothelial functions, maintain

vascular integrity, and promote vessel development by repressing VCAM1 and SPRED1 and activating VEGF signaling, both *in vitro* and *in vivo* [53]. The MiR-17-92 cluster has been implicated in regulating angiogenesis, proliferation and apoptosis [54]. MiR-221/222 has been found to inhibit EC survival, migration, and capillary tube formation, and regulate endothelial nitric oxide synthase (eNOS) in dicer-knockdown cells [48]. MiR-23/27/24 clusters are also abundant in ECs and are associated with vascular development, endothelial-mesenchymal transition, and angiogenic capacities [55]. Several recent studies have also reported that miR-143/145 levels are crucial for the switching of SMCs from contractile to synthetic phenotype, as well as the neo-intima formation in the development of atherosclerotic lesion [56]. These studies provide significant evidence, both *in vitro* and *in vivo*, supporting the pivotal role of miRNAs in regulating vascular functions, although the information is diverse and sometimes controversial. Of note, those reports may reflect complexity that one miRNA can modulate multiple targets in distinct pathways. The paucity of information of the systemic and cohesive regulation of mechanisms in the context of vascular functions indicates the need for further investigations. Understanding the underlying mechanisms may contribute to the prevention of vascular diseases and the usage of miRNAs as therapeutic targets.

The functional consequence of fluid shear stress on ECs is mediated by the “mechano-sensitive” genes, such as KLF2 and eNOS, that regulate vascular homeostasis [57, 58]. MiRNAs have been shown to play important roles in vascular biology, but it is unclear whether miRNAs are involved in the physiological adaption to mechanical stimuli. Using microarray and quantitative PCR, others and we recently demonstrated that various miRNAs are sensitive to mechanical stimuli such as shear stress [59-61], cyclic stretch [62], and cell-matrix adhesion [63]. In our hands, PS-

induced miR-23b and OS-induced miR-21 have been shown to be involved in EC anti-proliferative and pro-inflammatory responses, respectively [59, 64]. Parallel studies reported that laminar shear-induced miR-19a and OS-induced miR-663 also contribute to EC growth arrest and pro-inflammatory response, respectively [60, 61, 65]. Recent studies by Wu et al. and Fang et al. have confirmed that miR-92a targets KLF2 to modulate the EC athero-protective phenotypes associated with different regional flow patterns [66, 67]. In addition, it has been shown in zebrafish that flow-induced klf2a (KLF2 analog) is required for the expression of miR-126, which in turn activates vegf signaling and angiogenic sprouting of aortic arch vessels [68]. Beside miRNA regulation of EC functions, miR-143/145 has been shown to modulate SMC phenotype under static and stretch conditions [56, 69]. A recent report has shown that miR-143/145 are enriched in the extracellular vesicles secreted by KLF2-transduced or shear-stress-stimulated ECs. These miR-143/145 enriched vesicles can be taken up by the co-cultured SMC to regulate target gene expression and phenotypic change in SMCs [70]. This result suggests that athero-protective signal is transmitted from ECs to SMCs in the form of miRNAs. Furthermore, mechano-sensitive miRNAs have been identified to not only regulate vascular functions but also modulate inflammatory response in airway epithelial cells and stem cell differentiation under various conditions of mechanical loading [62, 71], further supporting the critical roles of miRNAs in mechanotransduction.

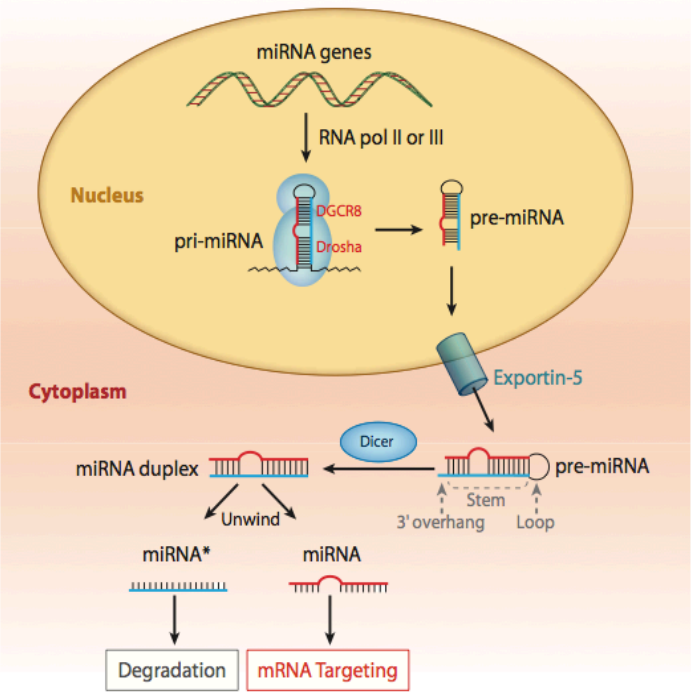

Figure 1.4 MicroRNA biogenesis and function. The biogenesis of miRNA begins with the transcription of pri-miRNA in the nucleus by RNA Polymerase II. The pri-miRNA is processed by the complex of Drosha and DGCR8, yielding a hairpin structure precursor (pre-miRNA) approximately 70 nucleotides. The pre-miRNA is exported from the nucleus to the cytoplasm and cleaved by Dicer, yielding the mature miRNA.The mature miRNA is incorporated into the miRISC (miRNA-induced silencing complex), which mediates gene silencing through either mRNA destabilization or translational inhibition. (adapted from Sun, W. et al., 2011).

1.5 Hypothesis and objectives

Fluid shear stress generated by blood flow over the surface of the endothelium plays a significant role in vascular physiology in health and disease. During the past two decades, a significant amount of effort went into understanding the molecular bases of mechanotransduction in ECs and the consequent gene expression and functional modulation. Others and we previously concluded that steady and pulsatile shear stresses (PS) with a net forward direction are athero-protective by decreasing EC turnover and suppressing the expression of inflammatory genes. In contrast, oscillatory shear stress (OS) without a significant forward direction is associated with high EC

turnover and up-regulation of pro-inflammatory genes, and hence is atherogenic. Based on new evidence in the literature and our recent studies that miRNAs play significant roles in regulating gene expression in ECs, **we hypothesize that athero-protective (PS) and atherogenic (OS) flow patterns induce distinct expression patterns of miRNAs in ECs, and hence differential gene/protein expressions and functional consequences.** As outlined in figure 1.5, this hypothesis was tested by experimental studies on cultured ECs *in vitro* and rat models *in vivo.*

In this dissertation, three objectives were proposed to study the role of miRNAs in mechanotransduction. First, to establish the miRNA signatures and corresponding functional outcomes in ECs subjected to atheroprotective and atherogenic flow, with the use of miRNA and cDNA microarrays. As demonstrated in Chapter 2, my results showed that flow patterns differentially regulated miRNA and mRNA profiles. Bioinformatics analyses of gene expression illustrated that PS led to the significant enrichment in cell cycle-related gene categories in comparison with static condition. Conversely, OS affected the gene set enrichments related to inflammatory response, cell adhesion, etc., in comparison to PS. Moreover, functional studies showed that PS suppressed EC growth through the regulation of miR-23b on cell cycle machinery, whereas OS caused sustained expression of miR-21 to contribute to pro-inflammatory responses.

The second objective is to identify the functional targets of miR-23b and elucidate the underlying mechanism that contributes to the anti-proliferative effect of PS on ECs. My results presented in Chapter 3 have identified and confirmed that CCNH is one of the direct targets of miR-23b in ECs. PS-induced miR-23b regulated the CCNH expression post-transcriptionally, thus leading to a reduction of the activities of cyclin-dependent kinase (CDK)-activating kinase (CAK) and RNA polymerase II (Pol II). Further

examination showed that the flow-regulation of miR-23b/CAK/Pol II pathway led to transcriptional inhibitions of cell cycle regulatory proteins and EC growth arrest.

The third objective is to validate the *in vitro* results in animals. In chapter 4, a rat carotid artery model was established to examine the expressions of miR-23b, CCNH, and proliferation markers in response to the alteration of flow patterns. Two approaches were used to produce the disturbed flow *in vivo*, including 1) local stenosis created by U-shaped clip, and 2) partial ligation of outflow branches of common carotid artery. My *in vivo* results obtained by using these two models with different types of disturbed flows validated my *in vitro* findings that miR-23b expression in disturbed flow region is lower than that in the pulsatile flow section and is inversely correlated to expressions of CCNH and Ki67.

Collectively, the studies conducted in this dissertation used a systematic approach to address the role of miRNAs in mechanotransduction. My findings have established the miRNA signatures and functional correlations in ECs in response to fluid shear stress with genome-wide microarray and provided mechanistic evidence that PS regulates EC proliferation through the miR-23b/CAK pathway. In addition, my *in vivo* findings validated that miR-23b expression is sensitive to flow pattern alterations in rat carotid artery. These findings reveal the mechanistic role of miR-23b in regulating EC gene expressions and functions, as well as the potential value of miR-23b in treating EC dysfunction in atherosclerosis.

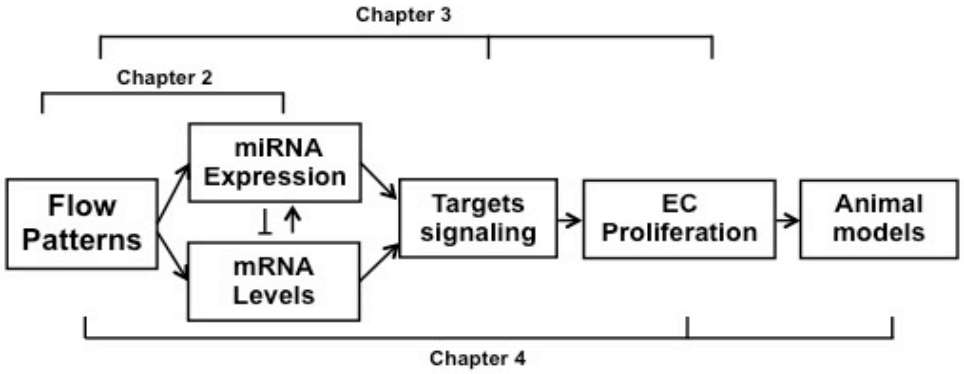

Figure 1.5 Outline of dissertation. *In vitro* (chapters 2 and 3) and *in vivo* (chapter 4) experiments were carried out to study the role of flow-regulated miRNAs in modulating gene expression and EC proliferation.

CHAPTER 2 FLOW REGULATION OF MICRORNA SIGNATURES AND ENDOTHELIAL PHENOTYPES

2.1 Abstract

The differential effects of flow patterns play important roles in regulating the vascular EC functions. The focal nature of atherosclerotic plaque formation reveals led to the understanding that the PS flow along the straight part of arterial tree exerts athero-protective effects on the ECs, while the disturbed flow (OS flow in the present study) found at the arterial bifurcation stimulates the pro-inflammatory response. The recent discovery of miRNAs reveals a novel powerful mechanism for post-transcriptional control of gene expression and modulation of many biological processes. However, the roles of miRNAs in regulating mechanotransduction and EC functions remain unclear. Using genome-wide microarray study, we profiled miRNA and mRNA expression levels in human ECs under 24-h PS and OS flows, as well as in static controls. Bioinformatics analyses of mRNA profiles indicated that PS predominantly regulates EC growth arrest, whereas OS modulates EC inflammatory response. Integration of miRNA and mRNA expression profiles with the use of computational approaches revealed the potential roles of miRNAs in regulating the PS-induced EC growth arrest and OS-induced pro-inflammatory response. Further miRNA studies showed that PS suppressed EC growth through the regulation of miR-23b on cell cycle machinery, and inhibition of miR-23b expression using antagomir-23b oligonucleotide attenuated the PS-induced G1/G0 cell cycle arrest. Furthermore, OS caused sustained expression of miR-21 to contribute to pro-inflammatory response. These results provide novel insights into the role of miRNAs in mechanotransduction. In conclusion, our study demonstrates that miRNA expression level can be differentially regulated by different flow patterns, consequently modulating the EC functions related to EC growth and inflammation.

2.2 Introduction

Cardiovascular dynamics involve different types of mechanical stimuli, including stretch and shear stress. These hemodynamic forces serve not only to provide the oxygen and nutrient to various tissues, but also to maintain cardiovascular homeostasis. ECs, which form the inner lining of the blood vessel, provide a barrier between the circulating blood and the vessel wall. Blood flow-induced hemodynamic forces act constantly on the endothelium; the variations in these forces due to vascular geometry, structural alterations, or hemodynamic factors can modulate EC signaling, gene expression, and physiological functions [2]. The atherosclerotic lesions in the arterial tree are found mainly at branch points where the blood flow is disturbed with a limited forwarding direction. Such lesions are generally spared at the straight parts of the arterial tree where the flow is laminar with a large forwarding direction [72]. Previous studies in our laboratory have demonstrated that exposure of ECs to 24 h of steady laminar shear flow at 12 dyn/cm^2 (approximating the hemodynamic force in the straight parts of the arteries) leads to anti-proliferative [34] and anti-inflammatory responses [57, 73]. In contrast, ECs exposed to disturbed flow that mimicks the hemodynamic condition at branch points exhibit the opposite responses [3, 74]. The PS-induced EC growth arrest involves the expression of CDK inhibitors (e.g., p21^{cip}, p27^{kip}), tumor suppressor p53, and Rb hypophosphorylation [33, 34]. The EC atherogenic phenotype induced by disturbed flow was examined by profiling the pro-inflammatory genes (including MCP-1, VCAM-1, SELE, etc.) and monocyte adhesion assay [74, 75]. Most of the knowledge in the field of mechanotransduction was acquired from studies at the protein and mRNA levels. There is little information on the role of miRNAs in regulating cardiovascular functions. With the recent advancements of knowledge that miRNAs are major regulator

for cell/tissue functions, it is important to examine its roles in EC proliferation and inflammatory response under different flow conditions.

Small noncoding RNAs, known as miRNAs, have been shown to regulate gene expression by binding to target mRNAs to cause either degradation or translational repression [44]. Currently, more than 800 miRNAs have been identified in the human genome and registered in the Sanger miRBase. These small RNAs provide a powerful mechanism for post-transcriptional control of gene expression at the mRNA level. There is growing evidence that miRNAs are involved in various biological processes in health and disease, including cell proliferation and differentiation, oncogenesis, and angiogenesis [46, 76-79]. It has also been shown that miRNAs play critical roles in cardiovascular homeostasis [80, 81]. In ECs, knockdown of dicer (a key molecule in the biogenesis of miRNAs) altered the expression of genes affecting EC biology and reduced EC proliferation and angiogenesis *in vitro* [46]. When both Dicer and Drosha (another important molecule in miRNA biogenesis) were knocked down in ECs, capillary sprouting and tube-forming activity were significantly reduced. Thus, the global reduction of miRNAs through the knockdown of Dicer and/or Drosha significantly affects EC functions *in vitro* and *in vivo*, suggesting the important roles of miRNAs in regulating vascular functions [47-49, 82].

In this study, I investigated the role of miRNAs in regulating EC gene expression and functions in response to pulsatile shear (PS) and oscillatory shear (OS) flows, respectively. The results indicate that miR-23b plays an important regulatory role in the inhibition of EC proliferation by PS flow, and that OS-induced miR-21 contributes to EC pro-inflammatory response.

2.3 Materials and Methods

2.3.1 Cell Culture

Human umbilical vein endothelial cells (HUVECs) were isolated by collagenase treatment of umbilical cord veins. Cells were cultured on 100-mm plates coated with collagen I (BD Biosciences, Bedford, MA) and maintained in medium M199 (Invitrogen, Carlsbad, CA) supplemented with 10% fetal bovine serum (Omega, Tarzana, CA), 10% endothelial cell growth medium (Cell Applications, San Diego, CA), 2 mM L-glutamine, 1 mM sodium pyruvate, and 1% penicillin/streptomycin. All cell cultures were kept in a humidified 5% CO2-95% air incubator at 37°C. HUEVCs within passages 4-7 were used in all experiments.

2.3.2 Shear Experiments

An *in vitro* circulating flow chamber system was used to impose fluid shear stress to the cultured HUVECs. Prior to the shear experiment, the HUVECs were seeded on collagen I (CN, BD Biosciences, Bedford, MA)-coated glass slides, which were assembled into the flow chamber for the shear experiments. The culture medium was maintained at 37˚C with a mixture of 95% air and 5% CO_2 and circulated through the chamber. Flow was generated through the chamber by the hydrostatic pressure difference between the perfusate reservoirs. Constant flow was maintained by pumping the culture medium from the collection flask back to the upper reservoir, which maintained the constant hydrostatic pressure. The cell cultured on slides were exposed to the shear stress with pulsatile (PS, 12 ± 4 dyn/cm^2, 1 Hz) and oscillatory (OS, 0.5 ± 4 dyn/cm^2, 1 Hz) flows, and the cells obtained from unsheared sample were used as the static control. All experiments were performed on ECs grown to confluent monolayers.

2.3.3 Transfection

Antagomirs used in this study, as well as negative control molecule, were purchased from Ambion (Austin, TX). The oligonucleotides were individually reverse transfected with siPort NeoFx (Ambion) reagent into HUVECs at the final concentration of 50 nM according to the manufacturer's protocol. Cells were incubated with the siRNA-transfection reagent complex in 2 mL of culture media on a glass slide (for flow experiment) overnight. Fresh culture medium was then added. 24 h post-transfection, the cells on slides were subjected to shear experiment.

2.3.4 miRNA and cDNA microarray analysis

Total RNA was isolated from ECs with mirVana kit (Ambion, Austin, TX) after PS or ST. Five μg of total RNA of each sample was sent to L.C. Sciences (Houston, TX) for miRNA profiling. The samples were enriched for small RNAs, labeled with fluorescent dyes, and hybridized to μParaFlo microfluidic chips, which contain 856 mature human microRNA probes (miRBase version 12.0) in multiple replicates, as well as the perfectly matched and mismatched probes for quality control. The raw data from the miRNA chips were normalized to the control probes on individual chips. Significantly up-regulated miRNAs were defined as those with >1.25 fold-changes in expression and down-regulated ones as those having <1.25 fold-changes in expression at $P<0.01$.

The cDNA microarray experiments were performed by the Genomic Core Facility on UCSD campus (Biogem, UCSD); 10 μg of total RNA was hybridized on Agilent 44K oligonucleotide microarrays (Agilent, Santa Clara, CA). Three biological repeats were performed for all array studies.

2.3.5 RT-PCR

Reverse transcription (RT) and polymerase chain reaction (PCR) were performed with TaqMan miRNA assays (Applied Biosystems, Foster, CA) using miRNA-specific primer sets in the 7900HT real-time PCR machine (Applied Biosystems, Foster, CA)

according to manufacturer's protocol. In general, three biological replicates were used for analysis, and all reactions were run in triplicates. The relative expression levels of miRNAs in ECs were determined with the $\Delta\Delta C_T$ method and compared with internal controls.

2.3.6 BrdU incorporation assay and flow cytometry

HUVECs were pulse-labeled with 10 mM BrdU during the last 4 h of shearing and static incubation. After labeling, the HUVECs were assayed using the Cell Cycle Analysis kit (BD Bioscience, San Jose, CA) according to the manufacturer's protocol. The cells were subjected to flow cytometirc analysis with FACScan (BD Bioscience, San Jose, CA).

2.3.7 Monocyte adhesion assay

THP-1 cells were grown in RPMI medium 1640 (Gibco) supplemented with 10% fetal bovine serum (Omega) and concentrated by centrifuging at 400 x *g* for 10 min at room temperature. The adhesion assay was performed by adding 2.0 mL of the concentrated THP-1 cells (preincubated with calcien-AM at 5 mM; Invitrogen) to the sheared slides for 30 min at 37°C. The unbound cells on the slides were removed by gently washing 3 times with PBS or RPMI, and the monolayers were fixed with 4% paraformaldehyde for 30 min. Fluorescent micrographs of the cells on the slides were taken with Olympus IX70. The number of adherent cells was determined using an image-processing algorithm that measures fluorescence intensity/area after background noise subtraction.

2.3.8 Immunoblotting

ECs were lysed in a lysis buffer: 25mM HEPES, pH 7.4, 1% Triton X-100, 1% deoxycholate, 0.1% SDS, 125mM NaCl, 5mM EDTA, 50mM NaF containing 1mM Na_3VO_4, 1mM PMSF, 10μg/ml leupeptin, and 2mM glycerophosphate. Equal amounts of

protein were loaded onto SDS-PAGE. After electrophoresis, the proteins were transferred to nitrocellulose membranes, blocked with 5% BSA-containing PBS, and incubated with the primary antibodies. The bound primary antibodies were detected using appropriate secondary antibodies coupled to horseradish peroxidase (Santa Cruz Biotech, Santa Cruz, CA) and the ECL detection system (Amersham, Piscataway, NJ).

2.3.9 Statistical analysis

Data are expressed as mean ± SEM and compared among separate experiments. For comparisons between two groups, statistical analyses were performed using the two-sample independent-groups *t* test. Comparison of multiple mean values was made by one-way ANOVA, and statistical significance among multiple groups was determined by Tukey's post-hoc test (for pair-wise comparisons of means). *P* values <0.05 are considered statistically significant.

2.4 Results

2.4.1 Long-term pulsatile laminar flow keeps vascular endothelium in a quiescent state

In agreement with previous studies on steady and pulsatile laminar shear stresses [33, 34, 83], we found that HUVECs subjected to 24-h PS had a significant reduction in cell proliferation rate in comparison to the static condition (ST). The BrdU staining in Figure 2.1A (top) shows that the number of BrdU-positive cells was substantially reduced under 24-h PS. The flow cytometric data on quantitative cell cycle analysis (Figure 2.1A, bottom) show that ECs subjected to 24-h PS had a significant increase in the percentage of cells in G0/G1 phase (72.43 ± 2.46 %) in comparison to ST (55.8 ± 4.32 %). PS also significantly reduced the cells in S-phase (4.18 ± 1.12 %) vs. ST (18.99 ± 4.35 %), but there is no significant difference for cells in G2/M phase between PS (24.13 ± 4.31 %) and ST (22.57 ± 3.2 %). These flow cytometric results are

consistent with those from immunofluorescence imaging analysis of BrdU staining in showing that 24-h PS causes growth arrest by preventing ECs from entering the S-phase.

2.4.2 Expression profiling analysis of mRNA in ECs under pulsatile flow and static condition

We investigated genome-wide mRNA expression profile in relation to EC growth arrest under PS. In three independent biological experiments, ECs were subjected to PS or kept as ST for 24 h. The results were analyzed using the GeneSpring GX software (Agilent, Santa Clara, CA). Gene expression ratios from each experiment were calculated by using the average normalized intensities (see Material and Methods). Differential gene expressions between PS and ST were selected with the cut-off at changes $\geq$ 1.75 fold and P value < 0.01. With these criteria, we were able to identify 1227 genes differentially expressed in response to PS, of which 569 (46%) were up-regulated and 658 (54%) were down-regulated.

The up-regulated and down-regulated gene lists were submitted to the DAVID online tool (http://david.abcc.ncifcrf.gov/home.jsp) to perform the Gene Ontology (GO) annotation and pathway enrichment analysis [84-86]. GO terms are grouped into three categories: biological process, cellular component, and molecular function. Table 2.1 lists the GO terms representing biological processes that have the highest enriched score and the most significant P-value. The top five GO terms under biological process are all cell cycle-related, these terms include cell cycle, mitotic cell cycle, cell division, DNA replication, and cell cycle check point. Functional classification of the differentially expressed mRNA transcripts by KEGG pathway database [87, 88](Table 2.2) also shows that the down-regulated genes are highly associated with cell cycle, p53 signaling, and DNA synthesis pathways, while the up-regulated genes are mostly

associated with metabolic pathways. Unsupervised clustering of the expression profile for cell cycle genes in ECs under PS and ST conditions is shown in Figure. 2.1B. Most cell cycle-related genes are down-regulated (e.g., CDK2, CDK4, most cyclins, and E2F1), while growth arrest genes are unchanged (e.g. p53, Rb) or up-regulated (e.g., $p21^{cip}$, $p27^{kip}$) in PS vs. ST. These results indicate that 24-h PS prevents ECs from entering the S phase by down-regulating key proteins in the cell-cycle network and up-regulating CDK inhibitors.

2.4.3 miRNA expression profiles in ECs under PS and ST conditions

To examine whether miRNAs are involved in the PS-regulated gene expression and growth arrest described above, we performed the analyses of miRNA profiles in ECs under PS and ST with LC Sciences μParaflo® microfluidic miRNA microarray. The array contains quadruplicate probes for 856 human miRNAs with the Sanger miRbase sequence database (Release 12.0). After filtering out the signals below the threshold level for detection and applying the criteria of fold change $\geq$ 1.25 and $P < 0.01$, the data of three independent biological experiments revealed that 21 miRNAs were differentially regulated in PS vs. ST (Fig. 2.2A), including 8 up-regulated and 13 down-regulated. PS caused the up-regulation of miR-23b cluster (miR-23b and miR-27b), and the down-regulations of miR-17-92 cluster (miR-17, 19b, 20a, 20b, 92a), miR-16 cluster (miR-15b, 16), and miR-221 cluster (miR-221 and 222) (Fig. 2.2B). Among these miRs, we selected nine miRNAs on the basis of functional interest for validation with RT-PCR. As shown in Table 2.3, the RT-PCR results of seven of these selected miRs (miR-23b, 27b, 923, 16, 106, 26b, and Let-7) matched the microarray data, but the other two (miR-19b, 221) did not.

To study the potential correlation between the miRNA expression induced by PS and vascular functions, we searched for potential mRNA targets of the 21 differentially

expressed miRNAs by using the algorithms TargetScan and PicTar, which are based on the conserved seed sequences of miRNAs matching the mRNA 3'UTR. By taking the consensus targets identified in common by both TargetScan 4.1 and PicTar, we were able to identify 1073 putative targets. [89-92]Among these, 68 genes (5.5% of these putative targets) were differentially expressed in ECs at the mRNA level under PS vs. ST (Fig. 2.2C). We also performed the GO analysis by submitting the predicted target gene list to the DAVID online tool, and the overlapping GO terms (representing biological processes) between the predicted targets and the differentially expressed genes are listed in Table 2.4, and cell cycle-related biological processes are among the top list.

2.4.4 Correlation of miRNA levels with functional gene sets in PS vs. ST

To investigate the potential functional consequences of the PS-regulated miRNAs, we first calculated the correlation coefficients between PS-induced miRNAs and differentially expressed genes (1227 mRNAs). We then ranked the correlation coefficients and used them to perform the Gene Set Enrichment Analysis (GSEA). 394 functional gene sets were identified from the curated gene sets in c.2 collection representing the functional pathways in GSEA database [93]. The associations of miRNAs with these functional gene sets were generated, hierarchically clustered, and plotted as a matrix based on the statistical significance (P-value) of the enrichment score obtained from the GSEA analysis. With this approach, we were able to identify the potential associations between miRNAs and the functional gene sets, and the strongest associations are shown in the boxed region. Upon further analysis of representative gene sets, we extracted protein-coding genes from these gene sets and performed the GO analysis. The top ten GO terms are shown in Figure. 2.3B. Again, cell cycle-related terms are highly enriched with this approach and strongly associated with the miRNA expression profile. The miR-23b cluster (miR-23b and 27b) is negatively associated with

these functional categories. Integration of miRNA and mRNA expression profiles, together with computational bioinformatics approaches (including miRNA-targets prediction, functional categorization with GO terms and KEGG database, and the association matrix) revealed the potential roles of miR-23b and 27b in regulating the PS-induced EC growth arrest.

2.4.5 Blockade of miR-23b, but not miR-27b, attenuated the PS-induced cell growth arrest

The abundance of miR-23b and miR-27b in HUVECs and their up-regulation by 24-h PS indicate that the miR-23b cluster may play significant roles in EC growth arrest. Therefore, we tested whether antagomirs against miR-23b and miR-27b can reverse the growth arrest effect of PS on ECs.

HUVECs were transfected with antagomir-23b (AM23b), antagomir-27b (AM27b), or anti-miR negative control (Neg. AM) and subjected to PS/ST experiments for 24 h with BrdU labeling during the last 4 h. In ECs transfected with Neg. AM, 24-h PS caused a significant increase of cell number in G0/G1 phase and a significant decrease in S phase, with no significant change in G2/M phase (Figure 2.4), giving the same response as the untreated ECs (Figure 2.1A). Blockade of endogenous miR-23b with AM23b partially reversed the PS-induced cell cycle arrest. Under 24-h PS, the cell number in S phase was markedly higher in AM23b+PS (9.87±0.79 %) than the Neg. AM+PS (4.88±0.96 %). Knocking down endogenous miR-27b expression with AM27b, however, did not block the growth arrest caused by 24-h PS, although miR-27b is in the same cluster as miR-23b. This suggests that the anti-proliferative response of HUVECs under 24-h PS is partially regulated by mechanism mediated by miR-23b, but not by miR-27b.

2.4.6 Roles of miR-23b and mir-27b in modulating the signaling molecules that mediate PS-induced cell growth arrest

To further investigate the signaling molecules that mediate the effects of miR-23b cluster on the 24-h PS-suppression of EC growth, we examined the actions of AM23b and AM27b on several cell cycle proteins regulating G1 to S transition under PS. Our previous study showed that steady laminar shear causes the dephosphorylation of the retinoblastoma (Rb) protein [34]. Rb in its hypophosphorylation state binds to the E2F family proteins and suppresses cell proliferation by inhibiting the cell cycle progression through G1 into S phase and preventing DNA synthesis [94, 95]. As shown in Figure 2.5A, 24-h PS decreased the phosphorylation of Rb without affecting the total Rb expression, and this presence of the hypophosphorylated form of Rb would inhibit EC proliferation. The PS-induced Rb hypophosphorylation was prevented by AM23b, but AM27b had no significant effect. Both AM23b and AM27b reversed the reduction of E2F1 expression caused by 24-h PS, but did not affect the expressions of p53 and $p27^{kip}$ (CDKN1B). These results suggest that miR-27b plays a role in down-regulating EC E2F1 expression, but this is not sufficient to modulate the PS-induced EC growth arrest without the accompanied Rb hypophosphorylation. In contrast, the PS-induced miR-23b expression can cause growth arrest through Rb hypophosphorylation, in addition to down-regulation of E2F family proteins

2.4.7 Prolonged OS flow promotes pro-inflammatory responses in ECs

In contrast with PS flow, disturbed flow (and OS flow) has been linked to the atherogenic phenotypes of ECs, particularly pro-inflammatory response, both *in vitro* and *in vivo*. To examine the differential regulation of flow patterns on EC pro-inflammatory response, ECs were exposed to 24-h OS and PS, respectively, and total RNA was isolated for cDNA microarray and RT-PCR validation. The profiling experiment and

analysis were performed as previously described. Determination of differential gene expressions between OS and PS with a cutoff at changes ≥1.75-fold and P-value <0.01 yielded 536 genes, of which 186 (34.7%) were up- and 350 (65.3%) were down-regulated by OS, in comparison to PS. Functional analysis of differentially expressed mRNA transcripts by GO annotation showed that inflammatory response, cell adhesion and cell growth are enriched in OS vs. PS group (Table 2.5). In agreement with previous studies, MCP-1 and VCAM-1 gene expressions were both significantly up-regulated by OS flow, compared to PS flow (Figure 2.6A). To further examine whether OS flow leads to the pro-inflammatory consequence, monocyte adhesion assay was performed as previously described. As shown in Figure 2.6B, the number of monocytes adhered to ECs under OS was significantly higher than the number caused by PS. These results show that the application of OS flow induces pro-inflammatory gene expressions and monocyte adhesion, compared to PS flow.

2.4.8 miRNA expression profile in ECs under OS and PS conditions

To examine the corresponding miRNA profile in OS vs. PS, small RNAs were enriched with mirVana kit from total RNA samples extracted from OS and PS and then subjected to miRNA microarray analysis as previously described. As shown in Figure 2.7, 36 miRNAs are differentially expressed with a cutoff at changes ≥1.25-fold and P-value <0.01, of which 22 are up-regulated and 14 down-regulated in OS as compared with PS. Selected miRNAs were confirmed with TaqMan miRNA assays. We further compared the overlaps of the miRNAs between PS and OS flows and all the significantly regulated miRNAs (no cutoff applied). 13 miRNAs were differentially regulated only for PS vs. ST, but not for OS vs. PS, while 31 miRNAs were differentially regulated only for. OS vs. PS, but not for PS vs. ST. 16 miRNAs were differentially regulated for both PS vs. ST and OS vs. PS.

2.4.9 OS induction of monocyte adhesion to ECs is mediated by miR-21

Although OS flow has been shown to cause the pro-inflammatory response of ECs, the underlying mechanism remains unclear. Among differentially expressed miRNAs in OS vs. PS, miR-21 is abundant in ECs and has been implicated to play important roles in cardiovascular diseases. To investigate the role of OS-induced miR-21 in pro-inflammatory response, ECs were transfected with antagomiR-21 (AM21) and control molecule. As shown in Figure 2.8, application of 24-h OS to ECs significantly induced the adhesiveness for monocytes, which was attenuated by AM21 transfection. In addition, the OS-induction of MCP-1 and VCAM-1 were also suppressed by the inhibition of miR-21, suggesting that OS-induced pro-inflammatory response, at least in par, is mediated by miR-21.

2.5 Discussion

The differential effects of flow patterns on ECs form the fluid mechanical basis of the predilection of regions of disturbed flow (e.g., arterial branch points and aortic arch) to atherosclerosis and regions of laminar flow with a significant forwarding direction (i.e., the straight parts of the arterial tree) to athero-protection. There have been many studies on the effects of different flow patterns (e.g., steady laminar and disturbed flows) on EC gene expression at the mRNA level [35, 36, 75] starting in 2001. Following the recent discovery that miRNAs provide a powerful mechanism for post-transcriptional control of gene expression at the mRNA level and that they are involved in various biological processes in health and disease, it is logical and timely to investigate the role of miRNAs in flow regulation of EC phenotypes.

Besides the steady laminar and disturbed flows that are widely studied in the literature, there is evidence demonstrating that the pulsatility imposed onto laminar flow due to heart beats may also contribute to the regulation of vascular cell functions [96,

97]. The present study was designed to determine the effects of pulsatile shear flow (PS) with a significant forwarding direction (12 ± 4 dynes/cm^2) and oscillatory shear flow (OS, 0.5 ± 4 dynes/cm^2) in modulating miRNA expression and to relate the miRNA modulation to mRNA expression by using bioinformatics algorithms and analysis. The results led to the discoveries that miR-23b plays a significant role in mediating the PS-induced suppression of several cell cycle genes and the consequent growth arrest, and that OS-induced miR-21 contributes to the pro-inflammatory responses of ECs.

We report for the first time that the application of 24-h PS to HUVECs causes (a) growth arrest, and (b) down-regulation of cell cycle genes by mRNA microarray analysis; these results show that PS and steady laminar cause the same anti-proliferation effects. The findings on PS-regulated gene expression correspond well with the cell cycle network shown in the red boxes of Figure 2.9. We then proceeded to determine the miRNA expression profile of ECs under PS and ST. The results show the differential regulation of miRNAs by PS, and demonstrate for the first time that PS causes the up-regulation of miR-23b cluster (miR-23b and miR-27b) and down-regulations of miR-17-92, miR-16, and miR-221 clusters in ECs. The differential expressions of these miRNA clusters in response to PS provide an excellent example of the potential roles of miRNA signatures in mechanotransduction.

Searching of the potential mRNA targets of the 21 differentially expressed miRNAs by using the algorithms TargetScan and PicTar led to the identification of 1073 putative targets that were in common with both algorithms, but only 68 of these genes (5.5%) were differentially expressed in ECs at the mRNA level under PS vs. ST. This indicates that the computational prediction can generate a very large number of false positives and that it needs validation with experimental approaches. It is also possible that miRNA regulation is through the inhibition of translation, and hence mRNA profile

does not sufficiently reflect the miRNA target prediction. Furthermore, there is the possibility of the collocation (or proximity) of miRNA and mRNA coding regions in the genome that regulates the protein products. Nevertheless, GO analysis shows that the overlapping GO terms (representing biological processes) between the predicted targets and the differentially expressed genes are highly enriched with cell cycle-related terms.

By ranking the correlation coefficients between the PS-induced miRNAs and the differentially expressed 1227 mRNAs and using the Gene Set Enrichment Analysis (GSEA), we found that twelve of the gene sets that represent cell cycle had the strongest association. miR-23b and miR-27b were negatively associated with these functional gene sets. Integration of miRNA and mRNA expression profiles, together with computational approaches, revealed the potential roles of miR-23b and 27b in regulating the PS-induced EC growth arrest.

Both miR-23b and miR-27b are highly conserved and lie within 0.5 kilobases (kb) of each other on human chromosome 9, and they are both up-regulated in ECs under PS vs. ST (Figure. 2.2). Although both AM23b and 27b can regulate E2F1 expression, only AM23b significantly reduced the PS-induced Rb hypophosphorylation and cell cycle arrest. It is known that the increase of Rb protein inhibits cell cycle progression and that Rb activities depend on its phosphorylation status [98]. The hypophosphorylated Rb binds to E2F family proteins in a cell cycle-dependent manner to modulate proliferation. Blocking Rb–E2F interaction with its endogenous genes has been reported to prevent the Rb- mediated growth arrest [99], and this probably involves the recruitment of other repressors (e.g., HDAC) to the Rb–E2F complex [100]. It seems that the decrease of E2F1 per se is not sufficient to cause growth arrest, but the hypophosphorylation of Rb with E2F1 binding plays an important role in regulating EC growth. Both AM23b and

AM27b did not have any effect on the PS-induced expressions of p53 and $p27^{kip}$; hence these molecules may not mediate the effects of miR-23b on growth arrest.

In this study, we have proposed a novel mechanism by which PS flow causes the up-regulation of miR-23b, which in turn decreases Rb phosphorylation, leading to the growth arrest. Since the regulatory mechanisms through miRNAs generally involve a network, there must be other miRNAs besides miR-23b that also mediate this PS-induced effect. It is most likely that miR-23b regulates EC proliferation through more complicated mechanisms than what is proposed here, including the interplays among different miRNAs and mRNAs. The partial blockade of the PS-actions by AM23b is in keeping with this line of thinking. It is known that Rb phosphorylation is also modulated by cyclins, CDKs, p53, and $p27^{kip}$. Our mRNA microarray results demonstrated that CDKs 1, 2 and 4, cyclins A, B, and E are down-regulated (Figure 2.9), and these may be one of the mechanisms that leads to Rb hypophosphorylation. We found that miR-23b does not significantly modulate p53, $p27^{kip}$, and CyclinD1. However, the effects of miR-23b on other cyclins and CDKs remained to be determined. The GO analysis of our predicted miRNA targets and mRNA data indicate that the regulation of kinase activities is one of the important features for EC gene signature in response to shear (Table 2.2); hence the signaling pathways may also involve kinase/phosphatase cascades. Moreover, the mechanism by which PS regulates miR-23b expression remains unclear. Recent study indicated that c-Myc, a known stimulator for cell proliferation, suppresses miR-23b expression in prostate cancer cells [101]. Further investigations will be needed to determine the role of myc in the PS regulation of miRNAs.

The miRNA regulation of gene and protein expressions not only involves a spatial network, but also temporal dynamics. Our collaborator has studied miRNA profiles in HUVECs under steady laminar flow at 12 and 24 h [65]. Their results indicate

that 12-h shearing caused a significant expression of miR-19a to mediate the shear-induced growth arrest, but this effect was not found after 24-h shearing. In contrast, they found miR-23b to be induced under 24-h shearing, which is the duration in our study, but the induction was not significant at 12 h. In contrast to miR-23b, which is shown in our study to regulate EC growth through the modulation of E2F expression and Rb phosphorylation, Qin et al. [65] found that the regulation of EC growth by miR-19a is mediated mainly through the modulation of cyclin D1. However, preliminary tests showed that the combined uses of AMs of miR-19a and -23b did not have any synergistic affect on EC growth arrest (data not shown). These two studies together show the participation of two miRNAs in regulating the PS-induced growth arrest with different temporal dynamics and different signaling pathways. These findings exemplify the complexity of the miRNA-mediated regulation of cellular functions and point out the need for further investigations on the interactions between different miRNAs on EC functions.

It has been reported that disturbed flow induces the pro-inflammatory responses of ECs *in vitro*, and that the disturbed flow pattern at branch points and curvatures of arterial tree causes the preferential localization of atherosclerotic lesions in vivo, Indeed, our results confirmed that the application of OS flow up-regulates the expressions of VCAM1 and MCP1 and promotes the monocyte adherence to ECs. These findings correspond well with the enriched functional gene sets, including cell adhesion and inflammatory response, identified by bioinformatics analyses of the cDNA microarray data in OS vs. PS group. In addition, we have reported the differential expression profiles of miRNAs in ECs in response to OS vs. PS identified by miRNA microarray. The expression of miR-21 is abundant in ECs and was found to be significantly up-regulated by OS relative to PS. A recent study in a swine model by Fang et al. [102]

reported that miR-21 expression is higher in ECs at the athero-prone region of aortic arch, where the blood flow is disturbed, as compared with the ECs in the straight segments, where the flow is pulsatile and laminar. These *in vitro* and *in vivo* findings implicate a potential role of miR-21 activation in the disturbed flow induction of EC pro-inflammatory phenotypes. Our functional study showed that inhibition of miR-21 with AM21 attenuates the OS-induced monocyte adhesion and up-regulations of VCAM1 and MCP1, confirming our hypothesis that OS-induced miR-21 expression, at least partially, contribute to the EC inflammation. The underlying mechanism was further demonstrated by a separate report by Zhou J. et al [64].

In conclusion, our findings indicate that flow patterns differentially regulate miRNA profiles, gene expressions, and EC phenotypes. 24-h PS significantly increases the miR-23b level, which decreases E2F1 expression, causes Rb hypophosphorylation, and results in EC growth arrest. On the other hand, 24-h OS sustained the induction of miR-21, which contributes to the pro-inflammatory responses of ECs. These results provide novel insights into the mechanism of mechanotransduction by which fluid shear stress modulates EC phenotypes through a miRNA-mediated mechanism. It is suggested that miRNAs may also act as a master switch to modulate various post-transcriptional processes in human ECs. Our findings have demonstrated that the shear-induced miRNA signature and the corresponding mechanisms are important for the understanding of the mechanisms of regulation of cardiovascular homeostasis in health and disease.

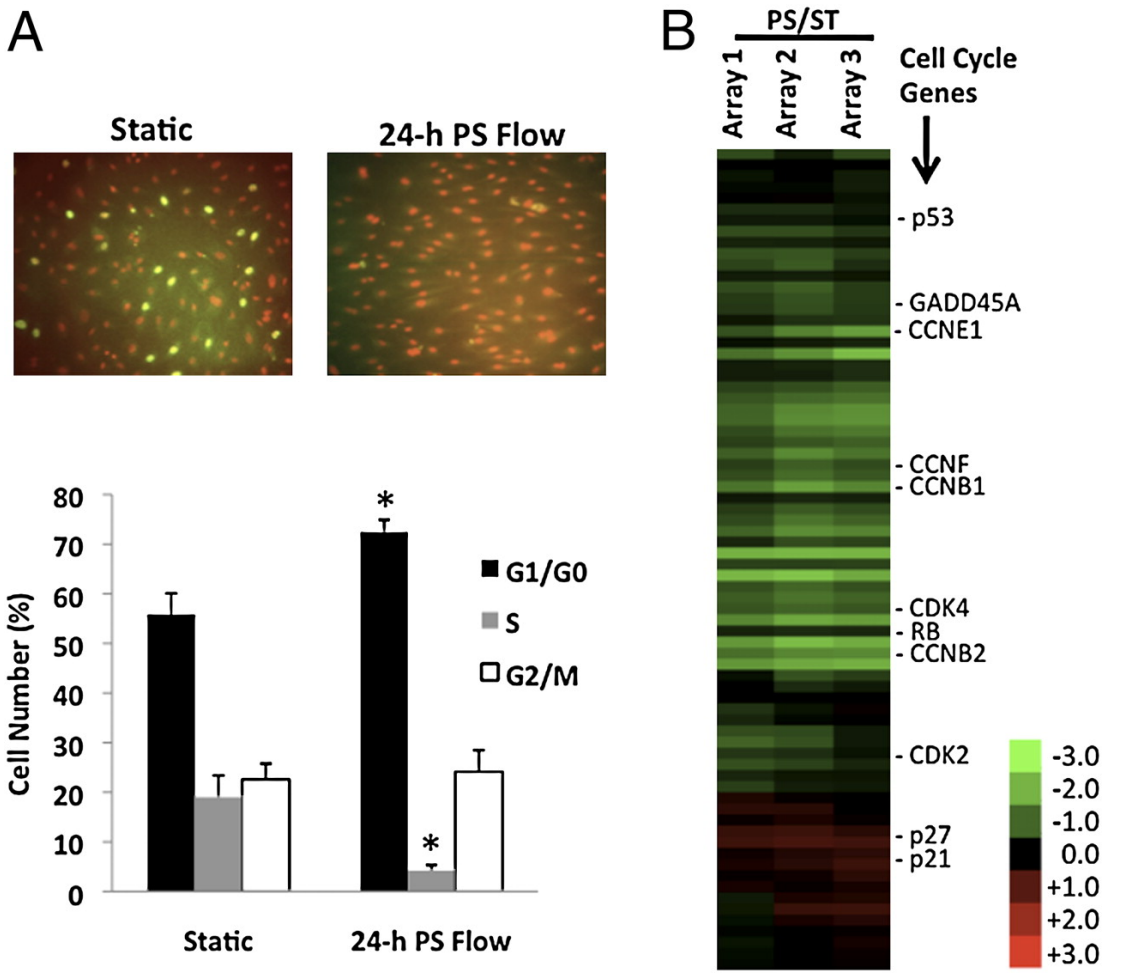

Figure 2.1 PS reduces cell proliferation and regulates cell cycle-related gene expression. (A) HUVECs were subjected to 24-h PS, with BrdU added during the last 4 h. Cells were fixed and stained (upper panel) with anti-BrdU and 7-AAD (for DNA staining). Flow cytometry (lower panel) showed a significant increase of cell number in G0/G1 phase and a significant decrease in S phase in comparison to the ones under static condition. The number of cells in G2/M phases was not significantly changed. (B) Hierarchical clustering of differentially expressed genes in cell cycle under PS vs. ST. Three biological repeats are shown at top of the heat map. Right column lists the selected gene symbols. Color of each band reflects fold change of mRNA in PS vs. ST. Red bands represent increases, and green bands for decreases. Exemplar mRNAs representing cell cycle components are shown in this heat map.

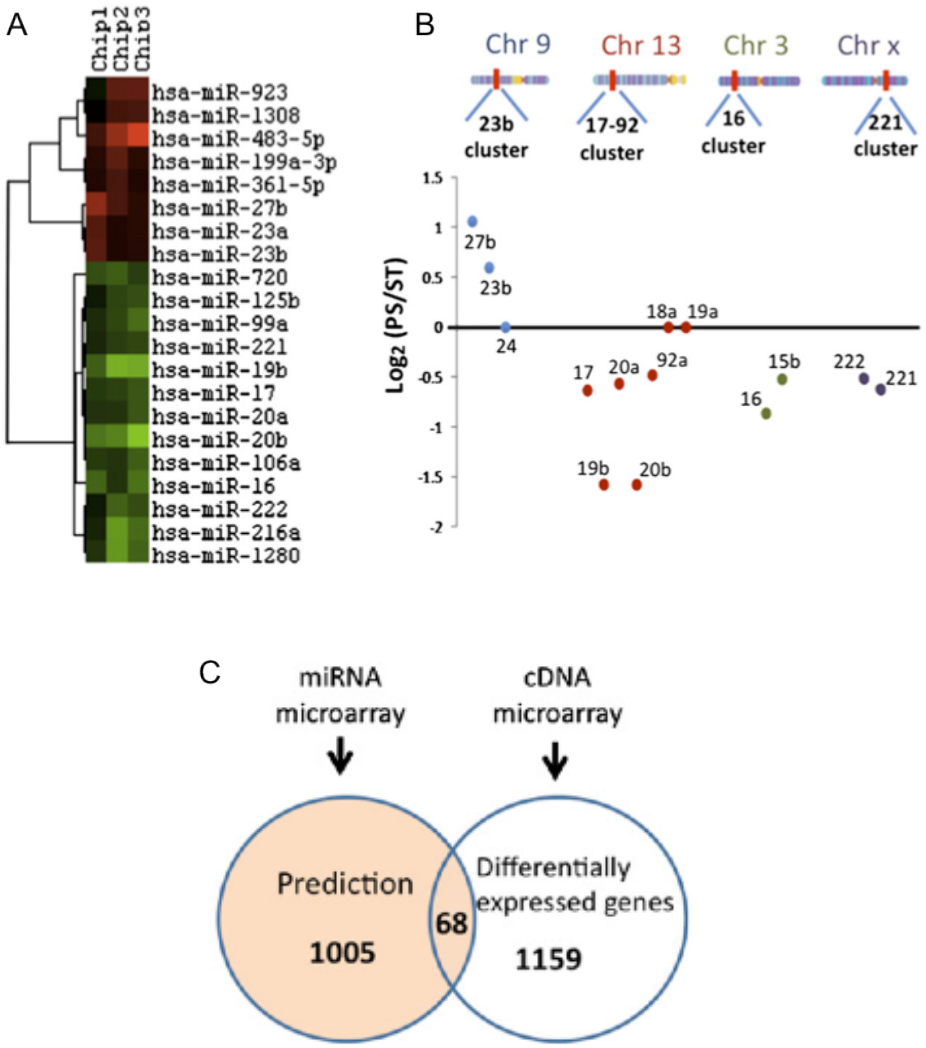

Figure 2.2 miRNA expression profile under PS vs. ST. Expression levels of 856 human miRNAs (Sanger miRBase 12.0) in ECs under PS and ST were measured with miR microarray (n = 3). (A) Unsupervised hierarchical clustering analysis of miRNA expression profile. Heat map shows PS vs. ST miRNA log2 ratios with a threshold of 1.25-fold and P < 0.05. Red bands represent upregulated miRNAs and green bands, downregulated miRNAs. (B) Differential expression of miRNA clusters. miRNAs are considered to belong to the same cluster if they are located in close proximity to each other in the genome. PS upregulates the miR-23b cluster in chromosome 9 and downregulates miR-17–92, -16, and -221 clusters in chromosomes 13, 3, and X, respectively. The images of chromosomes are adapted from **http://genomics.energy.gov**. (C) Venn diagram of the overlap between differentially expressed genes from mRNA microarray data and putative miRNA targets.

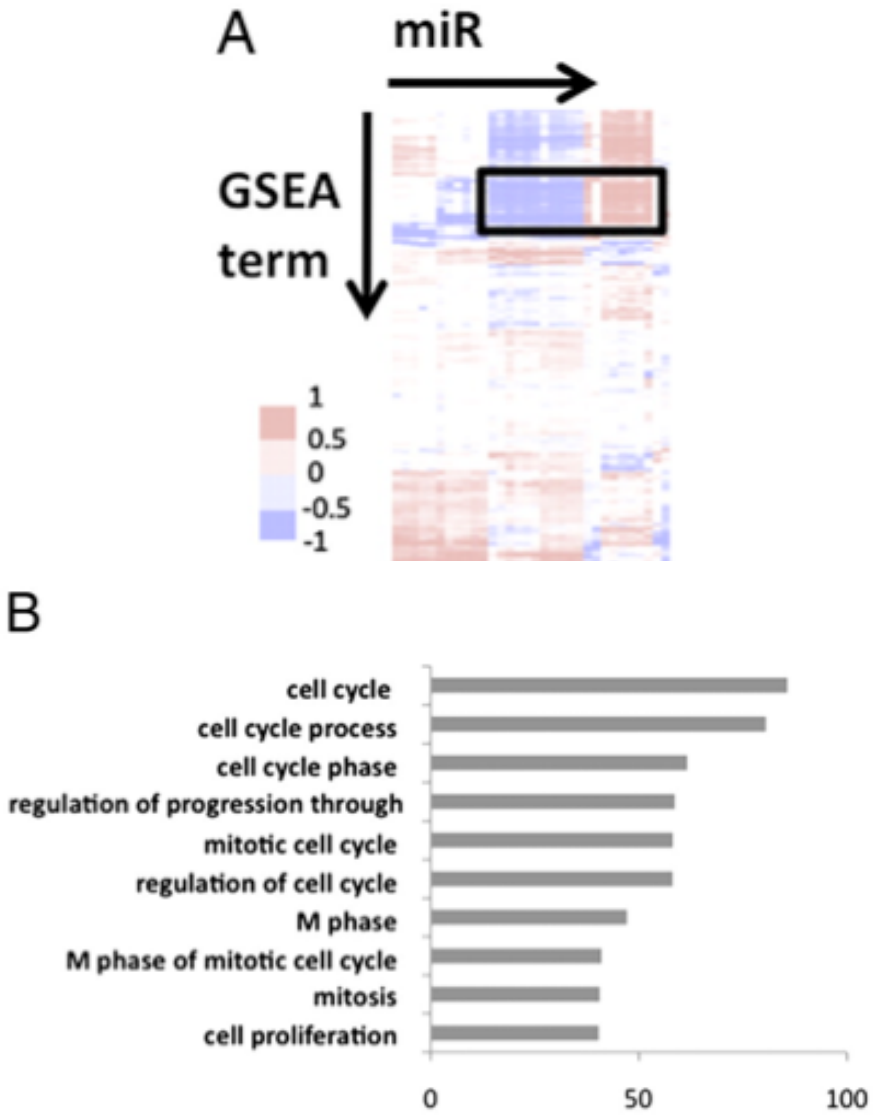

Figure 2.3 Association matrix of miRNA levels with functional gene sets under PS vs. ST. (A) Columns represent 394 functional gene sets, and rows represent flow-regulated miRNAs. Functional categories are positively (red bands), negatively (blue bands), or not (white bands) associated with miRNA expression profiles under PS vs. ST. The boxed region shows high associations between functional categories and miRNAs. The genes extracted from the functional gene sets in the box were used to perform the gene ontology (GO) analysis. (B) The −log (P values) of top 10 GO terms are plotted.

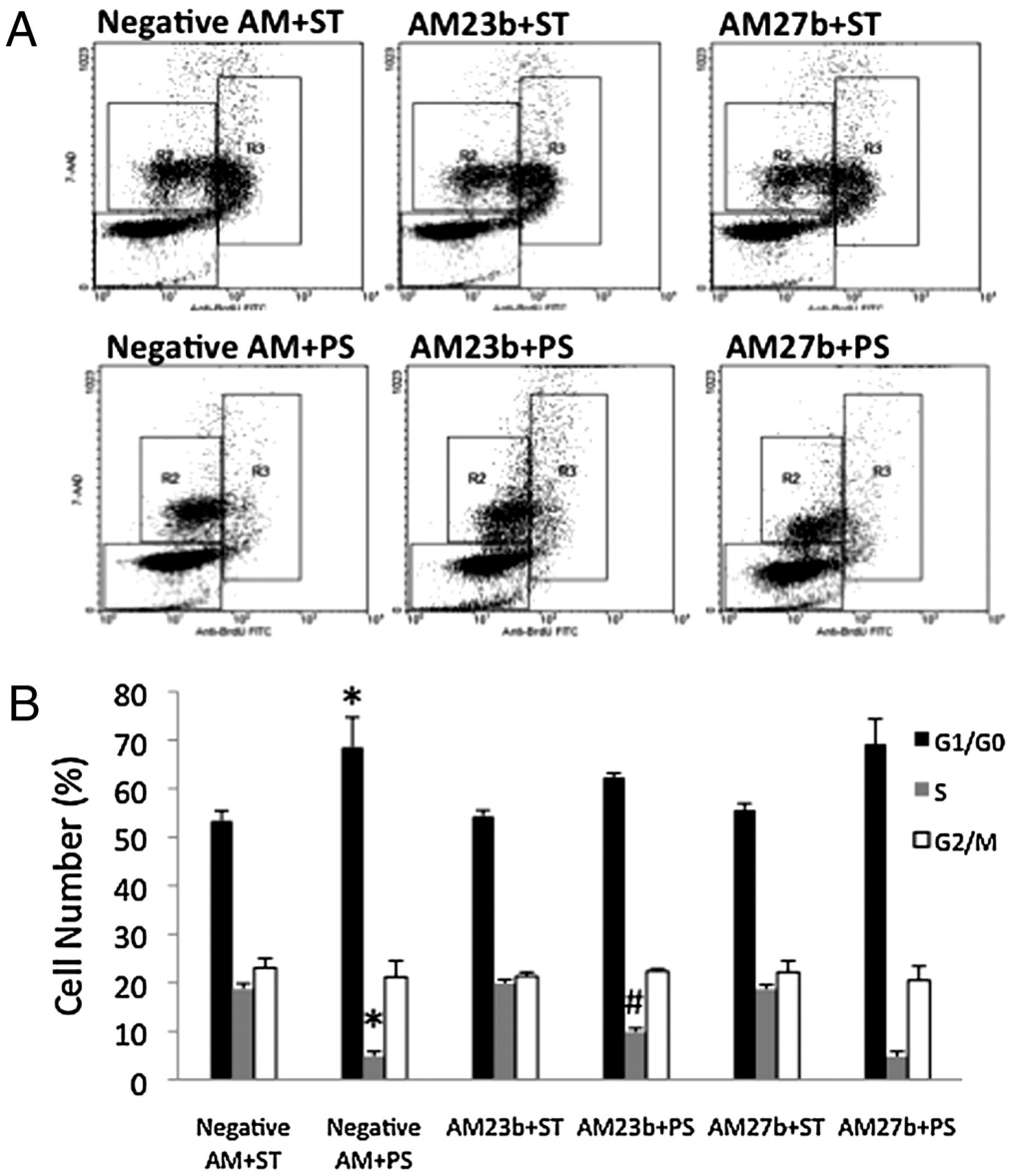

Figure 2.4 Antagomir against miR-23b attenuates the flow-induced EC growth arrest. (A) Flow cytometry for cells transfected with anti-miR negative control (right), AM23b (center), and AM27b (left) in ST (upper) vs. 24-h PS (lower). R1, R2, and R3 region gates denote cells in G1/G0, G2 + M, and S phases, respectively. (B) The bar graph summarized the percentage of cells in G1/G0, G2/M, and S phases under PS and ST with antagomir transfection. *,$P < 0.05$ in comparison with the corresponding data for negative AM transfection under static condition. #, $P < 0.05$ in comparison with the corresponding data for negative AM transfection under PS condition.

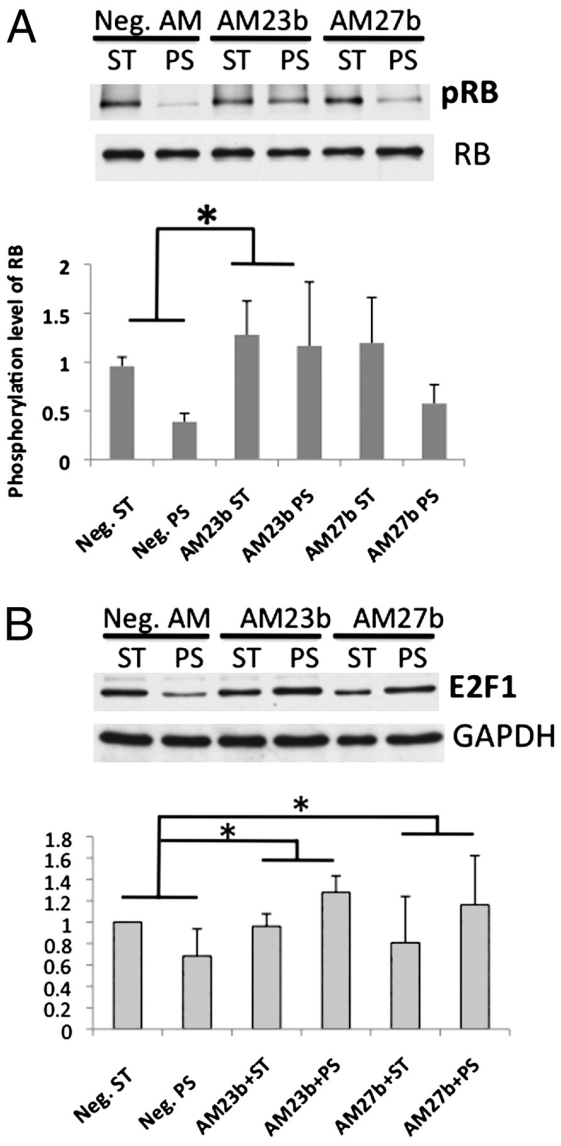

Figure 2.5 Effects of miR-23b and 27b on cell cycle proteins. HUVECs were transfected with Neg. AM, AM23b, and AM27b. Twenty-four-hour posttransfection, cells were then subjected to PS or ST for 24 h. Western blot analysis of cell cycle regulatory proteins, including (A) phosphorylation levels of Rb protein and (B) E2F1 expressions in total cell extracts, were determined with antibodies against phospho-Rb (BD Biosciences), Rb, and E2F1 (Santa Cruz). Blots shown here are representative of three independent experiments. *, $P < 0.05$ in comparison with the corresponding data for neg. AM transfection under ST.

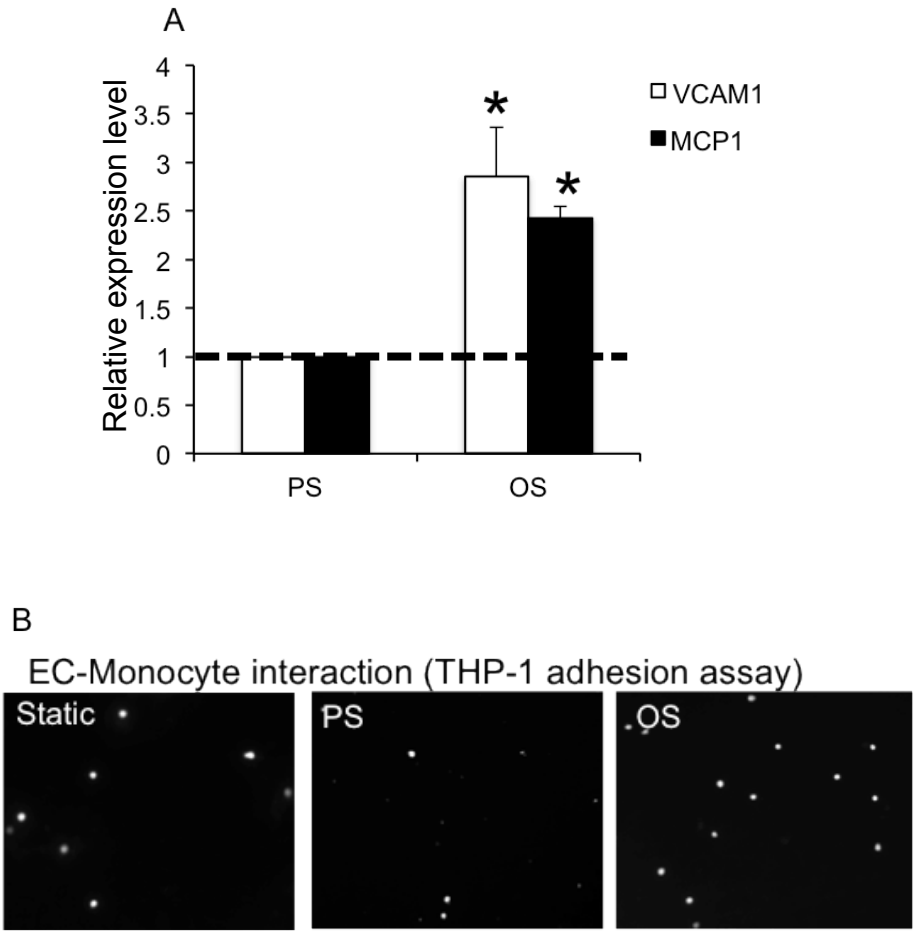

Figure 2.6 Long term OS flow induces pro-inflammatory gene expressions and monocyte adhesion. (A) HUVECs were subjected to 24-h PS or OS, or kept as static control. Total RNA was isolated, and the levels of VCAM1 and MCP1 were quantified by RT-PCR with the result normalized to GAPDH. The data represents mean ± SEM from 3 independent experiments. *P<0.05 vs. PS. (B) HUVECs were exposed to 24-h PS, OS, and static conditions, and then washed thoroughly, followed by overlaying with calcien-AM THP-1 cells for 30 min. Results were representative images of three independent experiments.

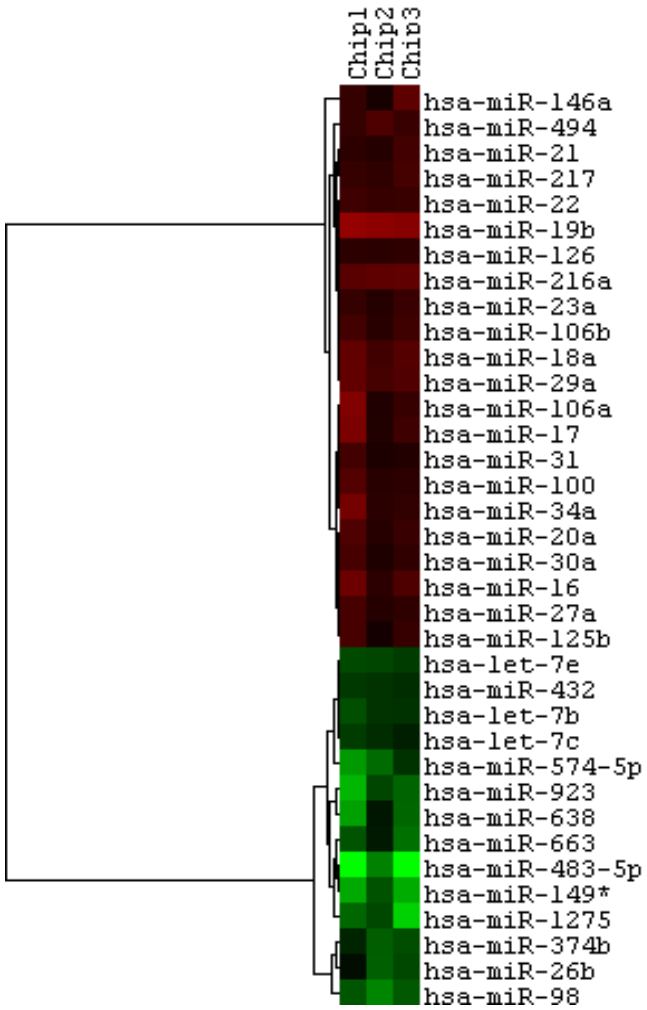

Figure 2.7 miRNA expression profiles under OS vs. PS. Expression levels of 856 human miRNAs (Sanger miRBase 12.0) in ECs under OS and PS were measured with miRNA microarray (n = 3). Heat map shows OS vs. PS miRNA log2 ratios with a threshold of 1.25-fold and $P < 0.05$. Red bands represent upregulated miRNAs and green bands for downregulated miRNAs.

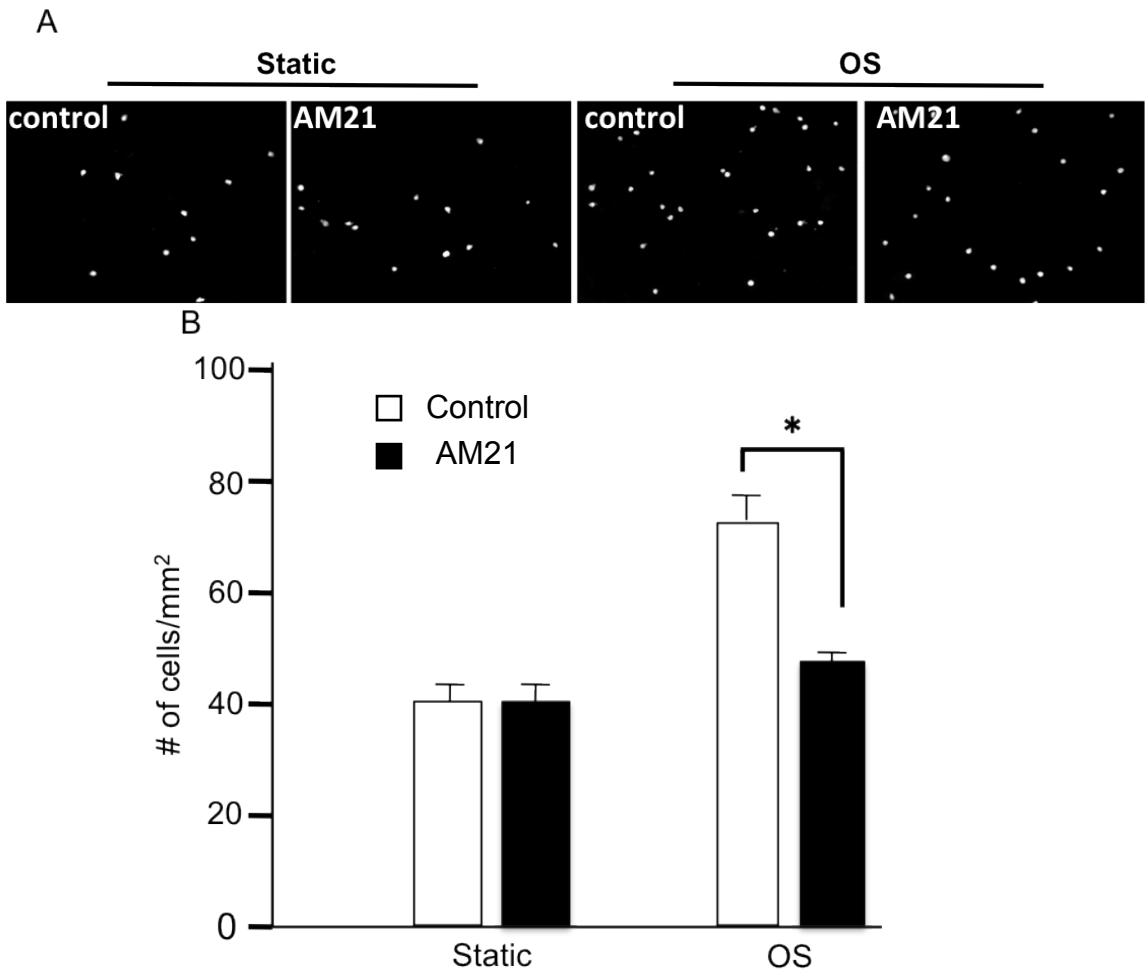

Figure 2.8 OS induction of functional miR-21 leads to inflammatory response in ECs. HUVECs were transfected with AM21 or the control molecule and kept as static controls or exposed to OS for 24 h, followed by incubating with calcien-AM THP-1 cells. (A) Representative images and (B) statistic results of THP-1 adhesion under static (left) or OS (right) conditions. THP-1 cell adherence was quantified by image processing software. The data represent mean ± SEM from 3 independent experiments using 6 fields in each experiment. *P < 0.05 vs. control oligomers.

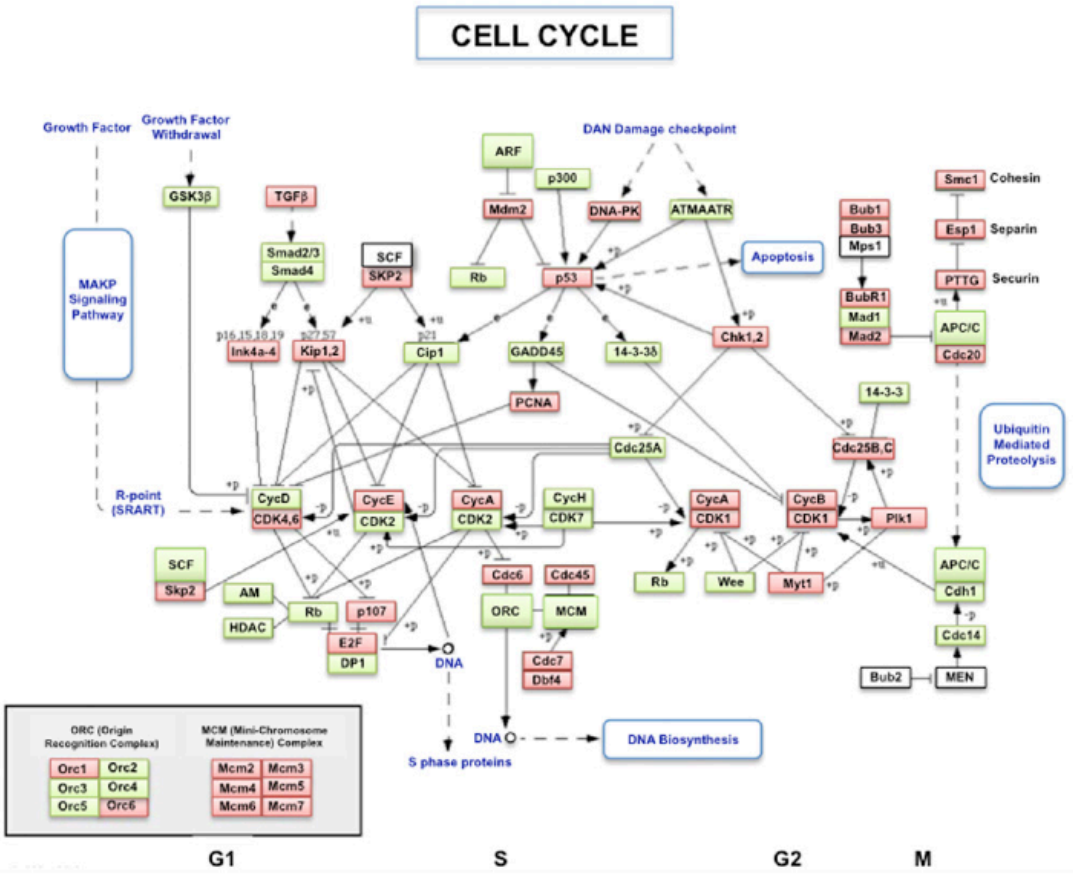

Figure 2.9 Mapping of the differential gene expression to cell cycle network. The cell cycle network was obtained from KEGG pathway database. The boxes represent the components in human cell cycle regulations. The red boxes indicate the corresponding mRNAs were differentially expressed in our PS vs. ST microarray data with the application of a cutoff of 1.5-fold changes. The green boxes represent the known molecules reported in the literature but are not regulated by PS , and open boxes indicate the predicted molecules by the pathway finder.

Table 2.1 Gene ontology analysis of up- and down-regulated genes in PS vs. ST.

GO	Biological Process	Enriched Score	P-value
GO:0007049	Cell cycle	42.17	2.20E-56
GO:0000278	Mitotic cell cycle	42.17	6.20E-43
GO:0051301	Cell division	42.17	1.10E-41
GO:0006260	DNA Replication	12.14	1.10E-10
GO:0000075	Cell cycle check point	11.42	1.00E-08

Only the top five GO terms representing biological process are listed in the tables.

Table 2.2 KEGG pathway analysis of up- and down-regulated genes in PS vs. ST.

	Pathway	Count	P-Value
Up	Glutathione metabolism	9	9.30E-03
Up	Arachidonic acid metabolism	10	2.50E-02
Up	Biosynthesis of steroids	6	3.50E-02
Up	Glycerolipid metabolism	9	3.80E-02
Down	Cell cycle	47	7.10E-22
Down	p53 signaling pathway	20	1.10E-06
Down	Pyrimidine metabolism	20	6.60E-05
Down	Purine metabolism	27	9.40E-05
Down	DNA polymerase	9	4.30E-04

Table 2.3 Validation of selected miRNAs

miRNA	Microarray	TaqMan PCR (FC)
miR-27b	2.3±1.1	2.6±0.4*
miR-23b	1.7±0.4	1.7±0.4*
miR-923	2.2±0.1	2.2±0.2*
miR-16	0.5±0.1	0.8±0.1*
miR-106a	0.6±0.1	0.6±0.1*
miR-19b	0.3±0.1	1.0±0.2
miR-221	0.7±0.1	1.3±0.1
miR-26b	NS	1.1±0.1*
let-7e	NS	1.1±0.1*

*Indicates the PCR result matched microarray data;
NS, not significant.

Table 2.4 Overlapping GO terms between putative miRNA targets and differentially expressed genes.

GO term	Biological Process	P-Value
GO:0000079	regulation of cyclin-dependent protein kinase activity	2.84E-06
GO:0022402	cell cycle process	6.82E-05
GO:0051329	interphase of mitotic cell cycle	0.000109
GO:0007017	microtubule-based process	0.000248
GO:0007001	chromosome organization and biogenesis	0.002711
GO:0043549	regulation of kinase activity	0.006631
GO:0050790	regulation of catalytic activity	0.009684
GO:0007050	cell cycle arrest	0.017707
GO:0007154	cell communication	0.03393
GO:0048839	inner ear development	0.043396
GO:0006865	amino acid transport	0.047237

Table 2.5 Gene ontology analysis of up- and down-regulated genes in OS vs. PS.

GO term	Biological Process	Enriched Score	P-value
GO:0007154	Cell Comunication	6.41	1.90E-08
GO:0007165	Signal Transduction	6.41	1.20E-07
GO:0048513	Organ Development	4.85	1.10E-04
GO:0006928	Cell Motility	4.36	1.00E-04
GO:0050896	Response to Stimulus	3.77	1.80E-02
GO:0006954	Inflammatory Response	3.77	1.00E-03
GO:0007155	Cell Adhesion	3.47	1.60E-03
GO:0001525	Angiogenesis/Blood vessel development	3.38	5.60E-04
GO:0016049	Cell Growth	3.25	1.60E-03
GO:0050817	Coagulation	2.33	3.90E-03

CHAPTER 3 ROLE OF MiR-23b IN THE ANTI-PROLIFERATIVE MECHANISM OF PULSATILE FLOW

3.1 Abstract

My study presented in Chapter 2 has identified that miR-23b plays an important role in the regulation of endothelial cells (ECs) proliferation by pulsatile shear (PS) flow. The studies presented in this Chapter were conducted with the objective to elucidate the underlying mechanism. Temporal expression studies revealed that miR-23b, miR-27b, as well as the host gene aminopeptidase O (APO), were up-regulated concomitantly in ECs under PS, but only miR-23b was shown to participate in the PS-induced EC growth arrest. The loss-of-function study demonstrated that miR-23b reversed the PS-induced retinoblastoma (Rb) hypo-phosphorylation, and that the PS reductions of upstream regulatory proteins (including CDK2, CDK4, and CCNH) by PS is mediated by miR-23b. Further investigation disclosed that PS-induced miR-23b directly suppressed CCNH expression posttranscriptionally, and that overexpression of miR-23b decreased CCNH at mRNA and protein levels and reduced BrdU-incorporation in ECs. The miR-23b-mediated CCNH reduction under PS flow suppressed the integrity and activity of CDK-activating kinase (CAK), which in turn resulted in the inactivation and transcriptional suppression of CDK2 and CDK4. Moreover, while PS flow induced miR-23b/CAK pathway that exerts anti-proliferative function on ECs, oscillatory shear (OS) flow had no significant effect. My findings highlight the anti-proliferative role of miR-23b/CAK pathway under PS and provide new insights to flow modulation of miRNAs in endothelial phenotypes.

3.2 Introduction

Hemodynamic forces play a pivotal role in modulating the physiological and pathological behavior of vascular endothelial cells (ECs) [2]. Pulsatile flow with a high shear stress and a clear forward direction, which exists in the straight part of arterial tree, is associated with quiescent ECs presenting the athero-protective phenotypes [7]. In contrast, the disturbed oscillatory flow without a clear direction, which exists at vascular curvatures and bifurcations, remodels the ECs toward the pro-inflammatory phenotypes and atherogenesis [3]. It is known that multiple physiological and patho-physiological pathways are involved in the mechanotransduction [10], but the feedback regulation between these pathways and posttranscriptional modulation of the signaling molecules remain largely unclear.

MicroRNAs (miRNAs) represent a class of small (~20-25 nucleotides), non-coding RNAs that bind to 3'-UTR of its target mRNAs and thereby destabilizes the transcripts or suppresses the translation [44, 45]. Recent studies indicate the pivotal role of miRNAs in vascular biology [46, 48, 78]. Emerging evidence suggests that mechanical stimuli modulate miRNA signatures, which contribute to vascular remodeling and development [62, 68, 69, 71]. By undertaking a comprehensive miRNA expression profiling analysis in vascular endothelial cells, we and others have shown that a series of miRNAs are differentially expressed both *in vitro* and *in vivo*, in response to different patterns of flow [59, 61, 65, 102, 103]. These studies with differences in the design of flow system and microarray platform indicate that post-transcriptional controls of gene expressions and signaling by miRNAs constitute a novel mechanism in mechanotranduction. Further functional dissection of miRNA target networks revealed that the up-regulations of miR-23b and 19a, which suppress EC proliferation [59, 65], and the down-regulation of miR-92a, which inhibits the anti-proliferative and anti-

inflammatory transcription factor KLF-2, synergistically confer the athero-protective effect of pulsatile shear stress (PS) [57, 66]. Conversely, the pro-inflammatory response of ECs induced by oscillatory shear stress (OS) can be attributed, at least in part, to miR-21 and miR-663 [33, 60, 64]. In addition, a higher expression of miR-10a and a lower expression of miR-92a are also found at the descending thoracic aorta [67, 102], in comparison to the internal curvature of aortic arch, suggesting these miRNAs are potentially regulated by the different flow patterns in the athero-protective and athero-prone regions.

Several recent studies, including ours, have shown the important roles of miR-23b in cell growth [59, 104], TGFb/BMP signaling [105], angiogenesis [55, 106], stem cell differentiation [107], tumorigenesis and metastasis [108]. More than twenty putative targets of miR-23b have been reported; and these have been confirmed in a variety of contexts by the paring of the seed sequence and mRNA 3' UTRs using luciferase reporter assay. For instance, Zhou at el. [106] demonstrated the pro-angiogenic role of miR-23b by targeting sprouty2; Zhang at el. [104] reported that miR-23b represses cancer cell proliferation and migration by regulating a cohort of pro-metastatic genes. I previously reported that inhibition of miR-23b reversed the PS-reduced E2F1 and Rb hypo-phosphorylation, and attenuated PS-induced EC growth arrest [59]. The significant functions of miR-23b in vascular biology motivated me to further investigate the underlying molecular mechanism.

Herein, I describe that the PS-induced miR-23b modulates cell cycle regulatory networks through the repression of cyclin H (CCNH) at posttranscriptional level. Importantly, down-regulation of CCNH impairs the integrity and activity of CDK-activating kinase (CAK) to deactivate CDK2, CDK4, and RNA Polymerase II (Pol II) and hence the transcriptional attenuation observed in PS-induced EC growth arrest. Moreover, PS and

OS flows differentially regulate miR-23b/CAK pathway and EC proliferation.

3.3 Materials and Methods

3.3.1 Cell culture and shear experiment

See section 2.3.1 and 2.3.2

3.3.2 RT-PCR

Total RNA was isolated using the mirVANA miRNA isolation kit with a manufacturer-suggested protocol (Ambion, Austin, TX). The concentration and quality of RNA were checked by Nanodrop spectrophotometer (Thermo). Reverse transcription of mRNA was carried out with 1 μg of total RNA using the MLV reverse transcriptase (Invitrogen) and oligo-dT primer, with incubation at 42°C for 1 h. The synthesized cDNA was used to perform real-time quantitative PCR (RT-PCR) with the iQ SYBR Green supermix (Bio-Rad) on the iCycler real-time PCR detection system (Bio-Rad). Reverse transcription of miRNA was carried out with miRNA-specfic RT primer, and the quantification was performed with TaqMan miRNA assay.

3.3.3 Immunoprecipitation and Kinase assay

For immunoprecipitation, 100 μg of lysate was incubated with 2 μg of CCNH antibody overnight at 4°C. Protein A/G-agarose was added for 1 h. The immunoprecipitated complexes were wash three times in RIPA buffer, and once in kinase buffer, and then assayed for CAK kinase activity on the substrate GST-CTD with ATP in kinase buffer. After 1h reaction at 30°C, the kinase assay samples were subjected to immunoblot analysis as previously described in section 2.3.8.

3.3.4 NOx bioavailability assay

The NO production from cells was detected as the accumulated nitrite (NO^{2-}) in perfusion media by using the Griess reagent (Sigma). An aliquot of cell culture media was mixed with an equal volume of Griess reagent and then incubated at room

temperature for 15 min. The azo dye production was analyzed by using a spectrophotometer at an absorbance setting at 540 nm.

3.3.5 Reporter construction and luciferase assay

To generate reporter vectors bearing the miR-23b binding site, the wild-type and mutated 3'UTR sequences of CCNH mRNA were synthesized and cloned into the pMir-Report luciferase vector (Ambion) according to the manufacturer's instruction. For luciferase assay, HUVECs were transfected with CCNH 3'UTR wt or CCNH 3'UTR mt, together with the precursor miR-23b (miR-23b) or control molecule, by using AMAXA Nucleofector™ (Lonza). The CMV-driven β-gal expressing vector was co-transfected as a normalizer. 48-h post-transfection, cell lysates were collected, and the luciferase activity was measured with the Dual-Glo Luciferase Assay System (Promega).

3.3.6 Chromatin Immuno-precipitation (ChIP) and RNA Immuno-precipitation

Chromatin was harvested from ~$1.5x10^6$ of HUVECs after shearing or being kept under static condition, as well as untreated controls. The cells were then crosslinked with 1% formaldehyde (Sigma) for 10 min at room temperature with rocking. The crosslinking procedure was quenched with the addition of 0.125M glycine for 10 min at room temperature followed by four washes with ice-cold PBS. The cells were collected and centrifuged at 700 x *g* for 8 min at 4°C, after which the pellet was snap-frozen in liquid nitrogen and stored at -80°C until further use. The frozen cell pellets were thawed on ice and resuspended in lysis buffer (1% NP-40, 1M KOH, pH 7.9, 85 mM KCl, 1 mM EDTA, pH 8.0) with protease inhibitors (Roche Complete, EDTA-free Protease Inhibitor Cocktail Tablets) and 1 mM PMSF on ice for 10 min. After centrifugation, nuclear pellets were resuspended in a nuclear lysis buffer (50 mM Tris/HCl, pH 7.4, 1% SDS, 0.5% Empigen BB (Sigma), 10 mM EDTA, pH 8.0) with protease inhibitors and 1 mM PMSF. The DNA was subjected to 10-sec sonication pulses on ice at a power setting of 13 W (out of 20)

on a 60 Sonic Dismembranator (Fisher Scientific, Pittsburgh, PA). The lysates were cleared by centrifugation (16,000 x *g*; 5 min at 4°C). Aliquot chromatin was incubated overnight with Pol II phospho-serine 5 antibody (H14), Pol II antibody (8WG16), or isotype control, and then pulled down with anti-IgM IgG-conjugated protein A/G agarose beads, pre-blocked with salmon sperm DNA. The cross-linking of immune-precipitated complex was reversed overnight, and proteins were digested with proteinase K treatment. Input DNA and DNA associated with specific immunoprecipitates or with negative control were purified (QIAquick PCR Purification Kit, Qiagen, Valencia, CA), and 2-4 mL were used as a template for qPCR to amplify promoter regions of various genes.

For RNA immune-precipitation (RIP), HUVECs subjected to different flow patterns were lysed in polysome lysis buffer. After centrifugation, supernatant was collected and subjected to immuno-precipitation as previously described with the antibody against AGO family proteins overnight. The pull-down mRNAs and miRNAs in miRISC complex were recovered with mirVana miRNA isolation kit (Ambion, Austin, TX) and subjected to qPCR analysis.

3.3.7 Statistical Analysis

Results are expressed as means ± SEM. Statistical analysis was performed by using an independent Student t test for two groups of data and analysis of variance (ANOVA), followed by Tukey's post-hoc test for multiple comparisons. A P value of <0.05 was considered significant.

3.4 Results

3.4.1 miR-23b participates in PS-induced EC growth arrest.

We and others have previously shown that PS and OS flows differentially regulate EC gene expressions and functional outcomes, such as cell cycle regulation

and pro-/anti-inflammatory responses, through the modulations of miRNAs [59, 64]. Among those miRNAs, the emerging roles of miR-23b cluster containing miR-23b, miR-27b, and miR-24-1 in cardiovascular biology led us to further investigate miR-23b-mediated regulation in mechanotransduction [55]. Human miR-23b, along with miR-27b, and miR-24-1, are located in the intron of c9orf3 gene on chromosome 9 (figure 3.1A). C9orf3 gene encodes aminopeptidase O (APO, a metalloprotease), and a recent study suggests human APO plays a role in the renin-angiotensin pathway through its activity in cleaving angiotensin III to angiotensin IV [109].

To explore the temporal expression profiles of the miR-23b cluster and its host gene in ECs in response to shear stress, we applied PS flow at 12 dyne/cm^2 to cultured HUVECs for various durations. RT-PCR studies revealed that PS increased expressions of both pri-miR-23b and miR-23b over 24 h, with the pri-miR-23b level peaking at 12 h and the mature miR-23b level being sustained at 24 h (figure 3.1B). Concomitant with the increase in miR-23b level, PS also augmented its host gene APO expression over 24 h, as well as the miR-27b expression (figure 3.2). Whether miR-23b cluster and its host gene APO regulated by PS flow cooperate to regulate EC functions deserve further investigation. To study the temporal effect of PS on EC proliferation, we performed the BrdU-incorporation assay with ECs subjected to various durations of PS. As shown in figure 3.3, PS transiently increased the number of BrdU-positive cells over the static control at 4 h, but led the ECs into a quiescent state later (12 and 24 h). To investigate the roles of miR-23b and APO in EC proliferation, we transfected ECs with either antagomiR-23b (AM23b) or APO siRNA (siAPO) to knockdown the levels of miR-23b and APO, respectively. Successful decreases of miR-23b and APO expression levels were verified by RT-PCR (figure 3.4A). Such perturbations of miR-23b and APO did not alter the expression of each other. As reported in Chapter 2 and the present Chapter,

the inhibition of miR-23b attenuated the PS-induced EC growth arrest. Notably, APO knockdown increased the number of BrdU-positive cells under static condition, but did not reverse the PS reduction of proliferating cells (figure 3.4B). These findings indicate that although PS flow induces concomitant changes of miR-23b, APO, and miR-27b (presented in Chapter 2), only miR-23b plays an important role in the anti-proliferative function of PS flow.

Because APO has been shown to cleave angiotensin III to generate the less active angiotensin IV and the consequential eNOS regulation, we further tested the role of the flow-induced APO on eNOS expression and nitric oxide production in ECs by using the siAPO. Western blot analysis (figure 3.5A) showed that APO-knockdown elevated the eNOS expression under both static and PS condition. NOx bioavailability assay (figure 3.5B) also indicated that the nitrite/nitrate concentration with APO knockdown in ECs was significantly higher than the control group. Since eNOS and NOx play important roles in regulating vascular homeostasis, our results suggest that both miR-23b and its host gene, APO, contribute to endothelial function under PS flow.

3.4.2 Involvement of β1 integrin in PS-induction of miR-23b and APO.

To investigate whether β1 integrin serves as a mechano-sensor for PS-induced miR-23b and APO expressions, ECs were transfected with β1 integrin siRNA (siβ1) or scramble control (Ctrl) and subjected to 4-h PS. The activation of β1 integrin was examined by western blot analysis using the antibodies against the ligand-induced binding site (LIBS) of β1 integrin (2079Z), and expressions of miR-23b and APO were examined with the RT-PCR analysis. As shown in figure 3.6A, 4-h PS induced EC β1 integrin activation, which was blocked by knocking down β1 integrin. RT-PCR analyses (figure 3.6B&C) indicated that the inductions of pri-miR-23b and APO by 4-h PS were inhibited by β1 knockdown. These results suggest that on collagen-I coating surface, the

PS-induction of miR-23b and APO expression in ECs is mediated through β1 integrin. The downstream signaling pathways and transcriptional factors leading to miR-23b and APO induction are under investigation.

3.4.3 PS-Induced miR-23b modulates the expressions and activities of cell cycle regulatory proteins.

In Chapter 2, I have identified that miR-23b serves as an important modulator of the EC growth arrest induced by PS flow. In the present study I further investigated the role of miR-23b in modulating cell cycle regulatory protein expressions in ECs. ECs were subjected to PS flow for various durations, or kept under static condition for 24 h as controls (ST). Western blot analysis (figure 3.7A) showed that exposure of ECs to PS for 24 h resulted in down-regulations of CCNA, CCNE, CDC2, CDK2, and CDK4, and up-regulations of the CDK inhibitor p27 (CDKN1B) and the hypo-phosphorylated state of Rb protein, compared with the static control. The temporal changes of these G1/S-related cyclins and CDKs agreed with the BrdU-incorporation assay. In comparison to the control group, transfecting ECs with AM-23b not only attenuated the PS-induced EC growth arrest, but also partially reversed the expressions of cell cycle regulatory proteins, including CDK2 and CDK4, which in turn hyper-phosphorylate Rb and lead ECs into the synthetic phase of cell cycle (figure 3.7B&C). The phosphorylation status of Thr160 on CDK2 and Thr172 on CDK4, which–represent the activities of these two CDKs, induced by PS is reversed by the AM23b transfection in ECs. The effect of AM23b on CDK2 and CDK4 was confirmed at the mRNA level with RT-PCR. In contrast, AM23b had no significant effects on other cell cycle regulators (CCNA, CCND1, CCNE, CDC2, and p27). To elucidate the molecular mechanism of miR-23b in the PS-induced growth arrest, I further explored the putative targets of miR-23b predicted by Pictar and TargetScan [89, 90]. However, based on the miRNA target prediction, neither CDK2 nor

CDK4 mRNAs contain miR-23b binding sequence in the 3'UTR. Since AM23b transfection reversed phosphorylation on Thr residues of CDK2 and CDK4, we further examined the potential miR-23b targets among the regulatory proteins of CDKs and found the miR-23b binding sequence in the 3'UTR of CCNH mRNA, which is highly conserved among the human, chimpanzee, mouse, rat, and dog CCNH 3'UTR (figure 3.8A). CCNH forms the CDK-activating kinase complex (CAK) with CDK7, and CAK phosphorylates the Thr residues on CDC2, CDK2, and CDK4. This information provides a strong rationale to test our hypothesis whether CCNH is a functional target of miR-23b in flow-induced EC growth arrest. Transfecting AM23b in ECs inhibited the PS-induced down-regulation of CCNH, but had no effect on CDK7 (figure 3.8B&C) at both mRNA and protein levels. These results suggest that PS flow causes EC growth arrest and modulates cell cycle regulatory proteins partially through the interplay of miR-23b and CAK.

3.4.4 CCNH is a direct target of miR-23b in EC under PS.

To determine whether CCNH is a direct target of miR-23b in ECs, we constructed pMIR-REPORTs containing the luciferase cDNA fused to either the wild type 3'UTR of CCNH mRNA (CCNH 3'UTR wt) or the mutant sequence (CCNH 3'UTR mt) and tested their luciferase activities in ECs. As shown in figure 3.9, in the presence of CCNH 3'UTR wt, PM-23b (precursor miR-23b) transfection repressed the luciferase activity to 0.64 ± 0.08 fold; the repression was diminished by introducing the mutation of miR-23b binding site into the CCNH 3'UTR (0.94 ± 0.12 fold), compared to the control group with empty vector transfection. Subsequently, ECs transfected with CCNH 3'UTR wt and CCNH 3'UTR mt were subjected to 24-h PS. In comparison with the ST condition, PS reduced the reporter activity of CCNH 3'UTR wt but did not have significant effect on the mutant. To further verify the association of miR-23b and CCNH mRNA in the miRISC complex, I

performed RNA immunoprecipitation (RIP) [110], using the anti-pan-argonaute (AGO) antibody, in cell lysates from PS and ST. The miR-23b and CCNH transcripts determined by using RT-PCR after RIP were normalized to the values of inputs and IgG control. The increases of miR-23b and CCNH mRNAs in miRISC were observed under PS in comparison to ST (figure 3.10A), indicating that PS flow induced the association of CCNH and miR-23b in miRISC and that CCNH modulation by PS is mediated, at least partially, through a miRNA-dependent mechanism. In addition, overexpression of miR-23b with PM23b in ECs decreased CCNH expression, at both mRNA and protein levels (figure 3.10 B&C). Overall, these data provided experimental evidence that the PS-induced miR-23b regulates CCNH expression by destabilizing its mRNA. To determine how miR-23b overexpression and CCNH knockdown affect cell cycle progression, we further performed the cell cycle / BrdU-incorporation assay. Flow cytometry analyses showed that miR-23b overexpression reduced the number of BrdU-positive cells, but CCNH knockdown had no significant effect on the EC proliferation (figure 3.10E).

3.4.5 PS-induced miR-23b modulates basal transcription by targeting CAK.

In addition to regulating the activities of CDKs, the CAK complex, as a component of the transcription factor II H (TFIIH), participates in basal transcriptional by phosphorylating the C-terminal domain (CTD) of RNA polymerase II (Pol II)[111, 112]. Pol II CTD consists of 52 repeats of the highly conserved sequence Tyr-Ser-Pro-Thr-Ser-Pro-Ser, and the Ser residues at position 2, 5, and 7 are targets for phosphorylation. The phosphorylation of Ser5 by CCNH-CDK7 complex is believed to regulate the transcription initiation and RNA splicing; the phosphorylation of Ser2 by CDK8/CDK9 is known to participate in the elongation, and the role of phosphorylation of Ser7 is unclear [113, 114]. To examine whether the CAK-Pol II activity is regulated by PS flow through miR-23b, we first investigated the effects of PS on the expressions of CCNH, CDK7, and

Pol II, and the phosphorylation of Pol II CTD over 24 h. Western blot analyses (figure 3.11A) indicated that PS flow induced transient increases (1 and 4 h) of phosphorylation at Ser2 residue and maintained basal phosphorylation level at Ser5, compared to static control. Prolonged PS flow up to 24 h abolished the phosphorylations of both Ser2 and Ser5 of CTD, and also decreased the expressions of Pol II, CCNH, and CDK7 in comparison with the static control at 24 h. In ECs kept under static condition for 24 h, the phosphorylation of CTD decreased significantly at Ser2, but was maintained at Ser5, suggesting that the CAK phosphorylation at the Ser5 is mainly regulated by PS flow, whereas the phosphorylating Ser2 may involve factors other than PS. To confirm the PS effect on CTD phosphorylation, we performed immunofluorescence staining with the antibody recognizing the phospho-Ser5, and the results agreed with the western blot analyses (figure 3.11B).

To investigate whether miR-23b can modulate the CAK activity and the phosphorylations of Pol II CTD in response PS, ECs were transfected with either AM23b or scramble control and then subjected to 24 h PS flow or kept as ST. As shown in figure 3.12A, AM23b transfection attenuated the PS-induced de-phosphorylation of Pol II CTD at Ser5 but had no significant effects on Ser2, and AM23 transfection reversed the PS-reduction of Pol II level. To confirm that miR-23b contributes to the CCNH down-regulation and consequent CAK activity, we co-immunoprecipitated the CAK complexes from AM23b- and scramble control-transfected cells in both ST and PS conditions. The result demonstrated that AM23b transfection not only reversed the expression of CCNH, but also restored the integrity of CAK complex (figure 3.12B). We further measured the kinase activity using a purified GST-CTD fusion substrate, and the result indicated that the PS-reduced CAK activity was restored by the transfection of AM23b. In addition, immunostaining (figure 3.12C) showed that AM23b transfection increased Ser5

phosphorylation in both the nuclei and peri-nuclear region under PS flow. Overall, these results indicate that PS flow modulates the CCNH expression and hence the CAK activity through the induction of miR-23b.

To investigate whether the altered transcription controls of the cell cycle regulatory proteins (CDC2, CDK2, and CDK4) in AM23b-transfected ECs under PS correlate with the phospho-CTD/Pol II occupancy, I performed chromatin-immunoprecipitation (ChIP) experiments using H14 and 8WG16 antibodies against phospho-CTD (Ser5) and total Pol II, respectively. The immunocomplexes were further analyzed using RT-PCR with primers specific to the proximal regions of transcription start sites (TSS) of CDC2, CDK2, and CDK4. PS significantly decreased both the phospho-Ser5 and total Pol II occupancy in the TSS of these selected genes (figures 3.13A and B), consistent with the reductions in mRNA levels and the global decreases of phospho-Ser5 and Pol II levels. As expected, AM23b transfection attenuated the reductions of phopho-Ser5 occupancy in the TSS of these genes, but had no significant effects on the total Pol II binding. Notably, the mRNA level of CDC2 was not affected by AM23b transfection even though the phospho-Ser5 binding in the TSS was enhanced, indicating that the increase of initiation complex may not be sufficient to progress through the following transcription events.

3.4.6 Differential regulation of miR-23b by flow patterns.

PS and OS flows differentially regulate EC gene expression and functions. To investigate whether the miR-23b expression can be differentially regulated by flow patterns, we compared the miR-23b levels in ECs subjected to PS and OS flows. As shown in figure 3.14A, RT-PCR analysis showed that PS, but not OS, significantly increased the miR-23b expression level in comparison with the static condition. To confirm this result, we further performed the fluorescence in situ hybridization (FISH)

with miR-23b-LNA probe in ECs under PS and OS conditions (figure 3.14B). Consistent with the increase in miR-23b level (figure 3.14A), the intensity of miR-23b staining under PS flow was much stronger than OS condition (figure 3.14B). In addition, the miR-23b staining under PS was localized in both the nuclei and peri-nuclear region, while miR-23b under OS was primarily in the peri-nuclear region. Since mature miRNAs regulate gene expression in the cytoplasm, the positive staining of miR-23b in nuclei might be the staining of pri-miR-23b and pre-miR-23b. These results suggest that the miR-23b transcription under PS is more active than OS. To further test the flow regulation of miR-23b/CAK pathway, we compared the phosphorylation of Pol II CTD and the expression levels of CAK components. Western analysis showed (figure 3.14C) that PS and OS flows had opposite actions on the activity and expression of CAK. The differential regulations of CAK under PS and OS may further modulate the EC proliferation. By BrdU-incorporation assay (figure 3.14D), PS flow significantly reduced the number of BrdU-positive cells in comparison with OS flow. These findings suggest that PS flow resulted in strong anti-proliferative effect on ECs through the interplay of miR-23b/CAK pathway.

3.5 Discussion

Our previous findings [59] showed that miR-23b knockdown reversed the PS-induced hypo-phosphorylation of Rb, and attenuated the anti-proliferative response to PS flow. In the present study, I have elucidated the mechanisms that the PS induction of miR-23b is through β1 integrin activation, and that miR-23b mediates the anti-proliferative effect of PS by repressing the CAK complex. As summarized in figure 3.15, the inhibitory effect of flow-induced miR-23b on CAK not only reduces CDK2 and CDK4 activities, but also decreases the basal transcriptions by keeping the Pol II-CTD (Ser5) in a hyper-phosphorylated state, which synergistically repressing the cell cycle

progression. I have further demonstrated that miR-23b/CAK pathway is highly responsive to flow patterns and is accompanied by inverse changes in endothelial proliferation *in vitro*.

There is increasing evidence that the miR-23b cluster plays an important role in cardiovascular biology, stem cell differentiation, and cancer [55, 104, 107]. The human miRNA-23b cluster, located in chromosome 9q22.32, contains miR-23b, miR-27b, and miR-24-1. It has been reported that pri-miR-23b, pri-miR-27b and pri-miR-24-1 are transcribed independently and that mature miR-23b, miR-27b, miR-24-1 are released from the corresponding primary transcripts in mice [95]. In HUVECs, there is similarity in the temporal expressions of pri-miR-23b and pri-miR-27b (figures 3.1B and 3.2), as well as the responses of the mature forms to PS are similar, suggesting the co-transcription of miR-23b and miR-27b under the same promoter in response to flow. My findings demonstrate that both miR-23b and miR-27b are regulated by PS, but miR-24-1 is not, indicating that miR-24-1 transcription does not play a role in PS regulation of EC functions. In addition to miR-23b and miR-27b, my current study provides the evidence that the host gene APO, which is highly conserved in vertebrates, is also induced by PS flow. Previous study reported that both the mmu-miR-23b cluster and mouse APO are expressed predominantly in blood vessels and highly vascularized tissues in mice [106], implicating their potential roles in vascular biology. Moreover, it has been reported that APO possesses the ability to modulate vasoactive peptides (Angiotensin III to Angiotensin IV) *in vitro* [109]. Indeed, I found that the expression of APO in response to PS contributes to the eNOS expression and bioavailable NO production (figure 3.5). Therefore, both miR-23b and its host gene APO may contribute to the vascular homeostasis in response to flow, which represents an example of functional cooperation between miRNAs and their host genes. It remains to be further investigated whether

APO participates in the renin-angiotensin system in hemodynamic regulation, and how APO interacts with its residential miRNAs in vascular homeostasis.

Integrins serve as fundamental mechano-sensors that transduce extracellular physical stimuli to intracellular biochemical signaling, thus leading to functional gene expression [24, 27], but the involvement of integrin activation in miRNA expression remains unknown. It has been reported that flow primarily induces α2β1 activation in ECs on collagen-I surface, and α5β1 and αvβ3 activation on fibronectin surface. Integrin activation controls the expression of key cell cycle proteins, including CCND1 and CDK inhibitors [115], but the mechanism mediating this process is not well understood. In the present study (figure 3.6), I observed that PS flow-activation of β1 integrin contributes to miR-23b and APO inductions in ECs on collagen-I coated slide, suggesting the role of β1 integrin in the PS-regulation of miR-23b-mediated EC growth arrest in this system. The signaling pathways and transcription factors involved in PS-induced β1 activation deserve further investigation.

Recently, several studies including ours investigated the role of miR-23b in cell growth and these results point to miR-23b as a key regulator of cell functions in both physiological and patho-physiological states and may be a potential therapeutic target in diseases. To understand the mechanism underlying the miR-23b-mediated hemodynamic regulation of vascular cell functions, I first examined the expression of cell cycle regulatory proteins under PS. Inhibition of miR-23b reversed the PS-reductions of CDK2 and CDK4 expressions and phosphorylations. The lack of miR-23b binding site in the 3'UTR of these mRNAs suggests that miR-23b regulation of these CDKs might be beyond the post-transcriptional stage. CAK (CCNH-CDK7) complex possesses dual capabilities of modulating basal transcription and phosphorylating the T-loop of CDKs that controls cell cycle progression [116]. My data demonstrated that AM-23b

transfection reversed the PS reduction of CCNH, but had no effect on the PS reduction of CDK7. These findings suggesting miR-23b induced by PS flow impairs the CAK integrity through repressing CCNH expression, and hence the phosphorylations of CDK2 and CDK4.

The following findings in my study indicate that CCNH is a direct target of miR-23b in HUVECs: (1) the complementary seed sequence of miR-23b is identified in the 3'UTR of CCNH mRNA, (2) the increased association of miR-23b and CCNH mRNA in miRISC under PS, and (3) the decrease of CCNH 3'UTR-luciferase reporter activity by miR-23b overexpression, and the abolition of this effect by mutation of the miR-23b seed binding site. The role of PS-induced miR-23b expression in EC proliferation and CCNH expression is further verified by the findings: 1) Inhibition of miR-23b reversed PS-reduction of CCNH and attenuated EC growth arrest under PS flow, 2) Overexpression of miR-23b with its specific synthetic precursor (PM23b) decreased CCNH expression and reduced the number of BrdU-positive cells. However, knocking down CCNH by itself did not affect EC proliferation significantly, similar to the report by Patel et al [117]. Therefore, the PS-induced miR-23b probably targets multiple components that synergistically suppress EC proliferation, and that repressing CCNH expression alone is not sufficient to arrest cell growth. Another possibility is the degree of CCNH reduction (~40%) by siCCNH in this study is not sufficient to inhibit cell cycle progression.

As mentioned above, CCNH is critical for maintaining the integrity and activity of CAK complex. In addition to CDK regulation, CAK activity is known to modulate the initiation event of transcription through phosphorylating Ser5 residue of Pol II CTD. A recent study has demonstrated that 6-h laminar shear in ECs increases the phosphorylation and recruitment of Pol II to eNOS gene [118]. In agreement with this finding, my present study shows that short-term PS (1 and 4 h) increases Pol II CTD

phosphorylation at Ser2 but not Ser5. The prolonged PS (12 and 24 h), however, causes a reduction in the phosphorylation of both Ser2 and Ser5 residues, in concert with the down-regulation of CAK components (CCNH and CDK7) after 24-h PS in ECs. Most importantly, miR-23b inhibition abolishes the PS-reduced EC CCNH expression and restores phosphorylation level at Ser5 residue of Pol II CTD, validating that PS regulation of CAK activity is mediated by miR-23b. It has also been reported that a global decrease of phosphorylation of Pol II CTD diminishes the capping efficiency, as well as the polyadenylation of mRNA [119]. PS causes the induction of miR-23b and a global reduction of Pol II phosphorylation may synergistically regulate mRNA stability. The reversal of CAK activity by the inhibition of miR-23b under PS is further supported by the finding that AM-23b transfection causes the positioning of phospho-CTD II (Ser5) in the transcription start sites of CDK2 and CDK4, consequently resulting in the expressions of these CDKs. These findings strongly support that concept that the decreased levels of CDK2/4 and Pol II Ser5 phosphorylation resulting from PS could be the result of a direct inhibition of CCNH by miR-23b. In this respect, the PS-induced miR-23b exerts the anti-proliferative effects on ECs through both inactivation and the transcriptional suppression of cell cycle regulatory proteins. However, I cannot rule out the possibility that CDK inhibitors, CTD phosphatases, as well as other miRNAs participate in the regulation of cell cycle progression and transcriptional control.

Earlier studies with culture ECs in flow chamber showed that PS flow caused ECs to be in a quiescent state, whereas disturbed flow patterns increased EC turnover in compared with PS and laminar flow [32-34, 41]. In agreement with these observations, my results in this Chapter demonstrate that PS flow causes significantly less BrdU-incorporation in ECs than OS flow does. In addition, miR-23b/CAK pathway is strongly induced by PS flow but maintained as basal levels by OS flow. These *in vitro* findings

suggest PS and OS cause differential effects on miR-23b expression that acts through CAK pathway to cause opposite changes in EC proliferation. It is known that EC turnover in athero-protective regions of arterial tree is much lower than that in the athero-prone regions. Hence, the miR-23b induction by PS flow and the resulting regulation through CAK pathway may contribute to the quiescent EC phenotype and counteract the risk factors associated with atherosclerosis. The differential regulations of miR-23b/CAK pathway and EC proliferation by disturbed vs. laminar flow was examined in rat carotid arteries with/without flow disturbance and presented in Chapter 4.

In summary, my findings in this Chapter demonstrate a novel mechanism by which PS-induced miR-23b exerts an anti-proliferative effect on ECs via the CAK/Pol II pathway to decrease cell cycle progression and basal transcription. Elucidation of the molecular basis of underlying the differential effects between PS and OS flows in the modulation of miR-23b/CAK pathway and EC proliferation may provide new insights into the role of miRNAs in vascular homeostasis and pathogenesis.

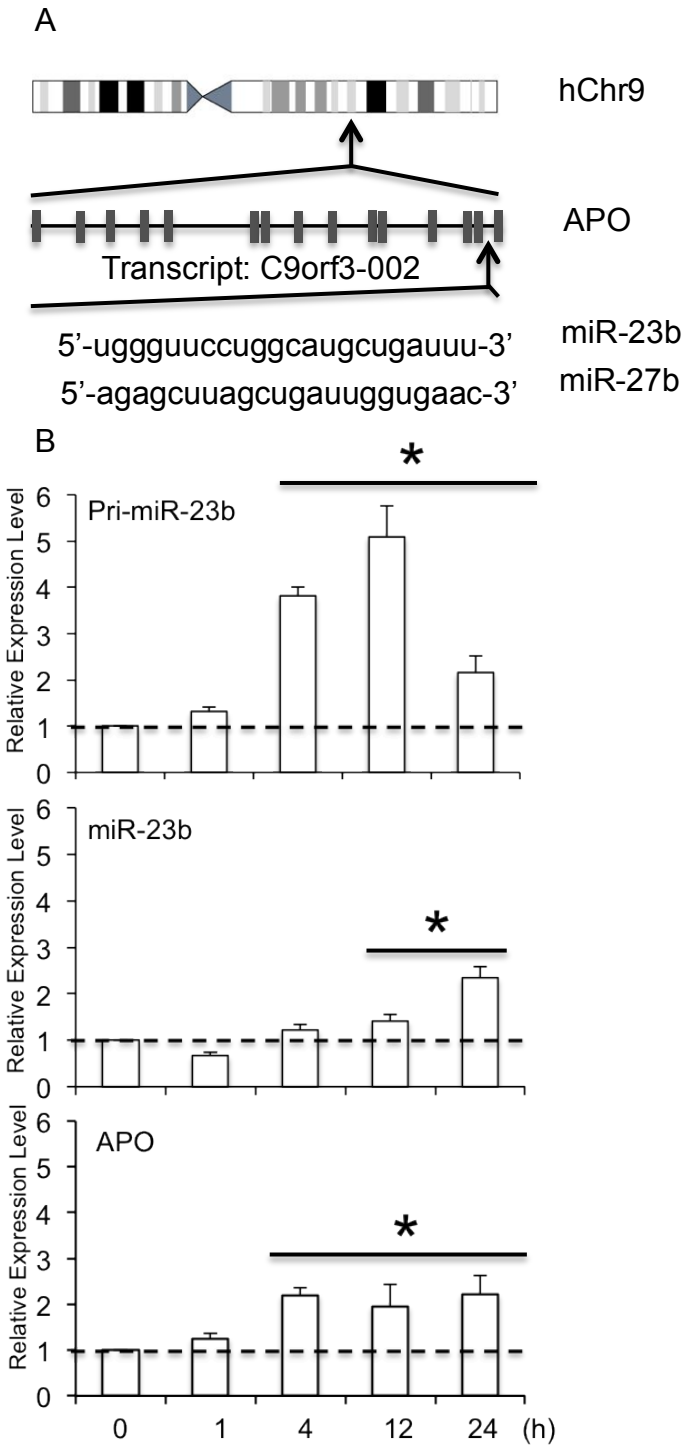

Figure 3.1 Prolonged PS flow induces the expressions of miR-23b and APO. (A) Gene structure of human miR-23b cluster and its host gene. (B) Expressions of pri-miR-23b, miR-23b, and APO in HUVECs subjected to PS flow for 1hr, 4hr, 12hr, 24hr, and static control (0hr). Data are shown as mean ± SEM from three independent experiments. *P < 0.05 vs. static control.

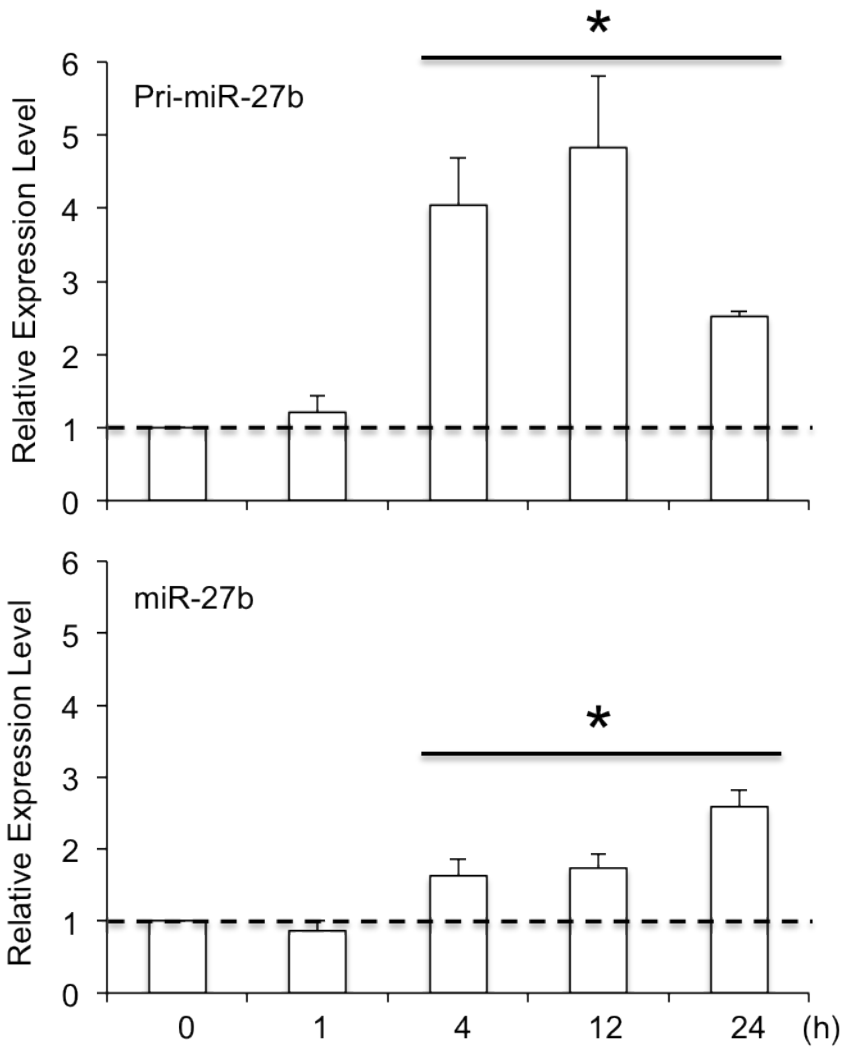

Figure 3.2 Prolonged PS flow induces the expressions of miR-27b. Expressions of pri-miR-27b (upper panel) and miR-27b (lower panel) in HUVECs subjected to PS flow for 1hr, 4hr, 12hr, 24hr, and static control (0hr). Data are shown as mean ± SEM from three independent experiments. *P < 0.05 vs. static control.

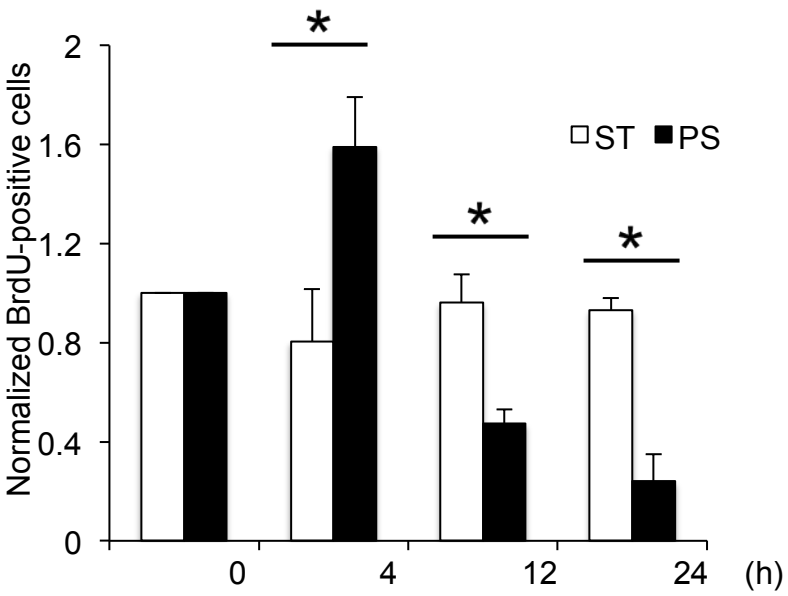

Figure 3.3 Prolonged, but not short-term, PS flow significantly reduces cell proliferation in HUVECs (BrdU-incorporation assay). Cells were subjected to PS flow or kept as static condition (ST) for 0hr, 4hr, 12hr, and 24hr, with BrdU added into the media during the last 4 hr of the periods. Cells were fixed and stained with anti-BrdU and subjected to flow cytometry analysis. Data are shown as mean ± SEM from three independent experiments. *P < 0.05 vs. static control.

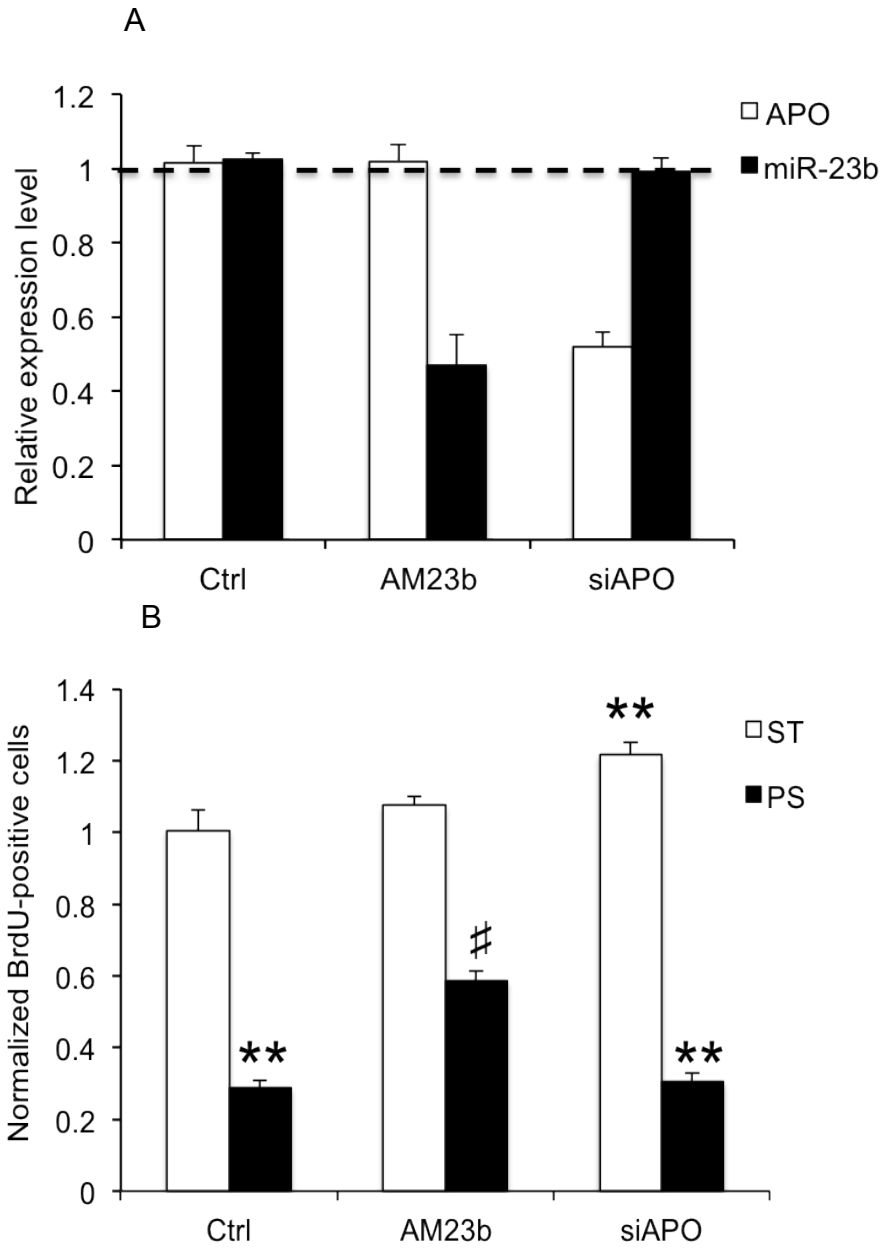

Figure 3.4 AM23b and siAPO significantly reduce levels of miR-23b and APO, respectively, but only AM23b reverses the anti-proliferative effect of 24-h PS flow. (A) Reverse transfections of AM23b and siAPO were used to knockdown the expressions of miR-23b and APO in HUVECs, respectively. RT-PCR analysis showed the successful knockdown of miR-23b and APO at mRNA levels. *P < 0.05 vs. scramble control. (B) 24-h PS flow led to a strong reduction of BrdU-positive cells in Ctrl-transfected cells. AM23b transfection but not siAPO significantly attenuated the PS-induced EC growth arrest. **P<0.05 vs. Ctrl_ST; #P<0.05 vs. Ctrl_PS.

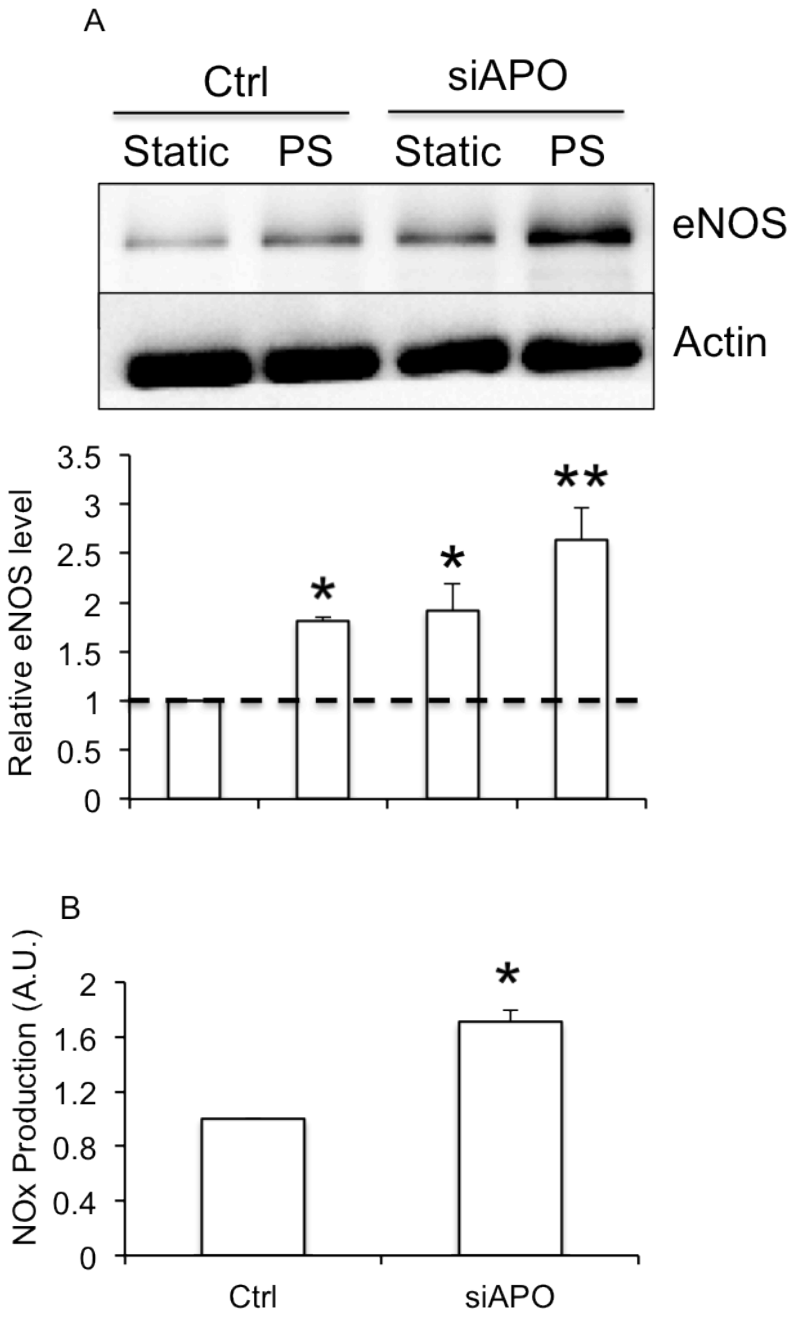

Figure 3.5 The effect of siAPO on PS induction of eNOS. (A) HUVECs were transfected with siAPO or scramble control before being exposed to 24-h PS or kept as static control (ST). The effect of siAPO on eNOS expression under ST and PS conditions was assessed by immunoblotting with the antibody against eNOS. *P < 0.05 vs. Ctrl_ST; **P<0.05 vs. Ctrl_PS. (B) The NO bioavailability in the perfusion medium was determined by Griess assay and expressed as NOx. *P < 0.05 vs. Ctrl. Image in (A) is a representative of triplicate experiments with similar results.

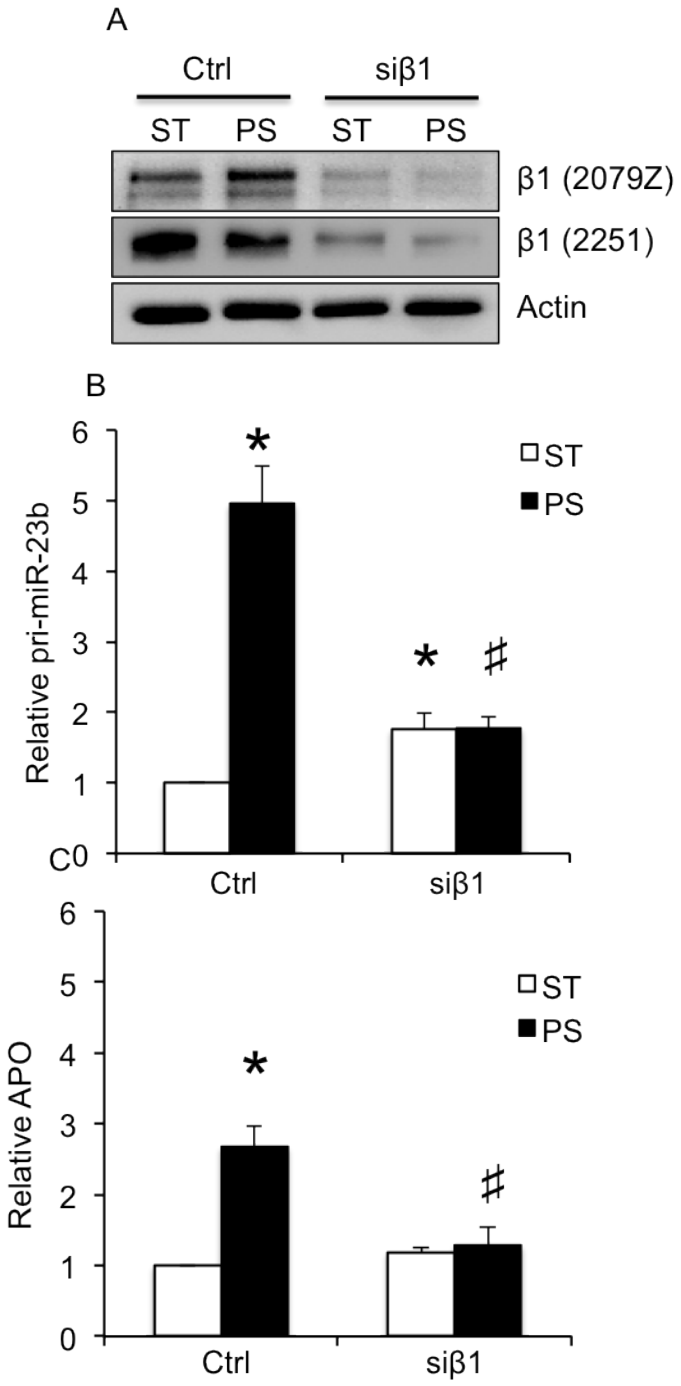

Figure 3.6 Integrin β_1 mediates the PS-induced miR-23b and APO expressions. (A) HUVECs were transfected with siβ_1 or scramble control before being subjected to 4-hr PS or kept as static control (ST). Cell lysates were immunoblotted with antibodies against LIBS- β_1 domain (2079Z), total β_1 (2251), and actin. (B) miR-23b and (C) APO expressions were analyzed with RT-PCR, *P < 0.05 vs. Ctrl_ST; #P<0.05 vs. Ctrl_PS. Results in (A) are representative of triplicate experiments with similar results.

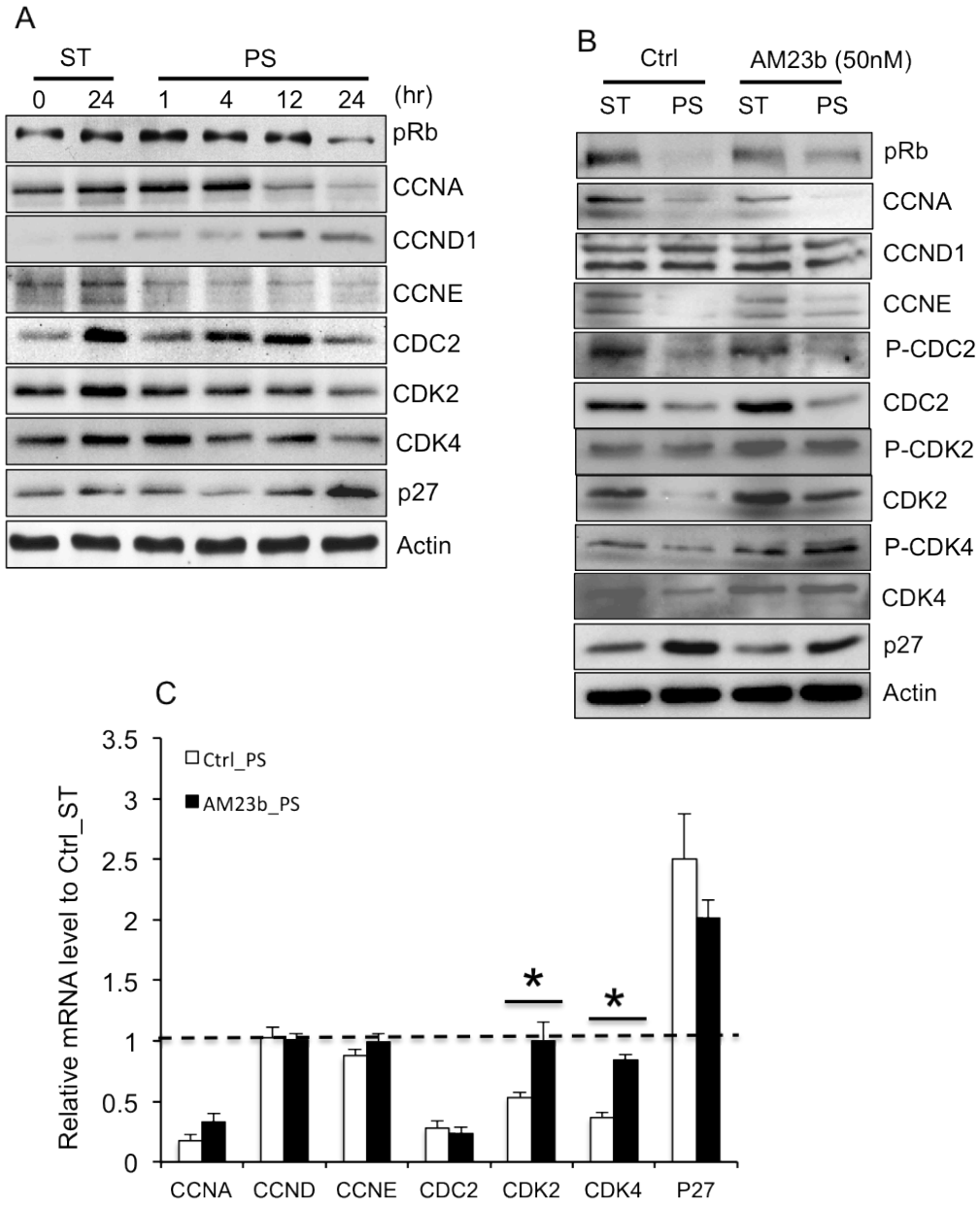

Figure 3.7 miR-23b mediates PS regulation of the phosphorylation and expressions cell cycle regulators CDK2 and CDK4. (A) HUVECs were kept under static condition (ST) or exposed to PS flow for the indicated times. Cell lysates were immunoblotted with antibodies against cell cycle regulatory proteins. Cells were transfected with AM23b 24 h before being subjected to PS flow or ST. Western blot (B) and RT-PCR (C) analyses were performed to examine the expressions of cell cycle regulatory proteins. Images in (A) and (B) are representative of triplicate experiments with similar results. *P < 0.05 vs. Ctrl_PS.

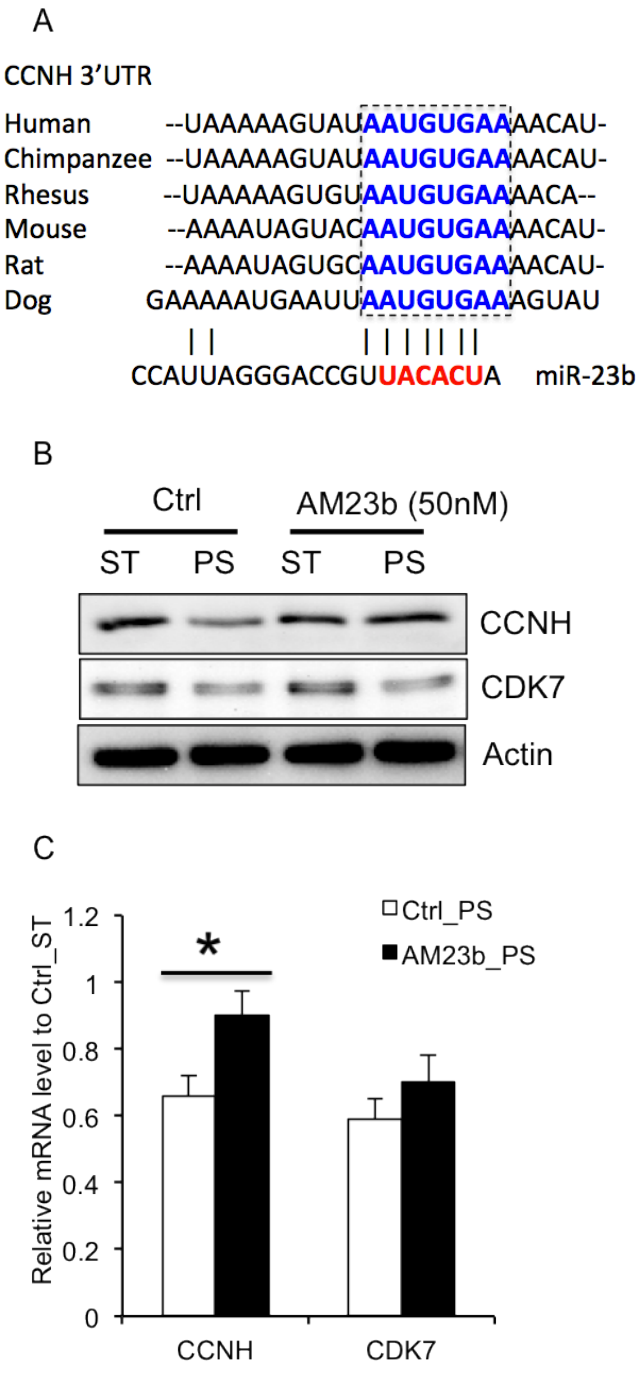

Figure 3.8 miR-23b mediates the PS reduction of CCNH. (A) The seed region of miR-23b and its target sequence at the CCNH 3'-UTR of several mammalian species. HUVECs were transfected with AM23b 24 hr before being subjected to PS or ST. Western blot (B) and RT-PCR (C) analyses were performed to examine the expressions of CCNH and CDK7. *P < 0.05 vs. Ctrl_PS. Results in (B) are representative of triplicate experiments with similar results.

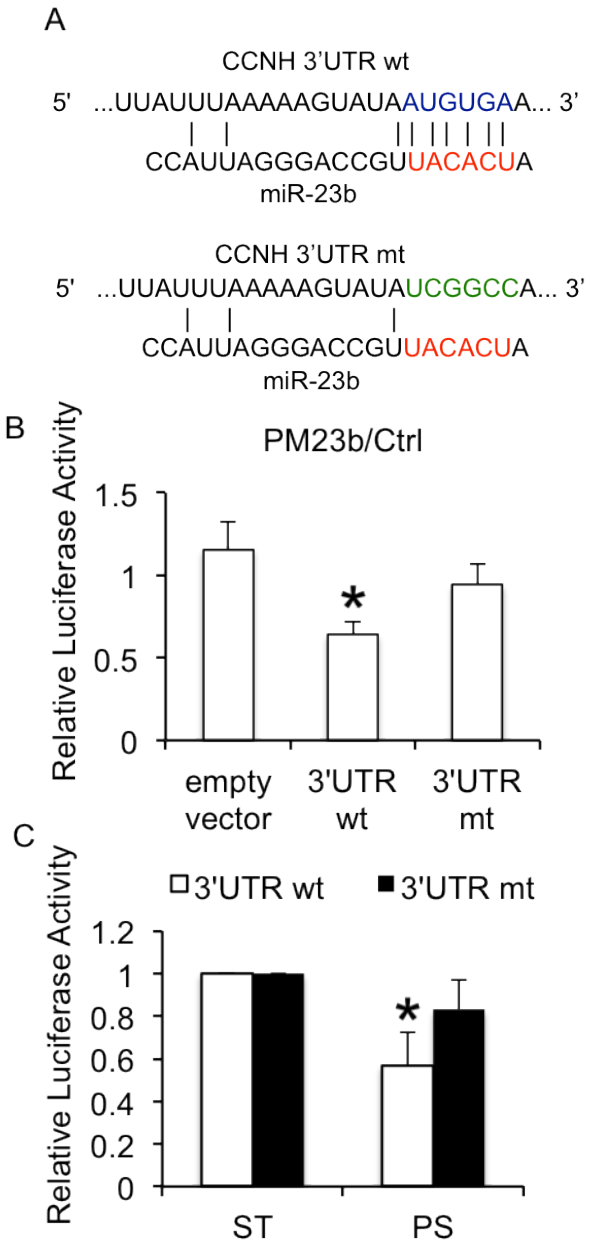

Figure 3.9 CCNH is a direct target of miR-23b. (A) Luciferase reporters containing wild-type CCNH 3'UTR (3'UTR wt) or the mutated CCNH 3'UTR (3'UTR mt) sequences were constructed. (B) HUVECs were transfected with empty vector, 3'UTR wt or 3'UTR mt together with CMV-β-gal, and PM23b or control molecule. Cell lysates were collected for luciferase activity assay, and the results were normalized to the β-gal. *P < 0.05 vs. empty vector. (C) Cells were transfected with 3'UTR wt or 3'UTR mt and subjected to 24-h PS or kept as static control (ST). Luciferase activity was measured and normalized as described above. *P < 0.05 vs. ST.

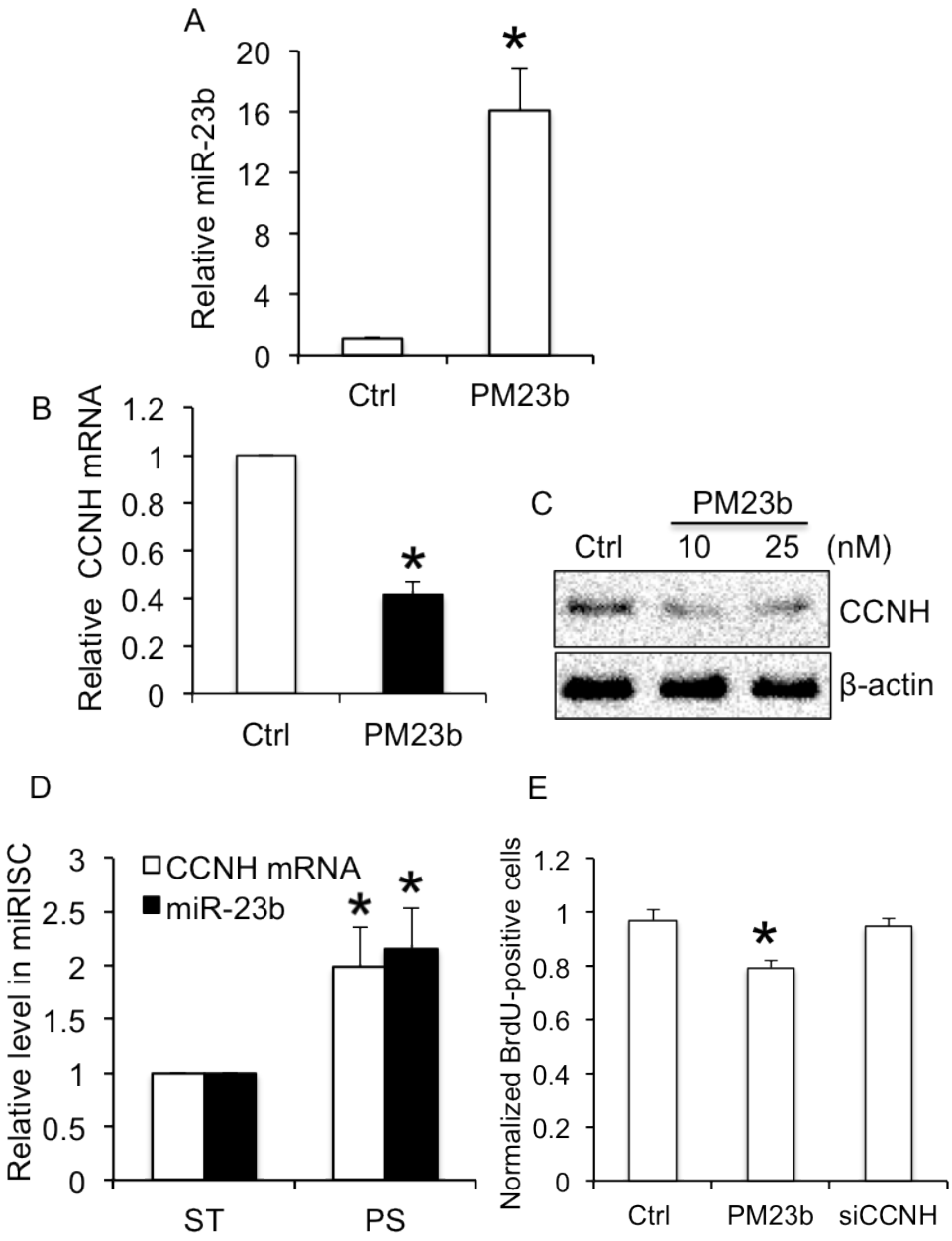

Figure 3.10 miR-23b decreases CCNH expression at both mRNA and protein levels. HUVECs were transfected with PM23b or control molecule. Fouty-eight-hr post-transfection, (A) the levels of miR-23b (relative to RNU48) and (B) CCNH (relative to GAPDH) were analyzed by RT-PCR. (C) CCNH levels was analyzed with immunoblotting. (D) AGOs-associated miR-23b and CCNH mRNA were immuno-precipitated with anti-pan-AGO and detected with RT-PCR. *P < 0.05 vs. ST. (E) Cells were transfected with PM23b or siCCNH, and BrdU incorporation assays were performed 48-hr post-transfection. *P<0.05 vs. Ctrl. Results in (C) are representative of triplicate experiments with similar results.

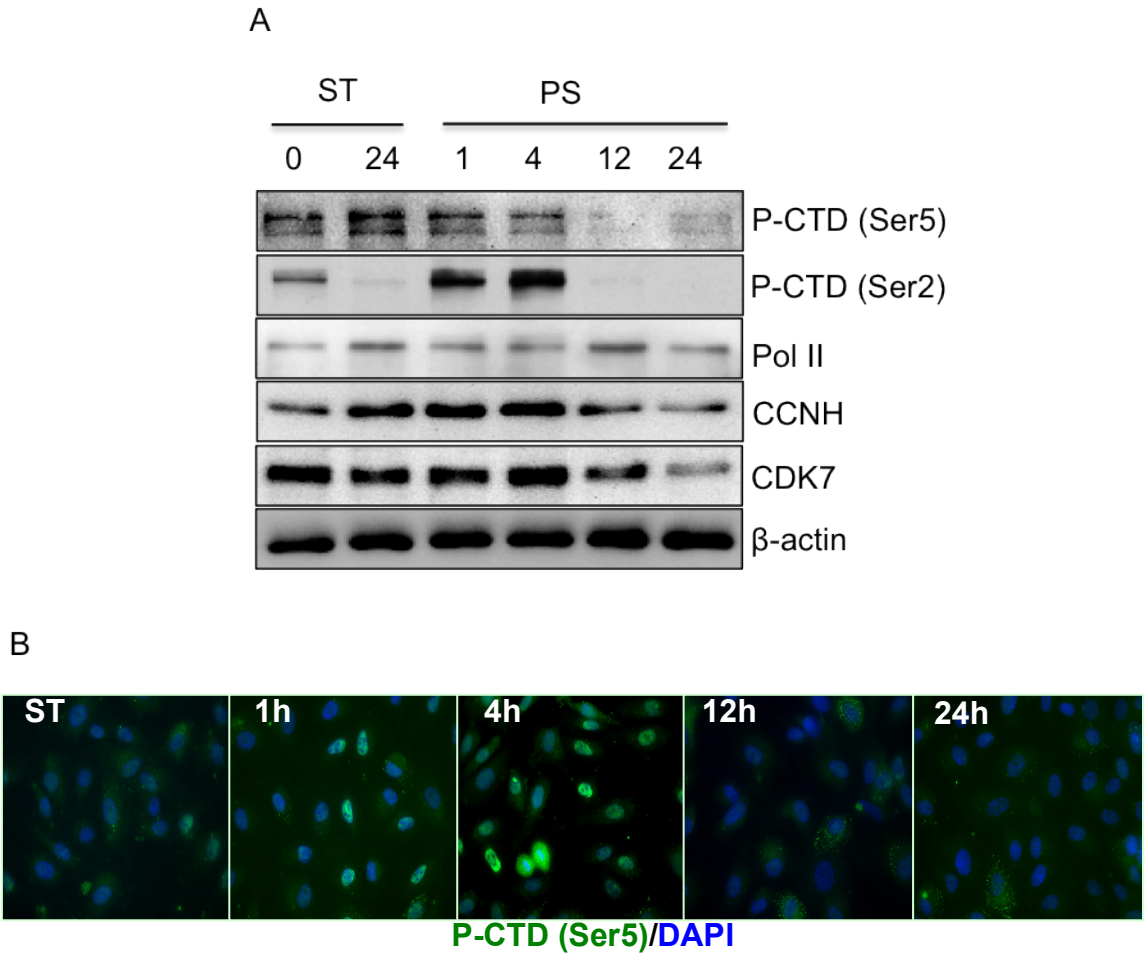

Figure 3.11 Prolonged PS flow decreases the expression and activity of CAK in ECs. HUVECs were subjected to PS flow or kept under static condition (ST) for indicated times. (A) Cell lysates were immunoblotted with antibodies against phospho-CTD (Ser2 and Ser5), Pol II (8WG16), CCNH, CDK7, and β-actin. (B) Phosphorylation of CTD at Ser5 under PS and ST0 was examined with immunofluorescence staining. Results are representative of triplicate experiments with similar results.

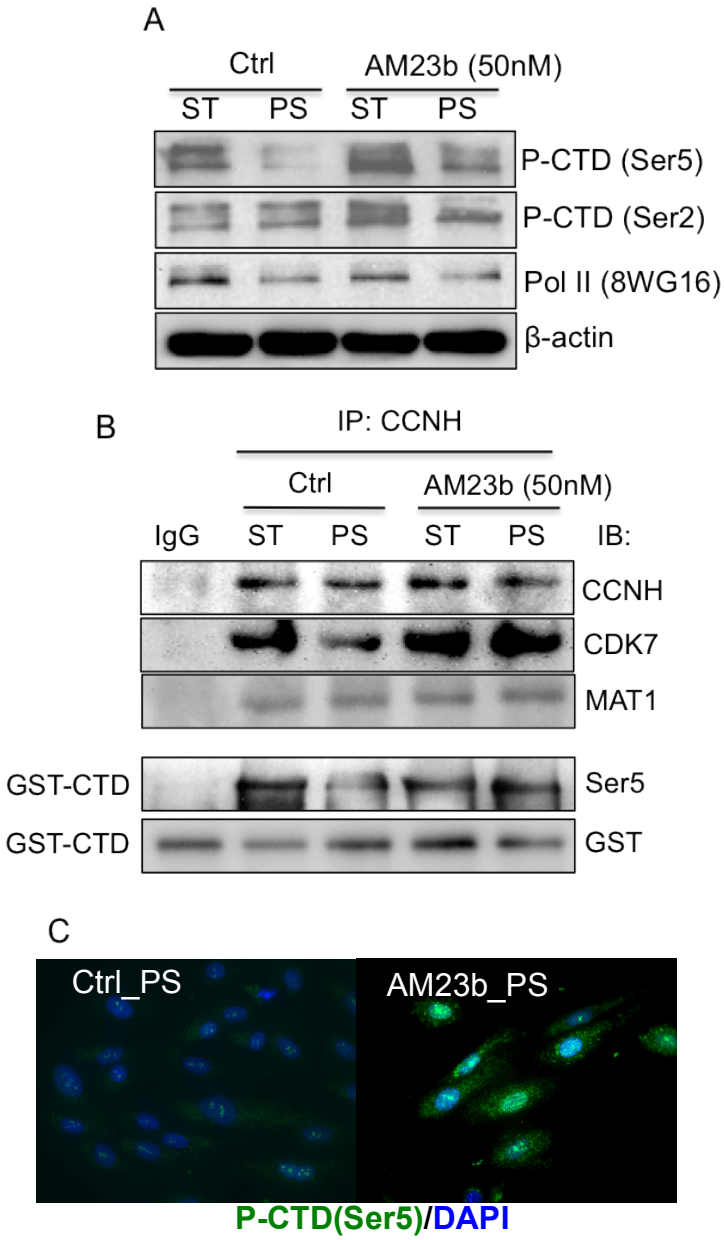

Figure 3.12 AM23b transfection restores CAK integrity and activity. (A) HUVECs were transfected with AM23b 24-h before being subjected to 24-h PS flow or kept under static condition (ST). (A) Western blot analysis performed to examine the phosphorylation and expression levels of Pol II. (B) CAK complex was pulled down with CCNH antibody and then incubated with GST-CTD, ATP, and kinase assay buffer. The CAK integrity and activity were examined with immunoblot. (C) Phosphorylation of CTD at Ser5 residue under Ctrl_PS and AM23b_PS conditions was further examined with immunofluorescence staining. Results are representative of triplicate experiments with similar results.

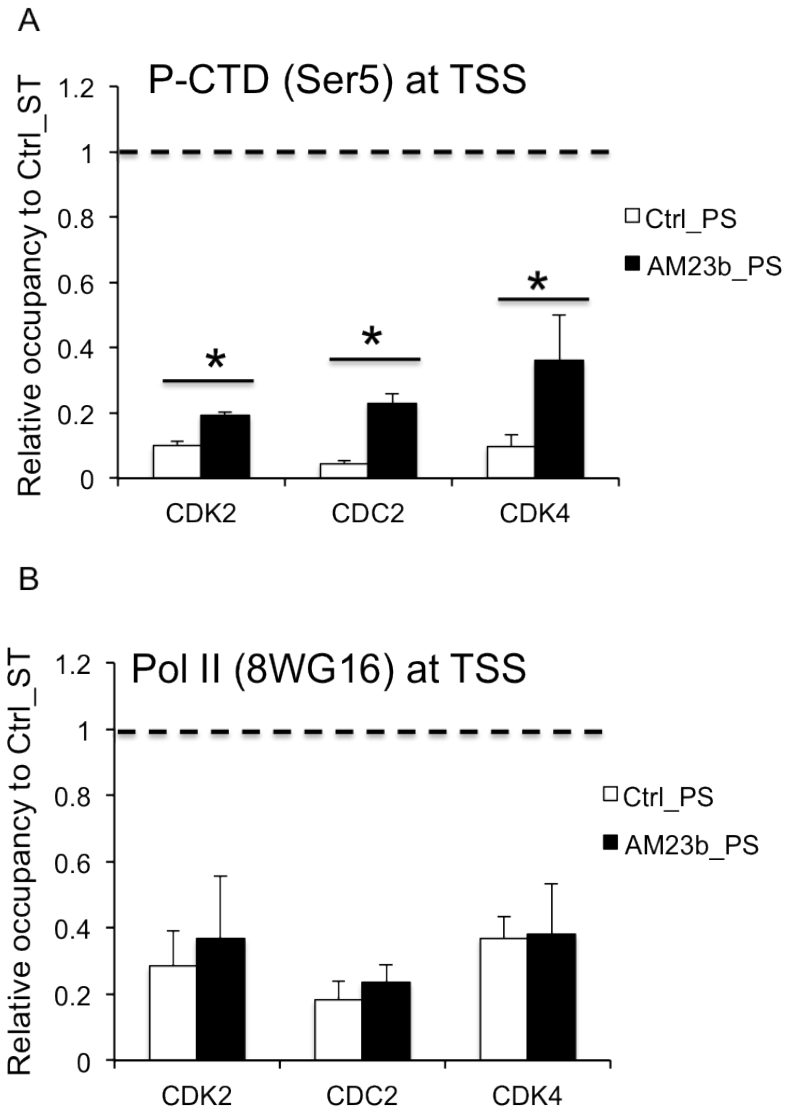

Figure 3.13 AM23b promotes the localization of phospho-CTD (Ser5) at CDC2, CDK2, and CDK4 transcription start sites (TSS). HUVECs were transfected with AM23b or scramble control before being subjected to 24-h PS or static condition (ST). The results show ChIP analysis of phospho-CTD (Ser5, H14) or Pol II (8WG16) binding to the TSS of CDC2, CDK2, and CDK4. Immunoprecipitated chromatin was analyzed by RT-PCR. Experimental samples were normalized to corresponding inputs and static controls and are represented as levels relative to static control. *p<0.05: AM23b_PS vs. Ctrl_PS.

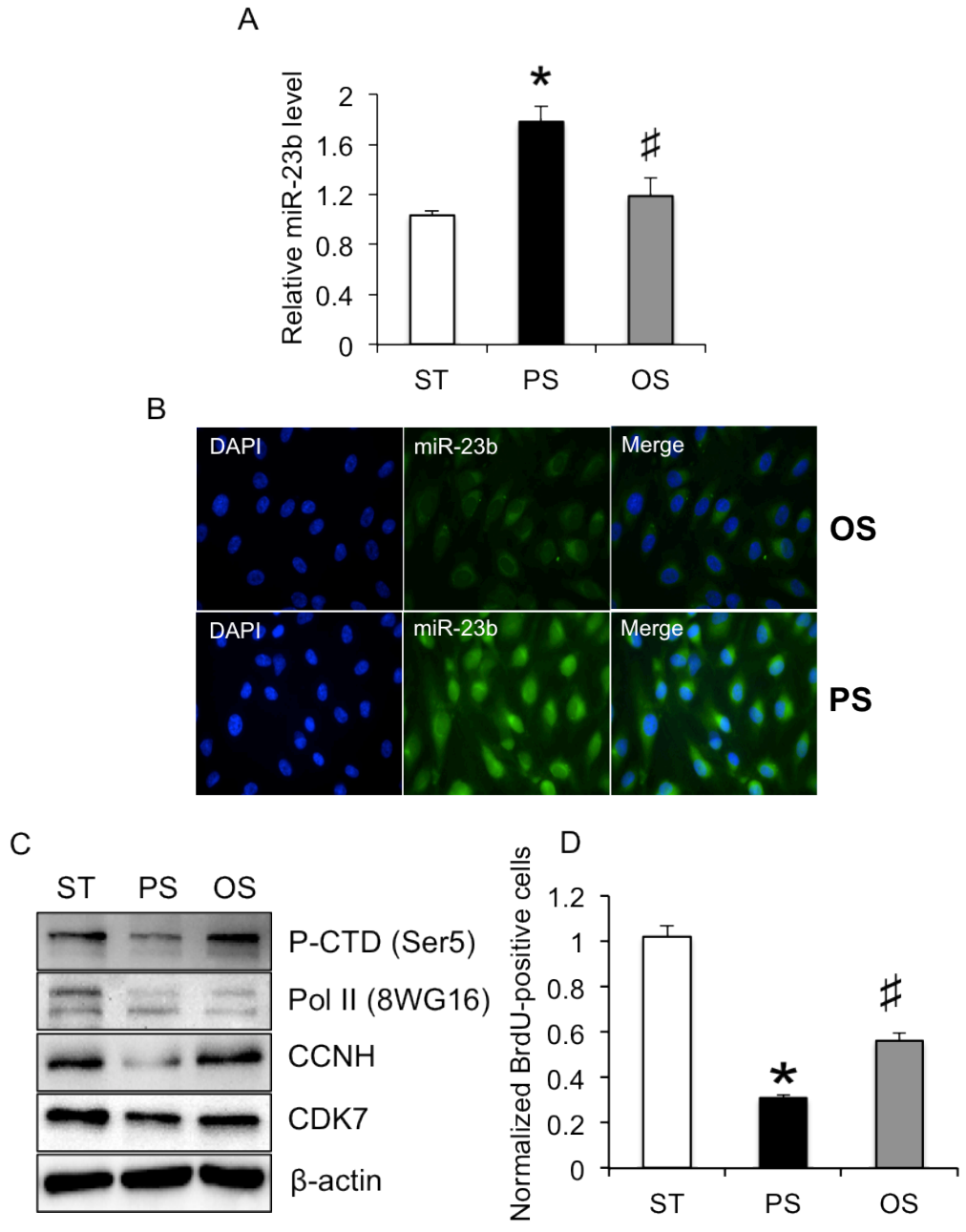

Figure 3.14 Flow patterns differentially regulate miR-23b/CAK pathway and EC proliferation. HUVECs were exposed 24-h PS and OS flows, or kept as static control (ST). The levels of miR-23b under different flow patterns were examined by (A) RT-PCR assay and (B) FISH staining. *P<0.05 vs. ST. (C) The activity and expression of CAK were assessed with western blot analysis. With BrdU added into the media during the last 4 hr of 24-h PS, OS, and ST conditions, BrdU-positive ECs were quantified by flow cytometry analysis. *PS<0.05 vs. ST and #P<0.05 vs. PS.

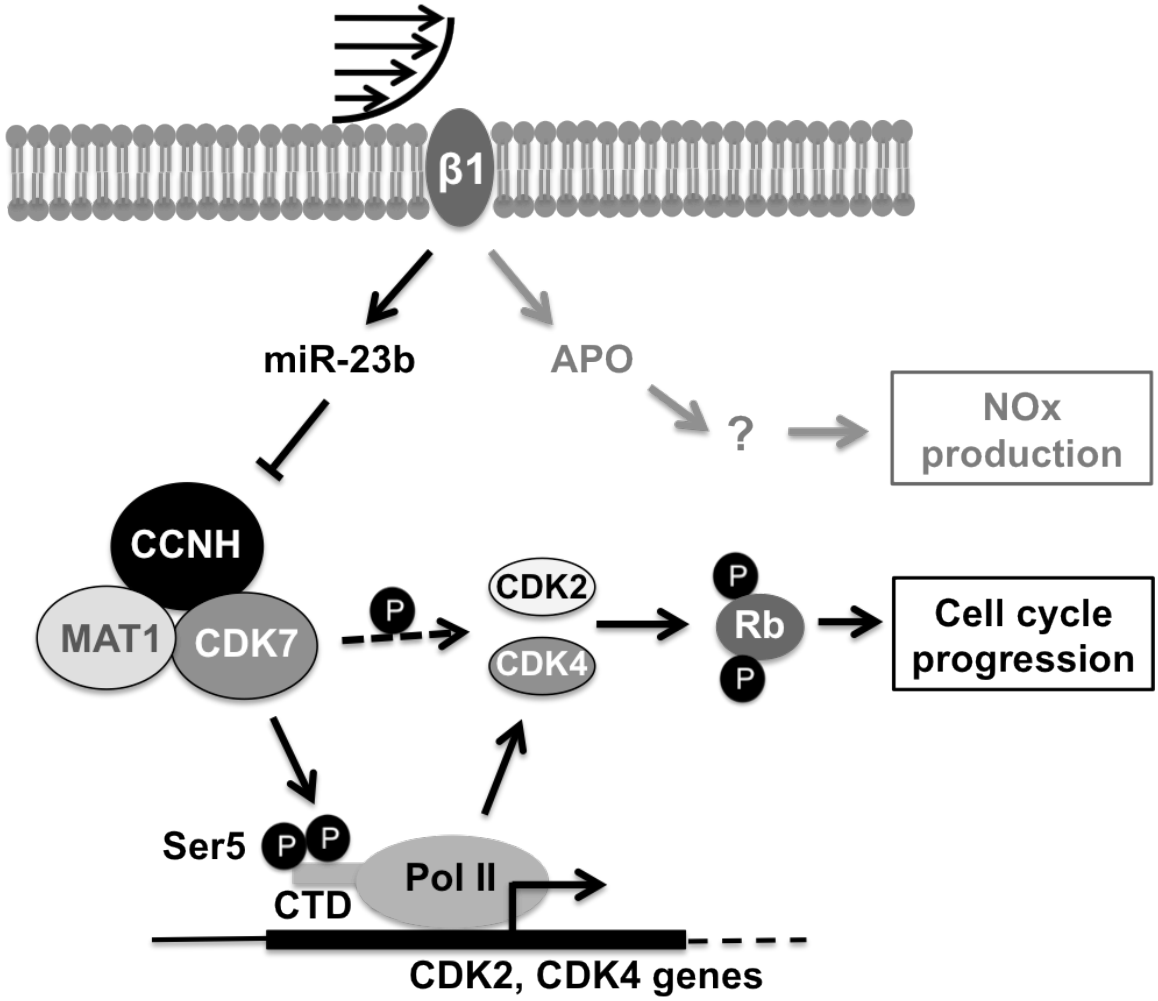

Figure 3.15 Schematic representation of the proposed role of miR-23b in flow regulation of EC growth. PS-induced miR-23b down-regulates CCNH expression and reduces CAK activity, which in turns modulates the expressions and activities of CDK2 and CDK4. Thus, Rb is altered to hypo-phosphorylated state and cell cycle progression is arrested. The up-regulation of APO contributes to the modulation of NOx production.

Table 3.1 Primer Sequences

Gene	Forward 5'-3'	Reverse 5'-3'
CCNA	GTCACCACATACTATGGACATG	AAGTTTTCCTCTCAGCACTGAC
CCND	AGACCTGCGCGCCCTCGGTG	GTAGTAGGACAGGAAGTTGTTC
CCNE	GTCCTGGCTGAATGTATACATGC	CCCTATTTTGTTCAGACAACATG
CCNH	GCATTGACGGATGCTTACCT	TGACATCGCTCCAACTTCTG
CDC2	CAGGATGTGCTTATGCAGGA	GGCCAAAATCAGCCAGTTTA
CDK2	CATTCCTCTTCCCCTCATCA	CAGGGACTCCAAAAGCTCTG
CDK4	TTCTGGTGACAAGTGGTGGA	CTGGTCGGCTTCAGAGTTTC
CDK7	GGCCGGACATGTGTAGTCTT	CATTTTCAGTGCCTGTGTGG
p27	TGCAACCGACGATTCTTCTACTC	CAAGCAGTGATGTATCTGAT
MCP-1	ATAGCAGCCACCTTCATTCC	TGGAATCCTGAACCCACTTC
VCAM	ATGGGAAGGTGACGAATGAG	ATCTCCAGCCTGTCAATGG
KLF2	AGACCTACACCAAGAGTTCGCATC	CATGTGCCGTTTCATGTGCAGC
eNOS	TGGTACATGAGCACTGAGATCG	CCACGTTGATTTCCACTGCTG
GAPDH	ATGACATCAAGAAGGTGGTG	CATACCAGGAAATGAGCTTG

CHAPTER 4 FLOW REGULATION OF MIR-23B IN EC PROLIFERATION *IN VIVO*

4.1 Abstract

Many studies using *in vitro* systems have demonstrated that PS flow exerts an anti-proliferative effect on ECs similar to that of steady laminar flow, while OS flow increases EC proliferation similar to the effect of disturbed flow. Although these *in vitro* findings are in agreement with the concept that PS is athero-protective and disturbed flow is atherogenic, there is a lack of *in vivo* evidence to elucidate the underlying mechanism. My *in vitro* studies using HUVECs and flow chambers showed that PS and OS have differential regulatory effects on miR-23b/CAK pathway and EC proliferation. In this Chapter, I extended these *in vitro* studies to examine the flow regulation of miR-23b and its role in modulating EC proliferation in rat carotid artery. Carotid stenosis and partial ligation procedures were used as two experimental models to alter the vascular flow patterns. The results of these *in vivo* studies showed that, similar to my *in vitro* findings, miR-23b levels were lower at the low and oscillatory shear stress regions in comparison to the high shear region, and that the expressions of CCNH and proliferation markers changed in direction opposite to miR-23b level. To the best of my knowledge, miR-23b is now the first flow-sensitive miRNA verified under both *in vitro* and *in vivo* conditions. These findings strengthen the role of miR-23b in mechanotransduction and vascular homeostasis and suggest the potential application of miR-23b as a therapeutic target.

4.2 Introduction

It is well established that the different patterns of shear stresses over the endothelium induced by regional variations in blood flow play a significant role in modulating vascular homeostasis, as well as the development of atherosclerotic lesions [3, 6]. This concept is based on the observations in humans and large animals that the distribution of vascular lesion formation is correlated to local blood flow patterns. *In vitro* studies corroborate the theory by showing that steady or pulsatile laminar flow decreases EC turnover, oxidative stress, and expression of inflammatory genes, and that oscillatory flow with the characteristics of disturbed flow results in high EC turnover and pro-inflammatory events in cultured ECs. Several animal models using knockout strains (such as ApoE-/- and LDL receptor-/- mice) or mechanical injuries (such as balloon injury and carotid artery ligation) have been used to study the development of atherosclerotic lesions [23], but there is still a lack of direct proof for phenotypic changes of ECs resulting from components of flow patterns *in vivo*.

The experiments described in previous Chapters demonstrated that miRNAs are differentially regulated in ECs under PS and OS *in vitro*, and that PS regulate EC proliferation through a miR-23b/CAK-dependent mechanism. In this study, the overall paradigm of miRNA regulation was proposed to be an important factor in modulating EC functions under physiological and pathophysiological conditions. Thus, in this Chapter, I proposed to examine the local correlation between miR-23b expression and EC proliferation in athero-protective and athero-prone sections using rat carotid artery as the animal model. The rat is an ideal candidate for my study because of the vessel sizes, ease of handling, availability of inbred strains, and the similarity of genetics to human. Of note, both the miR-23b cluster and the CCNH mRNA sequence (including 3'UTR) are highly conserved in the rat genome, thus making it possible for us to test our *in vitro*

findings in rat carotid artery *in vivo*. Wild-type rat is inherently resistant to atherogenesis, and the hemodynamics in the rat arterial tree may not faithfully reflect that in human. To overcome these limitations, I took advantage of two established methods to create flow disturbance in rat carotid artery: 1) carotid stenosis, and 2) partial carotid ligation.

The stenosis model, also known as peri-vascular cuff model [120-122], is achieved by applying the flow constrictor, such as a cast or U-shape metal clip, to the straight sections of large arteries (Figure 4.1). The constriction of blood vessel would change local hemodynamics and generate several regions with distinct flow patterns: normal or low shear stress at the proximal upstream of the constriction, high shear stress in the throat, and low and oscillatory shear stress (flow separation and vortices) downstream to the expansion. It has been reported that in ApoE-/- mice atherosclerotic lesions develop primarily in the upstream and downstream regions of the cuff [120], suggesting that low and oscillatory shear stress, which are characteristics of disturbed flow, may be associated with disease occurrence and progression.

Partial carotid ligation method was also used in this study to examine vascular responses to different flow patterns. This method was previously used in mice, rats, and rabbits to study the vascular remodeling and atherosclerosis in response to hemodynamic changes *in vivo* [123, 124]; blood flow is shown to be substantially reduced by ligating three out of four branches of the common carotid artery, leading to rapid vascular remodeling. According to the study by Nam D. et al. and Ni C. et al. [39, 125], disturbed flow resulted from partial ligation in ApoE-/- mice promotes the formation of atheroma in two weeks and advanced lesions in four weeks, indicating the atherogenicity of disturbed flow.

In this study, the stenosis or partial ligation was created in the left common carotid artery (LCA), while the right common carotid artery (RCA) was isolated and served as control vessels with laminar high shear. Although the disturbed flows created by these two models are not identical, both provide relevant disturbed hemodynamical environments for the examination of miRNA expression and functional consequences *in vivo*. I first confirmed the flow disturbances in both models with ultrasound Doppler study, and then validated that the expression of miR-23b and its inhibitory effect on EC proliferation are indeed flow pattern-dependent in the rat carotid artery.

4.3 Materials and Methods

4.3.1 Animals

Adult male Sprague-Dawley rats weighing 300-350 g were used in this study. Sixteen rats were used in each model, and four additional rats were used as the sham control group. The experimental protocol (S03003) was approved by the Animal Subject Committee of University of California, San Diego. All rats received humane care in accordance with the animal use principles of the American Physiological Society. All rats were maintained under constant environmental temperature (21 ± 1°C), humidity (60 ± 5%) and light/dark cycle, and had free access to water and normal rat diet.

4.3.2 Surgical procedures

Stenosis of LCA was produced by using a U-shaped titanium clip. Briefly, the animals were anesthetized with intraperitoneal ketamine (100 mg/kg body weight) and xylazine (10 mg/kg body weight). The general health conditions of animals (including body temperature, pulse rate, respiratory rate, mucous membrane color, shivering, jawtone, and gag) were monitored. The rat was laid supine, and its ventral side of the neck was de-haired and disinfected with Betadine. A ventral mid-line incision (~2 cm) was made in the neck, and a segment of the common carotid arteries (LCA and RCA)

was exposed by blunt dissection. The clip was held with a pair of forceps and placed on the LCA. The extent of clipping was controlled by placing a stopper of given size between the two arms of the forceps.

For the partial carotid ligation, the carotid bifurcation was exposed. Three branches (left external artery, left internal artery, and occipital artery) of the LCA were ligated with 6-0 silk suture, while the superior thyroid artery was left intact. The RCA was exposed but no ligation procedure was performed to serve as the control artery in the same animal. The wound was closed and the rat was returned to the cage for recovery. Post-op rats were monitored for 2 days to 4 weeks until sacrificed. Buprenophine was given at 0.05 mg/kg to each rat every 12 h to prevent post-operation pain. All care and experimental procedures were performed according to National Institute of Health guidelines and approved by the University of California, San Diego Animal Care Committee.

4.3.3 Ultrasound study

Doppler imaging was performed on the rat carotid artery at the Shared Animal Imagine Resource in UCSD Moores Cancer Center to visualize the flow alternations at/around the surgery sites, as well as the control vessels. The animal was anesthetized and placed in either supine or lateral recumbent position, and the neck was shaved to facilitate the ultrasound Doppler measurement. The ultrasound measurement was taken using the VisualSonic Vevo 770 ultrasound imaging system. Color Doppler mode was used to identify the location of carotid arteries and stenotic site. Pulse wave (PW) Doppler was used for measuring blood flow velocity in common carotid arteries in both models.

4.3.4 Vessel Preparation

At the end of each experiment, the rat was deeply anesthetized with an overdose of Ketamine-Xylazine cocktail and perfused with DEPC-treated phosphate-buffered saline (PBS) at a pressure of 120-140 mm Hg. For RNA extraction, carotid arteries were dissected from surrounding tissues, slit open longitudinally, and 1 ml TRIzol was applied to extract the RNA from intima layer. For immunohistochemistry, the vessels were perfusion-fixed with 4% paraformaldehyde (PFA) in PBS at a pressure of 120-140 mm Hg. The carotid artery was dissected out, and adventitia was carefully removed. The artery was further fixed by immersion in 1 ml of 4% PFA solution for 16 h before being subjected to frozen-section.

4.3.5 Frozen section and Immunohistochemistry

The PFA-fixed carotid artery was embedded with Tissue-Tek OCT compound in a tissue base mold and slowly submerged into pre-chilled 2-methyl butane until frozen completely. The frozen tissue block was then immediately stored at -80°C until sectioning. Serial sectioning (10 μm/section) was performed with cyrotome cryostat machine in UCSD Histology Core facility, and the tissue sections were placed on polylysine-treated glass slides. Tissue sections on slides were dried at room temperature for 30 min before staining.

For the detection of miR-23b expression, a modified fluorescence *in situ* hybridization (FISH) with miR-23b-LNA probe (Exiqon) was performed. Slides were first washed with PBS to remove residual OCT medium, and then treated with acetylation solution. The hybridization was performed in 150 μl hybridization buffer containing 1 μl DIG-labeled miR-23b LNA probe at 60°C for 4 h. After stringent wash, the slides were incubated with Alexa Fluor 594-conjugated DIG antibody at room temperature for 4 h, and then counterstained with Hoechst 33258 for 10 min.

For immunohistochemistry, the glass slides were blocked with 3% BSA in PBS

for 1 h, followed by incubation with antibodies against vWF, CCNH, Ki67 and APO (1:100) at 4°C for 12 h. Alexa Fluor 594-conjugated anti-rabbit and mouse antibodies were used (1:200) as secondary antibodies, and Hoechst 33258 was used for counterstaining. After mounting, images were acquired with an epi- fluorescence microscope.

4.4 Results

4.4.1 Disturbed flow at stenotic outlet reduces miR-23b expression but promotes EC proliferation

To assess the effects of different flow patterns on miR-23b expression and EC proliferation *in vivo*, a local stenosis was created using a U-shaped titanium clip at the rat LCA (figure 4.1). High-frequency ultrasonography at week 1 post-surgery was performed to verify the flow disturbance in LCA, and laminar flow in control RCA. As expected, color-mode echo studies (figure 4.2A) indicated that the placement of U-clip resulted in lumen narrowing and flow disturbance in LCA. The Doppler measurement (figure 4.2B) also showed that upstream from the stenotic site, flow velocity was relative low (~50% lower), compared with the flow velocity in RCA. Within the stenotic segment, forward flow acceleration was observed. Downstream of the flow constriction, forward flow with normal magnitude was measured with the existence of reversal flow, indicating vortices (or oscillatory flow) was successfully generated at that region. One week post-surgery, the stenotic vessel was fixed with saline and PFA perfusion, harvested, and frozen-sectioned. Hemotoxylin and eosin (H&E) staining of cross sections demonstrated the reduction of lumen size at the stenotic site, without any significant vessel wall thickening, intimal hyperplasia, or thrombus formation over one week (figure. 4.2C).

MiR-23b, CCNH, and Ki67 (proliferation marker) expressions were examined at the disturbed flow regions, as well as the control vessel, using FISH and

immunohistochemical staining. FISH results showed that miR-23b expression under high-shear condition in RCA was significantly higher than that under disturbed flow (low shear and oscillatory shear regions) in the stenotic LCA. Immunohistochemical studies demonstrated that the frequency and intensity of CCNH and Ki67 staining in endothelium were much higher at the immediate downstream of the constriction site, suggesting that the flow disturbance created by stenosis changed the quiescent ECs into a highly proliferative state. The proliferative state of ECs is inversely related to the miR-23b expression, as found *in vitro (*figure 4.3*)*.

4.4.2 Low and oscillatory flow reduces miR-23b expression and promote EC proliferation in partial carotid ligation model

The flow-regulation of miR-23b level and EC proliferative state *in vivo* was also studied in the rat carotid partial ligation model. As shown in figure 4.4A, three branches of LCA were ligated with sutures and the superior thyroid artery was left intact, and right common carotid artery (RCA) was kept as control. The echo studies using PW mode showed that flow velocity reduced significantly (~90%) in LCA one week after the ligation, while in RCA the blood flow slightly increased in comparison with the sham-operated rat (figure 4.4B). More importantly, reverse flow was detected in LCA during diastole as indicated by the white arrows in Figure 4.4B. These results confirmed that the partial carotid ligation created a low and oscillatory flow, which are the major components of disturbed flow, in LCA. The flow in RCA was maintained as high and laminar shear flow.

One week post-surgery, the animals were euthanized, and segments of LCA and RCA were isolated. Total RNA was extracted from the intima layer, and the levels of miR-23b, miR-27b, CCNH, and flow-sensitive genes such as KLF2 and eNOS were examined with RT-PCR. As shown in figure 4.5, the expressions of flow-sensitive genes,

including KLF2 and eNOS, in LCA were significantly lower than those in RCA; this is in agreement with the literature [39] and our *in vitro* finding (unpublished microarray/RT-PCR data) that KLF2/eNOS expression was lower under OS in comparison to PS. These *in vivo* results validated the *in vitro* findings on molecular responses to flow patterns. Furthermore, the miR-23b level in LCA was lower than that in RCA, and CCNH expression was higher in LCA than RCA.

Although the method used for mRNA isolation from LCA and RCA primarily targets the intima layer, the potential contaminations from SMCs or connective tissues may bias the result. To address this problem, we further analyzed the EC-specific responses by FISH and immunohistochemistry staining on the frozen cross sections of LCA and RCA tissues to spatially visualize the gene expression in endothelium (figure 4.6). Consistent with the RT-PCR studies, the level of miR-23b was significantly lower in the endothelium of LCA compared to the RCA. Furthermore, The intensity of CCNH and Ki67 staining in endothelium was much higher in LCA compared to the RCA, confirming that disturbed flow increases EC proliferation *in vivo*, while high and laminar flow keeps ECs in quiescence. APO staining, as miR-23b, was also weaker in LCA than in RCA, but the functional role of APO in regulating vascular functions remains to be explored.

4.5 Discussion

There is growing evidence indicating that miRNAs participate in the regulations of vascular homeostasis and pathogenesis. We and others have demonstrated that miRNAs are sensitive to fluid shear stress and modulate EC functional consequences *in vitro* [59, 64, 65, 103]. However, there is a paucity of studies validating these observations *in vivo* due to the lack of adequate animal models. Differential expression of endothelial miRNAs between athero-protective and athero-prone regions have been reported by Fang Y. et al in adult swine aorta [102]; they found high level of miR-10a

expression in the athero-protective region contributes to the suppression of chronic inflammation, The present study, by creating regions of disturbed flow vs. laminar flow with the use of two animal models, provides direct evidence for the regulation of miRNAs in modulating EC phenotypes flow disturbance with appropriate controls to assess *in vivo*.

It is known that ECs are primarily in the quiescent state throughout the arterial tree, and the limited number of proliferating ECs is usually associated with curvatures and branch sites, where the blood flow is disturbed. Pulsatile flow with high shear stress exerts an inhibitory effect on EC proliferation and is athero-protective, whereas disturbed flow has opposite effects. My *in vitro* studies presented in Chapter 3 demonstrated that PS flow repressed EC proliferation through a miR-23b-dependent mechanism, and that the miR-23b/CAK pathway was differentially regulated by flow patterns. In this Chapter, I have extended my study to *in vivo* conditions with experimentally created flow disturbances and examined the resulting changes in miR-23b and EC proliferation in rat carotid arteries. Ultrasonography showed that flow disturbances with low shear and flow reversal were successfully generated using carotid stenosis and partial ligation in LCA, and that the flow in the control RCA was pulsatile with high shear stress. Although the detailed patterns of low and oscillatory shear stresses resulting from the two models are not exactly the same, the pathological responses to the flow variation such as EC proliferation were similar. Von Willebrand factor (vWF) staining showed that the endothelium remained continuous and there was no thrombosis observed in the LCA, thus these surgical procedures did not cause damage to the endothelium to elicit injury effects. There were little to no structural change of vascular wall (in terms of luminal area reduction and SMC proliferation) at the disturbed flow regions of the LCA in both models, suggesting that the differential regulations of miR-23b and EC proliferation are the

primary responses to disturbed flow variation, rather than secondary to vascular derangement.

Using the carotid stenosis and partial ligation models, I have verified the differential effects of pulsatile flow vs. disturbed flow on miR-23b expression rat carotid arteries: miR-23b expression is higher in ECs in the control RCA under high shear stress than that in the LCA under low and oscillatory shear stress. In addition, the RCA had little or no Ki67-positive ECs, in contrast to the large number of Ki67-positive proliferating ECs in the LCA with disturbed flow. The results in the sham-ligated carotid arteries are similar to those in the RCA. These findings suggest that miR-23b is highly expressed in the endothelium of healthy arteries and may be critical for maintaining ECs in a resting, non-activated state. In this respect, disturbed flow in the carotid artery (LCA in the two models with different patterns of disturbed flow) suppresses miR-23b expression, thus impairing its inhibitory effect on EC proliferation and inducing the ECs into an active state.

Several studies including ours have previously shown that PS repressed EC proliferation through cell cycle regulatory network, and my report in Chapter 3 provided further evidence that, while PS induces miR-23b expression to exert the anti-proliferative action on ECs through a CAK/Pol II pathway, OS flow does not. My mechanistical studies showed that the PS-induced miR-23b directly represses CCNH expression at posttranscriptional level, thus impairing the CAK activity on cell cycle progression and basal transcription. The results of the two animal models are in agreement with my *in vitro* findings: CCNH expression is lower in quiescent ECs in the RCA under pulsatile flow than that in proliferating ECs in the LCA under disturbed flow. These findings suggest that the miR-23b → CAK/Pol II → cell proliferation pathway is also applicable to *in vivo* regulations. To further validate interplays between miR-23b and EC proliferation

in vivo, local perturbation of miR-23b in carotid arteries will be needed. However, delivery of miRNA precursor or antagomir to endothelium in a specific region of artery is still a major challenge and remains to be established.

In summary, the *in vitro* studies in Chapter 3 have demonstrated the miR-23b/CAK pathway on the effects of different flow patterns on proliferation. In this Chapter 4, I have used two well-defined animal models to generate the important findings that different flow patterns have effects on miR-23b and EC proliferation *in vivo* that verify the *in vitro* findings in Chapter 3. The important role of miR-23b in relaying the anti-proliferative effects of sustained pulsatile flow on the endothelium *in vitro* and *in vivo* is indicated by the high level of miR-23b expression and its suppression of CAK pathway, cell cycle and basal transcription. Disturbed flow suppresses the endothelial miR-23b expression to lead to atherogenic phenotype changes. These findings provide new insights into the physiological and therapeutic importance of miRNAs in vascular biology.

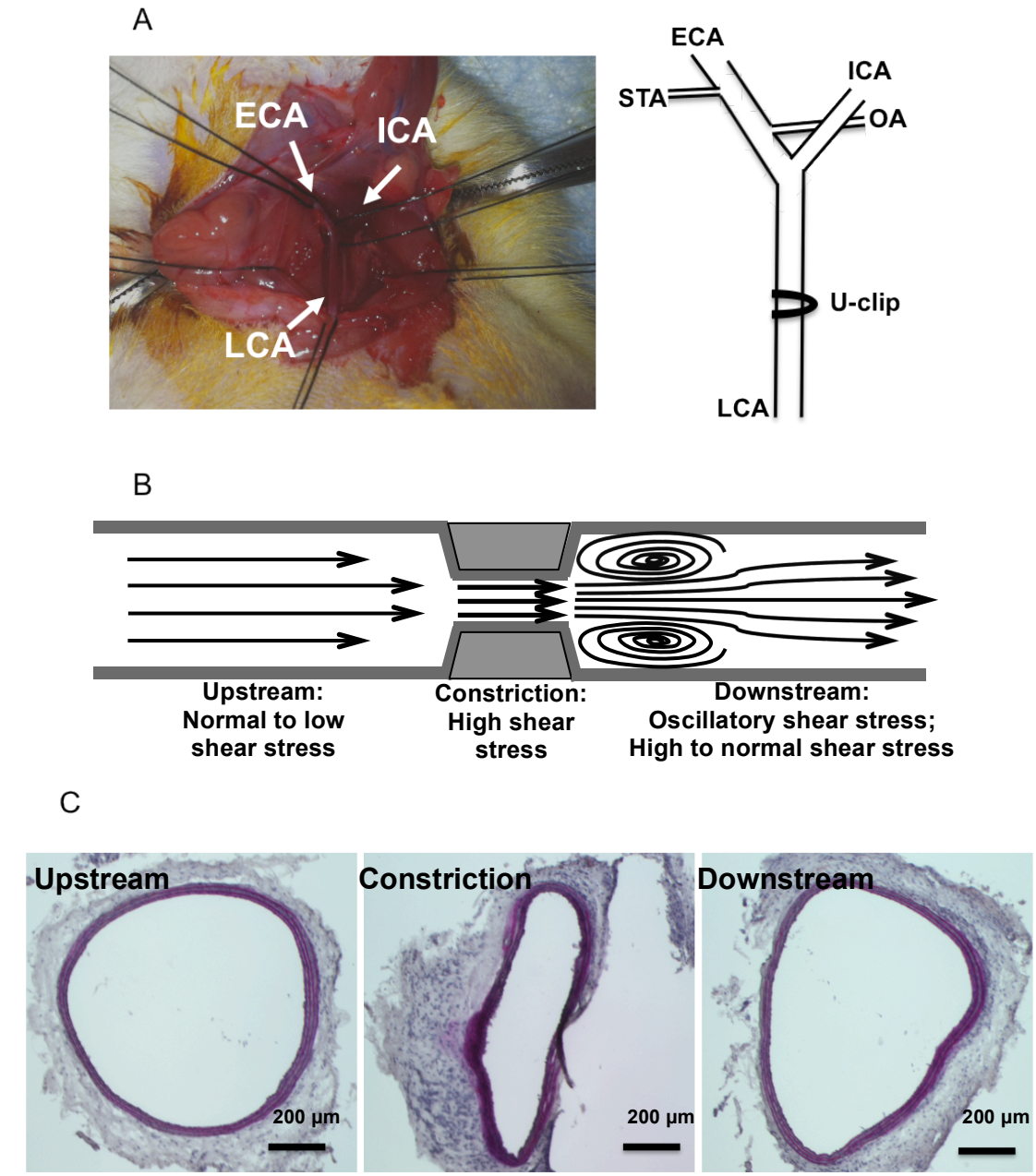

Figure 4.1 Rat carotid stenosis model to create flow disturbance. (A) Transverse placement of U-shaped metal clip onto left common carotid artery (LCA). (B) Schematic representation of shear stress patterns created by the stenosis. (C) Hematoxylin and Eosin staining of the cross-sections from different regions of carotid artery. Results in C are representative of triplicate experiments with similar results

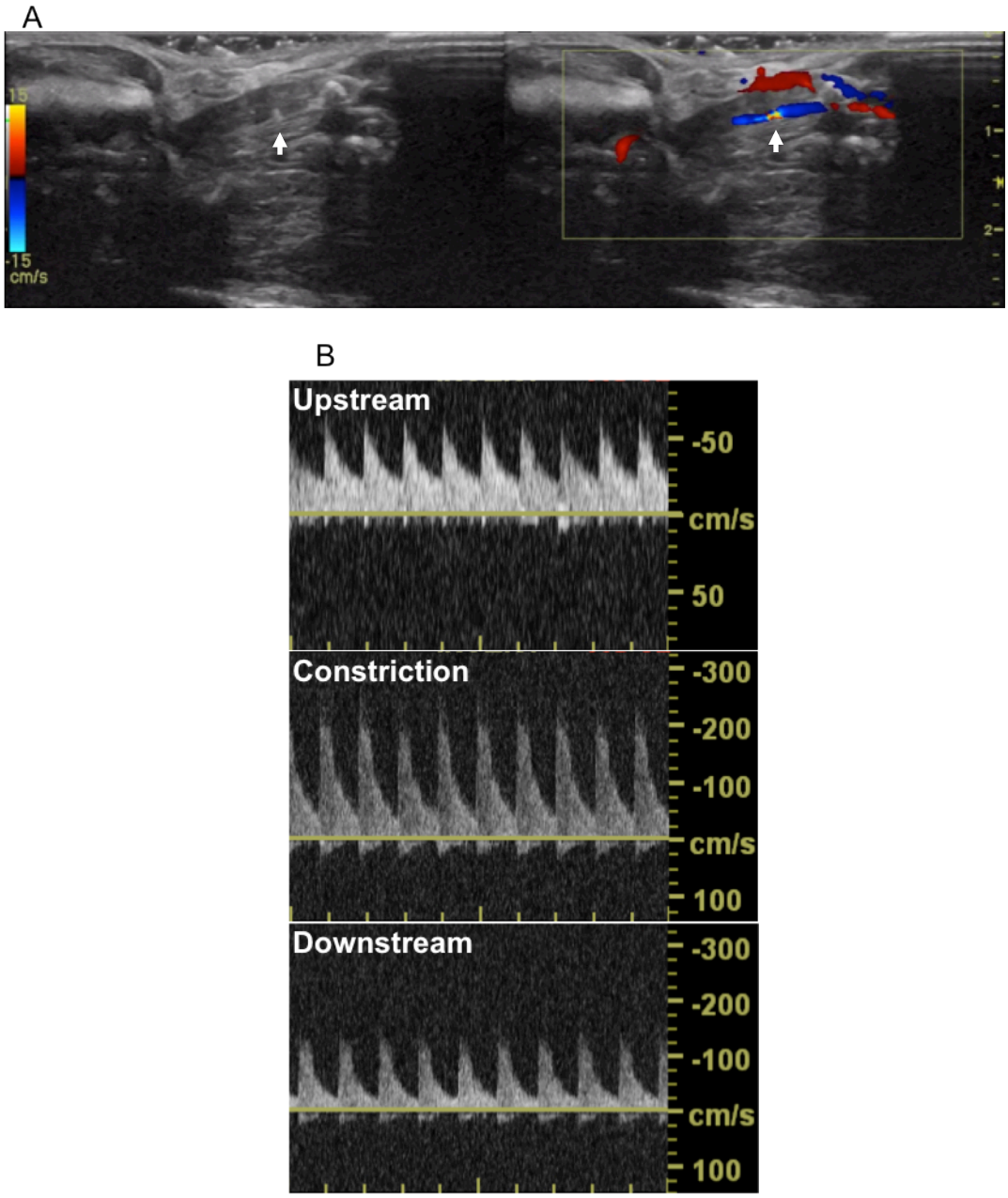

Figure 4.2 Ultrasonography measurement of blood flow in rat carotid artery. (A) Identification of carotid stenosis and flow disturbance with color Doppler. (B) Measurement of blood flow velocity from various regions in carotid artery with pulse-wave Doppler. Results are representative of triplicate experiments with similar results.

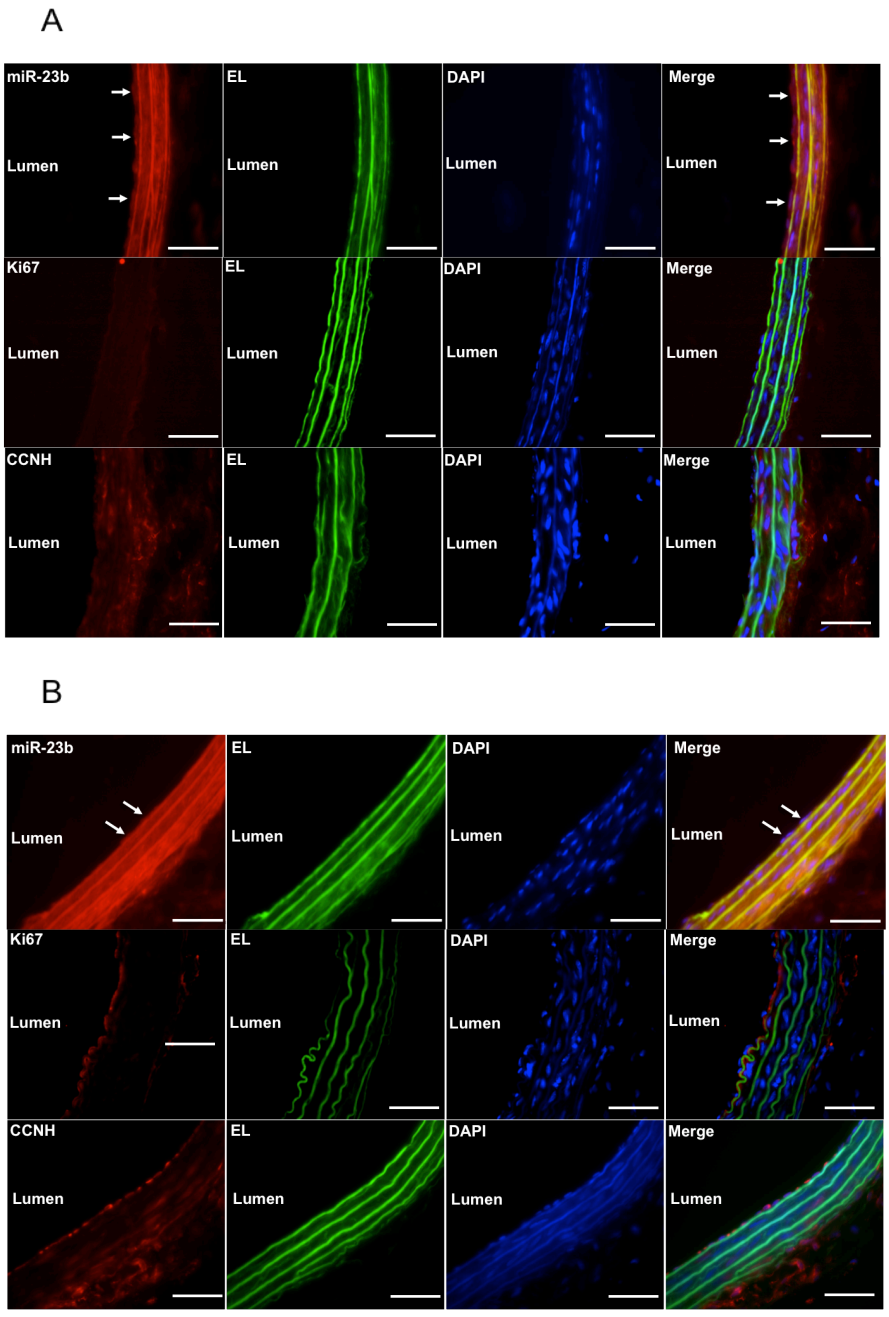

Figure 4.3 Disturbed flow at stenotic outlet reduces miR-23b expression but promotes EC proliferation. The control vessels (RCA) and the stenotic cartotid arteries (LCA) were isolated one week post-operation from Sprague-Dawley rats. Frozen sections from (A) control RCA and (B) disturbed flow site at stenotic outlet in LCA were stained with fluorescence in situ hybridization (FISH) and immunohistochemistry for miR-23b, Ki67, and CCNH (red).

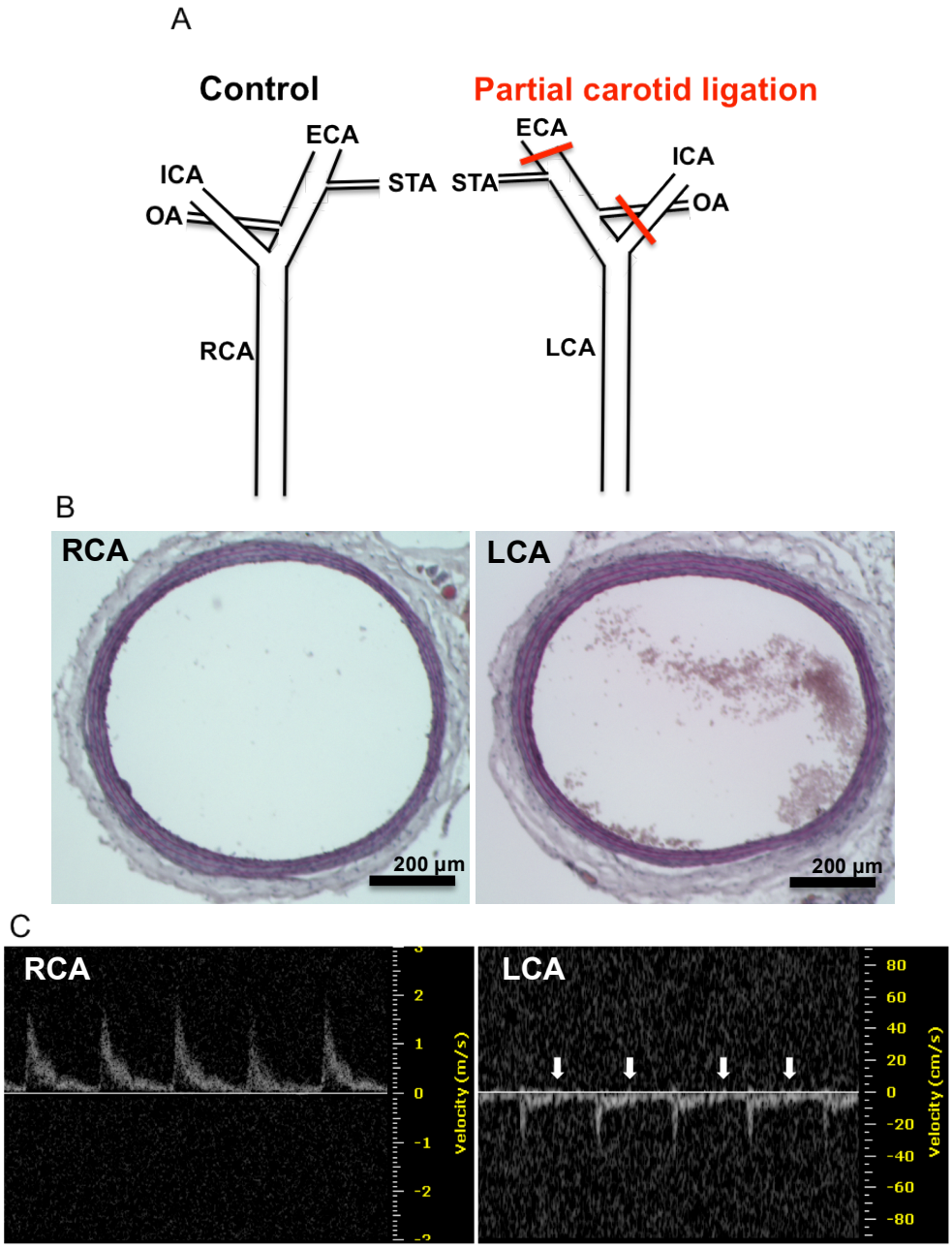

Figure 4.4 Rat carotid partial ligation significantly reduced the flow. (A) Schematic presentation of the partial LCA ligation. RCA: right common carotid artery; LCA: left common carotid artery; ICA: internal carotid artery; ECA: external carotid artery; OA: occipital artery; STA: superior thyroid artery. (B) Hematoxylin and Eosin staining of the cross-sections from RCA and partial ligated LCA (C) Ultrasonography measurements of flow velocity in LCA and RCA one week post-ligation. Results are representative of triplicate experiments with similar results.

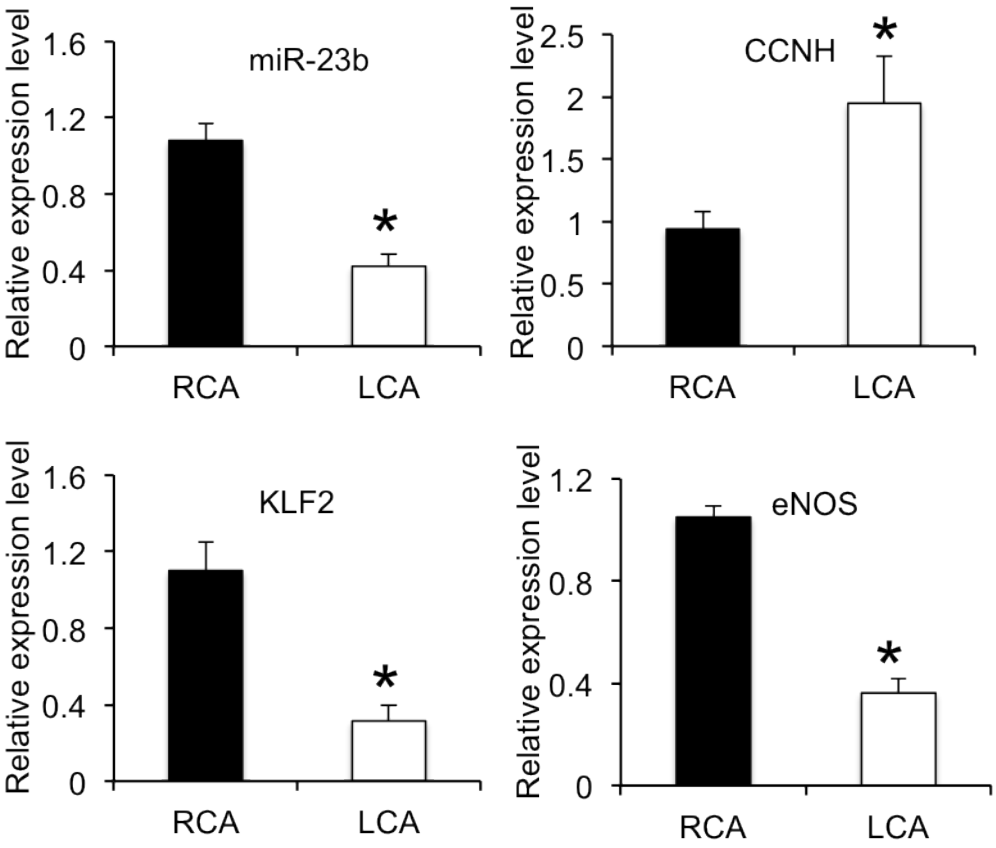

Figure 4.5 Partial ligation in LCA reduces the expressions of arthero-protective genes miR-23b, KLF2, and eNOS, but increases proliferative CCNH expression. Sprague-Dawley rats underwent partial carotid ligation, and one week post-ligation the rats were sacrificed and total RNA was isolated from the intima layer. The expressions of miR-23b, CCNH, KLF2, and eNOS in RCA (high shear stress) and LCA (low and oscillatory shear stress) were examined with RT-PCR. The results were normalized to U6 snRNA (for miR-23b) and GAPDH (for CCNH, KLF2, and eNOS), *$p<0.05$: LCA vs. RCA.

A. RCA

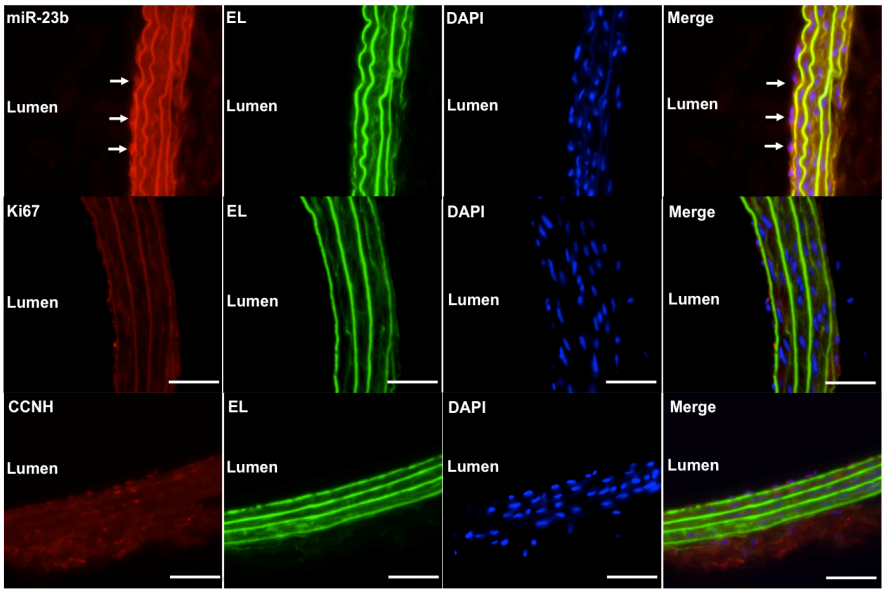

B. LCA

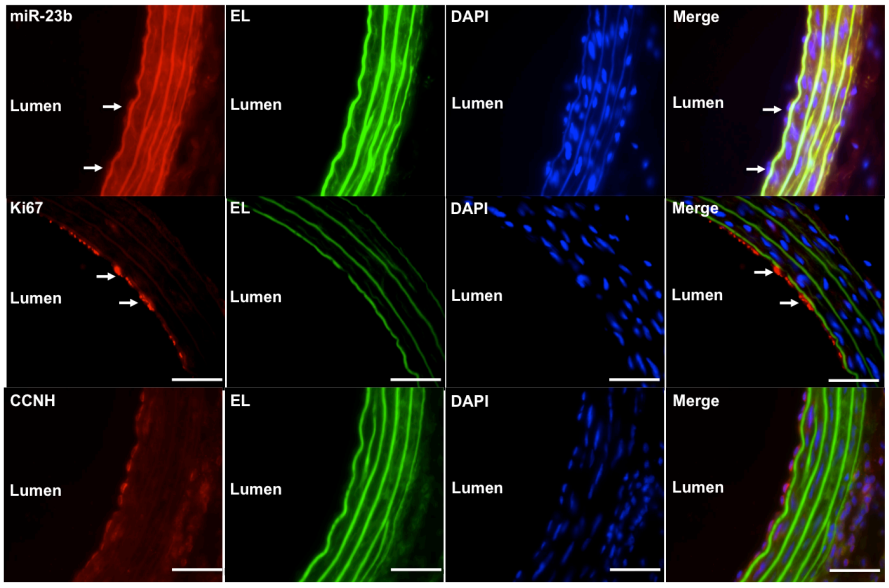

Figure 4.6 Low and oscillatory flow reduces miR-23b expression and promote EC proliferation in partial carotid ligation model. The Control vessels (RCA) and post-ligated carotid arteries (LCA) were isolated one week post-operation. Frozen sections from (A) RCA and (B) LCA were analyzed with FISH and immunohistochemistry for miR-23b and Ki67 (red).

CHAPTER 5 CONCLUSION and PROSPECTIVES

5.1 Conclusion

Atherosclerotic lesions preferentially form at vessel branch points and regions with high curvature in the arterial tree, but are usually absence along the straight part of the arterial tree. These observations led to a well-accepted concept that the site-specificity of atherogenesis is attributable, at least in part, to the local hemodynamic forces generated by blood flow. Endothelial cells (ECs) lining the innermost layer of vessel wall respond to different patterns of fluid shear stresses to differentially modulate athero-protective or athero-prone phenotypes. Recent studies suggest a vital role of microRNAs (miRNAs) in regulating vascular functions; however, the roles of miRNAs underlying the differential gene expressions and phenotype modulations of athero-protective *and* athero-prone flows remain largely unknown. Studying the flow regulations of endothelial miRNAs is essential for understanding the relation of miRNAs to vascular homeostasis and diseases.

The goals of this dissertation are (1) to investigate the mechano-sensitive miRNAs that regulate EC phenotypes under different flow patterns, (2) to elucidate the underlying molecular mechanism by which mIRNAs regulate EC phenotype, and (3) to examine the flow regulation of miRNAs *in vivo*. In Chapter 2 of this dissertation, a systematic approach was used to profile the miRNA signatures and functional regulations in ECs subjected to pulsatile shear stress (PS), oscillatory shear stress (OS), or kept as static control (ST). First, using miRNA microarray, I have shown that 21 miRNAs (8 up- and 13 down-regulated) are differentially expressed in PS vs. ST group, while 36 miRNAs (22 up- and 14 down-regulated) are differentially expressed in OS vs. PS group. In addition, mRNA profiles under the same experimental conditions were examined. Bioinformatics analyses of the mRNA profiles provide evidence that PS flow

predominantly suppresses EC proliferation, whereas OS flow promotes EC pro-inflammatory responses. Functional analyses using BrdU-incorporation validated that PS flow exerts the anti-proliferative effect on ECs, and that such regulation is mediated through a mechanism that is miR-23b-dependent. The results of monocyte adhesion assays show that OS causes sustained expression of miR-21 to contribute to pro-inflammatory response. The results from Chapter 2 demonstrate that endothelial miRNAs are differentially regulated by different flow patterns, and that mechano-sensitive miRNAs, including miR-23b and miR-21, indeed modulate EC phenotypes under PS and OS flows, respectively. The direct target of miR-23b in ECs and the underlying mechanism that mediates the anti-proliferative effects of PS flow are further investigated in experiments presented in Chapter 3.

The focus of Chapter 3 is to elucidate the molecular mechanism by which the PS-induced miR-23b exerts anti-proliferative effects on ECs. The results demonstrate that the application of PS induces the biogenesis of miR-23b/27b, as well as the host gene aminopeptidase O (APO) in ECs. Interestingly, the inhibition of miR-23b attenuates the PS-induced EC growth arrest, but APO and miR-27b (in Chapter 2) knockdowns have no significant effect on the anti-proliferative response. I have shown that the PS-induced miR-23b directly represses cyclin H (CCNH) expression post-transcriptionally to lead to impairments of the activity and integrity of CDK-activating kinase (CAK). The inhibitory effect of miR-23b on CAK pathway causes the suppression of cell cycle progression and basal transcription by deactivating CDK2/CDK4/RNA polymerase II (Pol II). While PS induces miR-23b/CAK pathway that exerts anti-proliferative response on ECs; OS has little effects on miR-23/CAK pathway and hence no EC growth arrest. These findings indicate that the miR-23b/CAK pathway serves as an important anti-proliferative mechanism of the PS-dependent EC response.

In chapter 4, two well-defined animal models for creating flow disturbance were employed for comparative analyses of differential regulations of miR-23b expression and EC proliferation under different flow patterns *in vivo*. Disturbed flow patterns were created by (1) carotid stenosis or (2) partial carotid ligation in the left common carotid arteries (LCA), while pulsatile flow with high shear stress was maintained in the control right common carotid arteries (RCA). The difference in flow velocities between LCA and RCA was determined with the Doppler ultrasound device. *In situ* hybridization and immuno-histochemical studies showed that, in comparison to the quiescent ECs in the RCA, disturbed flow in the stenotic or partial ligated LCA decreases miR-23b expression to lead to the increase of ECs proliferation. The findings presented in Chapter 3 and this Chapter have established that flow patterns significantly affect the expression of EC miR-23b expression and proliferation *in vitro* and *in vivo*. The results suggest the miR-23b/CAK regulatory mechanism presented in Figure 3.15 also applies *in vivo*.

Collectively, the studies presented in this dissertation used a combination of cell perfusion systems and experimental animals to demonstrate flow regulation of miR-23b in modulating endothelial proliferation both *in vitro* and *in vivo*. The novel findings of this dissertation include 1) the identification of the miRNA signatures and the corresponding gene expression profiles in ECs under PS and OS flows, 2) the elucidation of a novel mechanism that PS exerts anti-proliferative effects on ECs through a miR-23b/CAK/Pol II pathway, and 3) flow patterns differentially regulate miR-23b/CAK pathway and EC proliferation state *in vitro* and *in vivo*. This dissertation has contributed to the understanding of the role of miRNAs in regulating vascular functions in response to hemodynamic forces, and in particular, the miR-23b-mediated anti-proliferative response of ECs. These findings implicate miR-23b as one of the potential therapeutic candidates for atherosclerotic diseases.

5.2 Prospectives

In Chapter 2, the miRNA signatures in ECs under different flow patterns showed that 21 miRNAs in PS vs. ST and 36 miRNAs in OS vs. PS group were identified as mechano-sensitive miRNAs. Up to now, only three miRNAs have been studied and functionally associated to EC responses (miR-23b, miR-21, and miR-92a, for anti-proliferation, pro-inflammatory, and athero-protective effects, respectively). The functions of other flow-regulated miRNAs remain unexplored. It is also expected that miRNAs modulate target networks and EC functions as cohorts, the interactions among multiple miRNAs require further investigations. Moreover, temporal profiling of miRNAs, mRNAs, as well as the signaling networks, will provide more clues on the dynamic regulation of vascular responses under different flow patterns. The systematic approaches to profile the temporal networking among miRNAs, signaling pathways, gene expressions, as well functional consequences will be needed to further decipher the comprehensive roles of miRNAs in vascular biology.

As shown in Chapter 3, I have identified a novel mechanism that miR-23b targets CCNH to modulate CAK activity, which in turns regulates the phosphorylation of Pol II and the transcriptional control cell cycle genes. Since the phosphorylation levels of Pol II CTD significantly modulate the multifactorial transcription events, it will be interesting to study the role of miR-23b in global regulation of EC transcription machinery under different flow patterns. Chromatin Immunoprecipitation-Sequencing (ChIP-Seq) using antibodies against specific Pol II phosphorylated residue, with or without miR-23b perturbation, will provide valuable information of the comprehensive role of miR-23b in transcriptional controls.

In Chapter 4, my findings show that flow variations in stenotic and partially ligated arteries lead to the differential expression of miR-23b in ECs versus control arteries, and

that increased EC proliferation is associated with low miR-23b expression in disturbed flow regions. Further studies on miR-23b perturbation in rat carotid arteries should be employed to validate the anti-proliferative role of miR-23b in EC responses to flow patterns. The ultimate goal of the studies is to assess the potential therapeutic role of miR-23b as a candidate for atherosclerotic diseases, and such studies require further tests to be performed in the atherosclerotic animals. To address this issue, disease-based models, such as apoE-/- or LDL receptor-/- stains, should be employed to test the role of miR-23b in the formation and progression of atherosclerotic lesions.

REFERENCES

1. Chien, S., S. Li, and Y.J. Shyy, *Effects of mechanical forces on signal transduction and gene expression in endothelial cells.* Hypertension, 1998. **31**(1 Pt 2): p. 162-9.
2. Chien, S., *Mechanotransduction and endothelial cell homeostasis: the wisdom of the cell.* American journal of physiology. Heart and circulatory physiology, 2007. **292**(3): p. H1209-24.
3. Chiu, J.J. and S. Chien, *Effects of disturbed flow on vascular endothelium: pathophysiological basis and clinical perspectives.* Physiological reviews, 2011. **91**(1): p. 327-87.
4. Chien, S., et al., *Blood rheology after hemorrhage and endotoxin.* Advances in experimental medicine and biology, 1972. **33**(0): p. 75-93.
5. Ross, R., *Atherosclerosis is an inflammatory disease.* American heart journal, 1999. **138**(5 Pt 2): p. S419-20.
6. VanderLaan, P.A., C.A. Reardon, and G.S. Getz, *Site specificity of atherosclerosis: site-selective responses to atherosclerotic modulators.* Arteriosclerosis, thrombosis, and vascular biology, 2004. **24**(1): p. 12-22.
7. Hahn, C. and M.A. Schwartz, *Mechanotransduction in vascular physiology and atherogenesis.* Nature reviews. Molecular cell biology, 2009. **10**(1): p. 53-62.
8. Davies, P.F., et al., *Endothelial heterogeneity associated with regional athero-susceptibility and adaptation to disturbed blood flow in vivo.* Seminars in thrombosis and hemostasis, 2010. **36**(3): p. 265-75.
9. Gimbrone, M.A., Jr. and G. Garcia-Cardena, *Vascular endothelium, hemodynamics, and the pathobiology of atherosclerosis.* Cardiovascular pathology : the official journal of the Society for Cardiovascular Pathology, 2012.
10. Li, Y.S., J.H. Haga, and S. Chien, *Molecular basis of the effects of shear stress on vascular endothelial cells.* Journal of biomechanics, 2005. **38**(10): p. 1949-71.
11. Ando, J. and K. Yamamoto, *Effects of shear stress and stretch on endothelial function.* Antioxidants & redox signaling, 2011. **15**(5): p. 1389-403.
12. Haga, J.H., Y.S. Li, and S. Chien, *Molecular basis of the effects of mechanical stretch on vascular smooth muscle cells.* Journal of biomechanics, 2007. **40**(5): p. 947-60.
13. Chiu, J.J., et al., *Shear stress inhibits adhesion molecule expression in vascular endothelial cells induced by coculture with smooth muscle cells.* Blood, 2003. **101**(7): p. 2667-74.
14. Wang, H.Q., et al., *Shear stress protects against endothelial regulation of vascular smooth muscle cell migration in a coculture system.* Endothelium : journal of endothelial cell research, 2006. **13**(3): p. 171-80.
15. Gan, L.M., et al., *Temporal regulation of endothelial ET-1 and eNOS expression in intact human conduit vessels exposed to different intraluminal pressure levels at physiological shear stress.* Cardiovascular research, 2000. **48**(1): p. 168-77.

16. Dekker, R.J., et al., *Endothelial KLF2 links local arterial shear stress levels to the expression of vascular tone-regulating genes.* The American journal of pathology, 2005. **167**(2): p. 609-18.

17. Malek, A.M., et al., *Endothelial expression of thrombomodulin is reversibly regulated by fluid shear stress.* Circulation research, 1994. **74**(5): p. 852-60.

18. Khachigian, L.M., et al., *Egr-1 is activated in endothelial cells exposed to fluid shear stress and interacts with a novel shear-stress-response element in the PDGF A-chain promoter.* Arteriosclerosis, thrombosis, and vascular biology, 1997. **17**(10): p. 2280-6.

19. Aromatario, C., et al., *Fluid shear stress increases the release of platelet derived growth factor BB (PDGF BB) by aortic endothelial cells.* Minerva cardioangiologica, 1997. **45**(1-2): p. 1-7.

20. Hsieh, H.J., N.Q. Li, and J.A. Frangos, *Shear-induced platelet-derived growth factor gene expression in human endothelial cells is mediated by protein kinase C.* Journal of cellular physiology, 1992. **150**(3): p. 552-8.

21. Kukreti, S., et al., *Molecular mechanisms of monocyte adhesion to interleukin-1beta-stimulated endothelial cells under physiologic flow conditions.* Blood, 1997. **89**(11): p. 4104-11.

22. Davignon, J. and P. Ganz, *Role of endothelial dysfunction in atherosclerosis.* Circulation, 2004. **109**(23 Suppl 1): p. III27-32.

23. Rezvan, A., et al., *Animal, in vitro, and ex vivo models of flow-dependent atherosclerosis: role of oxidative stress.* Antioxidants & redox signaling, 2011. **15**(5): p. 1433-48.

24. Tzima, E., et al., *A mechanosensory complex that mediates the endothelial cell response to fluid shear stress.* Nature, 2005. **437**(7057): p. 426-31.

25. Kuchan, M.J. and J.A. Frangos, *Shear stress regulates endothelin-1 release via protein kinase C and cGMP in cultured endothelial cells.* The American journal of physiology, 1993. **264**(1 Pt 2): p. H150-6.

26. Chachisvilis, M., Y.L. Zhang, and J.A. Frangos, *G protein-coupled receptors sense fluid shear stress in endothelial cells.* Proceedings of the National Academy of Sciences of the United States of America, 2006. **103**(42): p. 15463-8.

27. Wang, Y., et al., *Interplay between integrins and FLK-1 in shear stress-induced signaling.* American journal of physiology. Cell physiology, 2002. **283**(5): p. C1540-7.

28. Brakemeier, S., et al., *Shear stress-induced up-regulation of the intermediate-conductance Ca(2+)-activated K(+) channel in human endothelium.* Cardiovascular research, 2003. **60**(3): p. 488-96.

29. Sumpio, B.E., et al., *MAPKs (ERK1/2, p38) and AKT can be phosphorylated by shear stress independently of platelet endothelial cell adhesion molecule-1 (CD31) in vascular endothelial cells.* The Journal of biological chemistry, 2005. **280**(12): p. 11185-91.

30. Iomini, C., et al., *Primary cilia of human endothelial cells disassemble under laminar shear stress.* The Journal of cell biology, 2004. **164**(6): p. 811-7.

31. Frank, P.G. and M.P. Lisanti, *Role of caveolin-1 in the regulation of the vascular shear stress response.* The Journal of clinical investigation, 2006. **116**(5): p. 1222-5.

32. Guo, D., S. Chien, and J.Y. Shyy, *Regulation of endothelial cell cycle by laminar versus oscillatory flow: distinct modes of interactions of AMP-activated protein kinase and Akt pathways.* Circulation research, 2007. **100**(4): p. 564-71.

33. Akimoto, S., et al., *Laminar shear stress inhibits vascular endothelial cell proliferation by inducing cyclin-dependent kinase inhibitor p21(Sdi1/Cip1/Waf1).* Circulation research, 2000. **86**(2): p. 185-90.

34. Lin, K., et al., *Molecular mechanism of endothelial growth arrest by laminar shear stress.* Proceedings of the National Academy of Sciences of the United States of America, 2000. **97**(17): p. 9385-9.

35. Chen, B.P., et al., *DNA microarray analysis of gene expression in endothelial cells in response to 24-h shear stress.* Physiological genomics, 2001. **7**(1): p. 55-63.

36. McCormick, S.M., et al., *DNA microarray reveals changes in gene expression of shear stressed human umbilical vein endothelial cells.* Proceedings of the National Academy of Sciences of the United States of America, 2001. **98**(16): p. 8955-60.

37. Garcia-Cardena, G., et al., *Distinct mechanical stimuli differentially regulate the PI3K/Akt survival pathway in endothelial cells.* Annals of the New York Academy of Sciences, 2000. **902**: p. 294-7.

38. Dekker, R.J., et al., *Prolonged fluid shear stress induces a distinct set of endothelial cell genes, most specifically lung Kruppel-like factor (KLF2).* Blood, 2002. **100**(5): p. 1689-98.

39. Ni, C.W., et al., *Discovery of novel mechanosensitive genes in vivo using mouse carotid artery endothelium exposed to disturbed flow.* Blood, 2010. **116**(15): p. e66-73.

40. Dai, G., et al., *Biomechanical forces in atherosclerosis-resistant vascular regions regulate endothelial redox balance via phosphoinositol 3-kinase/Akt-dependent activation of Nrf2.* Circulation research, 2007. **101**(7): p. 723-33.

41. Davies, P.F., et al., *Turbulent fluid shear stress induces vascular endothelial cell turnover in vitro.* Proceedings of the National Academy of Sciences of the United States of America, 1986. **83**(7): p. 2114-7.

42. Lee, D.Y., et al., *Role of histone deacetylases in transcription factor regulation and cell cycle modulation in endothelial cells in response to disturbed flow.* Proceedings of the National Academy of Sciences of the United States of America, 2012. **109**(6): p. 1967-72.

43. Zhou, J., et al., *Force-specific activation of Smad1/5 regulates vascular endothelial cell cycle progression in response to disturbed flow.* Proceedings of the National Academy of Sciences of the United States of America, 2012. **109**(20): p. 7770-5.

44. Bartel, D.P., *MicroRNAs: genomics, biogenesis, mechanism, and function.* Cell, 2004. **116**(2): p. 281-97.

45. Sun, W., et al., *microRNA: a master regulator of cellular processes for bioengineering systems.* Annual review of biomedical engineering, 2010. **12**: p. 1-27.

46. Suarez, Y., et al., *Dicer dependent microRNAs regulate gene expression and functions in human endothelial cells.* Circulation research, 2007. **100**(8): p. 1164-73.

47. Poliseno, L., et al., *MicroRNAs modulate the angiogenic properties of HUVECs.* Blood, 2006. **108**(9): p. 3068-71.

48. Kuehbacher, A., et al., *Role of Dicer and Drosha for endothelial microRNA expression and angiogenesis.* Circulation research, 2007. **101**(1): p. 59-68.

49. Hua, Z., et al., *MiRNA-directed regulation of VEGF and other angiogenic factors under hypoxia.* PloS one, 2006. **1**: p. e116.

50. Wienholds, E., et al., *The microRNA-producing enzyme Dicer1 is essential for zebrafish development.* Nature genetics, 2003. **35**(3): p. 217-8.

51. Bernstein, E., et al., *Dicer is essential for mouse development.* Nature genetics, 2003. **35**(3): p. 215-7.

52. Pan, Y., et al., *Conditional deletion of Dicer in vascular smooth muscle cells leads to the developmental delay and embryonic mortality.* Biochemical and biophysical research communications, 2011. **408**(3): p. 369-74.

53. Harris, T.A., et al., *MicroRNA-126 regulates endothelial expression of vascular cell adhesion molecule 1.* Proceedings of the National Academy of Sciences of the United States of America, 2008. **105**(5): p. 1516-21.

54. Concepcion, C.P., C. Bonetti, and A. Ventura, *The microRNA-17-92 family of microRNA clusters in development and disease.* Cancer journal, 2012. **18**(3): p. 262-7.

55. Bang, C., J. Fiedler, and T. Thum, *Cardiovascular importance of the microRNA-23/27/24 family.* Microcirculation, 2012. **19**(3): p. 208-14.

56. Rangrez, A.Y., et al., *miR-143 and miR-145: molecular keys to switch the phenotype of vascular smooth muscle cells.* Circulation. Cardiovascular genetics, 2011. **4**(2): p. 197-205.

57. Young, A., et al., *Flow activation of AMP-activated protein kinase in vascular endothelium leads to Kruppel-like factor 2 expression.* Arteriosclerosis, thrombosis, and vascular biology, 2009. **29**(11): p. 1902-8.

58. Chen, Z., et al., *Shear stress, SIRT1, and vascular homeostasis.* Proceedings of the National Academy of Sciences of the United States of America, 2010. **107**(22): p. 10268-73.

59. Wang, K.C., et al., *Role of microRNA-23b in flow-regulation of Rb phosphorylation and endothelial cell growth.* Proceedings of the National Academy of Sciences of the United States of America, 2010. **107**(7): p. 3234-9.

60. Ni, C.W., H. Qiu, and H. Jo, *MicroRNA-663 upregulated by oscillatory shear stress plays a role in inflammatory response of endothelial cells.* American journal of physiology. Heart and circulatory physiology, 2011. **300**(5): p. H1762-9.

61. Weber, M., et al., *MiR-21 is induced in endothelial cells by shear stress and modulates apoptosis and eNOS activity.* Biochemical and biophysical research communications, 2010. **393**(4): p. 643-8.

62. Mohamed, J.S., M.A. Lopez, and A.M. Boriek, *Mechanical stretch up-regulates microRNA-26a and induces human airway smooth muscle hypertrophy by suppressing glycogen synthase kinase-3beta.* The Journal of biological chemistry, 2010. **285**(38): p. 29336-47.

63. Yu, X., D.M. Cohen, and C.S. Chen, *miR-125b Is an adhesion-regulated microRNA that protects mesenchymal stem cells from anoikis.* Stem cells, 2012. **30**(5): p. 956-64.

64. Zhou, J., et al., *MicroRNA-21 targets peroxisome proliferators-activated receptor-alpha in an autoregulatory loop to modulate flow-induced endothelial inflammation.* Proceedings of the National Academy of Sciences of the United States of America, 2011. **108**(25): p. 10355-60.

65. Qin, X., et al., *MicroRNA-19a mediates the suppressive effect of laminar flow on cyclin D1 expression in human umbilical vein endothelial cells.* Proceedings of the National Academy of Sciences of the United States of America, 2010. **107**(7): p. 3240-4.

66. Wu, W., et al., *Flow-Dependent Regulation of Kruppel-Like Factor 2 Is Mediated by MicroRNA-92a.* Circulation, 2011. **124**(5): p. 633-41.

67. Fang, Y. and P.F. Davies, *Site-specific microRNA-92a regulation of Kruppel-like factors 4 and 2 in atherosusceptible endothelium.* Arteriosclerosis, thrombosis, and vascular biology, 2012. **32**(4): p. 979-87.

68. Nicoli, S., et al., *MicroRNA-mediated integration of haemodynamics and Vegf signalling during angiogenesis.* Nature, 2010. **464**(7292): p. 1196-200.

69. Turczynska, K.M., et al., *MicroRNAs are essential for stretch-induced vascular smooth muscle contractile differentiation via microRNA (miR)-145-dependent expression of L-type calcium channels.* The Journal of biological chemistry, 2012. **287**(23): p. 19199-206.

70. Hergenreider, E., et al., *Atheroprotective communication between endothelial cells and smooth muscle cells through miRNAs.* Nature cell biology, 2012. **14**(3): p. 249-56.

71. Huang, Y., et al., *miR-146a regulates mechanotransduction and pressure-induced inflammation in small airway epithelium.* FASEB journal : official publication of the Federation of American Societies for Experimental Biology, 2012. **26**(8): p. 3351-64.

72. Chien, S., *Mechanical and chemical regulation of endothelial cell polarity.* Circulation research, 2006. **98**(7): p. 863-5.

73. Wang, N., et al., *Shear stress regulation of Kruppel-like factor 2 expression is flow pattern-specific.* Biochemical and biophysical research communications, 2006. **341**(4): p. 1244-51.

74. Hsiai, T.K., et al., *Monocyte recruitment to endothelial cells in response to oscillatory shear stress.* FASEB journal : official publication of the Federation of American Societies for Experimental Biology, 2003. **17**(12): p. 1648-57.

75. Garcia-Cardena, G., et al., *Biomechanical activation of vascular endothelium as a determinant of its functional phenotype.* Proceedings of the National Academy of Sciences of the United States of America, 2001. **98**(8): p. 4478-85.

76. Lu, J., et al., *MicroRNA expression profiles classify human cancers.* Nature, 2005. **435**(7043): p. 834-8.

77. Bonauer, A., et al., *MicroRNA-92a controls angiogenesis and functional recovery of ischemic tissues in mice.* Science, 2009. **324**(5935): p. 1710-3.

78. Urbich, C., A. Kuehbacher, and S. Dimmeler, *Role of microRNAs in vascular diseases, inflammation, and angiogenesis.* Cardiovascular research, 2008. **79**(4): p. 581-8.

79. Suarez, Y. and W.C. Sessa, *MicroRNAs as novel regulators of angiogenesis.* Circulation research, 2009. **104**(4): p. 442-54.

80. Parmacek, M.S., *MicroRNA-modulated targeting of vascular smooth muscle cells.* The Journal of clinical investigation, 2009. **119**(9): p. 2526-8.

81. Care, A., et al., *MicroRNA-133 controls cardiac hypertrophy.* Nature medicine, 2007. **13**(5): p. 613-8.

82. Shilo, S., et al., *Evidence for the involvement of miRNA in redox regulated angiogenic response of human microvascular endothelial cells.* Arteriosclerosis, thrombosis, and vascular biology, 2008. **28**(3): p. 471-7.

83. Levesque, M.J., R.M. Nerem, and E.A. Sprague, *Vascular endothelial cell proliferation in culture and the influence of flow.* Biomaterials, 1990. **11**(9): p. 702-7.

84. Dennis, G., Jr., et al., *DAVID: Database for Annotation, Visualization, and Integrated Discovery.* Genome biology, 2003. **4**(5): p. P3.

85. Ashburner, M., et al., *Gene ontology: tool for the unification of biology. The Gene Ontology Consortium.* Nature genetics, 2000. **25**(1): p. 25-9.

86. Huang da, W., B.T. Sherman, and R.A. Lempicki, *Systematic and integrative analysis of large gene lists using DAVID bioinformatics resources.* Nature protocols, 2009. **4**(1): p. 44-57.

87. Kanehisa, M. and S. Goto, *KEGG: kyoto encyclopedia of genes and genomes.* Nucleic acids research, 2000. **28**(1): p. 27-30.

88. Kanehisa, M., et al., *From genomics to chemical genomics: new developments in KEGG.* Nucleic acids research, 2006. **34**(Database issue): p. D354-7.

89. Creighton, C.J., et al., *A bioinformatics tool for linking gene expression profiling results with public databases of microRNA target predictions.* RNA, 2008. **14**(11): p. 2290-6.

90. Krek, A., et al., *Combinatorial microRNA target predictions.* Nature genetics, 2005. **37**(5): p. 495-500.

91. Lewis, B.P., et al., *Prediction of mammalian microRNA targets.* Cell, 2003. **115**(7): p. 787-98.

92. Wang, X., *Systematic identification of microRNA functions by combining target prediction and expression profiling.* Nucleic acids research, 2006. **34**(5): p. 1646-52.

93. Subramanian, A., et al., *Gene set enrichment analysis: a knowledge-based approach for interpreting genome-wide expression profiles.* Proceedings of the National Academy of Sciences of the United States of America, 2005. **102**(43): p. 15545-50.

94. Giacinti, C. and A. Giordano, *RB and cell cycle progression.* Oncogene, 2006. **25**(38): p. 5220-7.

95. Sun, F., et al., *Characterization of function and regulation of miR-24-1 and miR-31.* Biochemical and biophysical research communications, 2009. **380**(3): p. 660-5.

96. Davies, P.F., et al., *Influence of hemodynamic forces on vascular endothelial function. In vitro studies of shear stress and pinocytosis in bovine aortic cells.* The Journal of clinical investigation, 1984. **73**(4): p. 1121-9.

97. Li, M., et al., *High pulsatility flow induces adhesion molecule and cytokine mRNA expression in distal pulmonary artery endothelial cells.* Annals of biomedical engineering, 2009. **37**(6): p. 1082-92.

98. Poznic, M., *Retinoblastoma protein: a central processing unit.* Journal of biosciences, 2009. **34**(2): p. 305-12.

99. He, Y., et al., *Identification of E2F-3B, an alternative form of E2F-3 lacking a conserved N-terminal region.* Oncogene, 2000. **19**(30): p. 3422-33.

100. Brehm, A., et al., *Retinoblastoma protein recruits histone deacetylase to repress transcription.* Nature, 1998. **391**(6667): p. 597-601.

101. Gao, P., et al., *c-Myc suppression of miR-23a/b enhances mitochondrial glutaminase expression and glutamine metabolism.* Nature, 2009. **458**(7239): p. 762-5.

102. Fang, Y., et al., *MicroRNA-10a regulation of proinflammatory phenotype in athero-susceptible endothelium in vivo and in vitro.* Proceedings of the National Academy of Sciences of the United States of America, 2010. **107**(30): p. 13450-5.

103. Holliday, C.J., et al., *Discovery of shear- and side-specific mRNAs and miRNAs in human aortic valvular endothelial cells.* American journal of physiology. Heart and circulatory physiology, 2011. **301**(3): p. H856-67.

104. Zhang, H., et al., *Genome-wide functional screening of miR-23b as a pleiotropic modulator suppressing cancer metastasis.* Nature communications, 2011. **2**: p. 554.

105. Rogler, C.E., et al., *MicroRNA-23b cluster microRNAs regulate transforming growth factor-beta/bone morphogenetic protein signaling and liver stem cell differentiation by targeting Smads.* Hepatology, 2009. **50**(2): p. 575-84.

106. Zhou, Q., et al., *Regulation of angiogenesis and choroidal neovascularization by members of microRNA-23~27~24 clusters.* Proceedings of the National Academy of Sciences of the United States of America, 2011. **108**(20): p. 8287-92.

107. Ham, O., et al., *The role of microRNA-23b in the differentiation of MSC into chondrocyte by targeting protein kinase A signaling.* Biomaterials, 2012. **33**(18): p. 4500-7.

108. Salvi, A., et al., *MicroRNA-23b mediates urokinase and c-met downmodulation and a decreased migration of human hepatocellular carcinoma cells.* The FEBS journal, 2009. **276**(11): p. 2966-82.

109. Axton, R., et al., *Aminopeptidase O contains a functional nucleolar localization signal and is implicated in vascular biology.* Journal of cellular biochemistry, 2008. **103**(4): p. 1171-82.

110. Hendrickson, D.G., et al., *Systematic identification of mRNAs recruited to argonaute 2 by specific microRNAs and corresponding changes in transcript abundance.* PloS one, 2008. **3**(5): p. e2126.

111. Fujii, W., et al., *CDK7 and CCNH are components of CDK-activating kinase and are required for meiotic progression of pig oocytes.* Biology of reproduction, 2011. **85**(6): p. 1124-32.

112. Feaver, W.J., et al., *Relationship of CDK-activating kinase and RNA polymerase II CTD kinase TFIIH/TFIIK.* Cell, 1994. **79**(6): p. 1103-9.

113. Kim, H., et al., *Gene-specific RNA polymerase II phosphorylation and the CTD code.* Nature structural & molecular biology, 2010. **17**(10): p. 1279-86.

114. Egloff, S. and S. Murphy, *Cracking the RNA polymerase II CTD code.* Trends in genetics : TIG, 2008. **24**(6): p. 280-8.

115. Schwartz, M.A. and R.K. Assoian, *Integrins and cell proliferation: regulation of cyclin-dependent kinases via cytoplasmic signaling pathways.* Journal of cell science, 2001. **114**(Pt 14): p. 2553-60.

116. Paternot, S., et al., *Rb inactivation in cell cycle and cancer: the puzzle of highly regulated activating phosphorylation of CDK4 versus constitutively active CDK-activating kinase.* Cell cycle, 2010. **9**(4): p. 689-99.

117. Patel, S.A. and M.C. Simon, *Functional analysis of the Cdk7.cyclin H.Mat1 complex in mouse embryonic stem cells and embryos.* The Journal of biological chemistry, 2010. **285**(20): p. 15587-98.

118. Moore, J.P., M. Weber, and C.D. Searles, *Laminar shear stress modulates phosphorylation and localization of RNA polymerase II on the endothelial nitric oxide synthase gene.* Arteriosclerosis, thrombosis, and vascular biology, 2010. **30**(3): p. 561-7.

119. Helenius, K., et al., *Requirement of TFIIH kinase subunit Mat1 for RNA Pol II C-terminal domain Ser5 phosphorylation, transcription and mRNA turnover.* Nucleic acids research, 2011. **39**(12): p. 5025-35.

120. Cheng, C., et al., *Atherosclerotic lesion size and vulnerability are determined by patterns of fluid shear stress.* Circulation, 2006. **113**(23): p. 2744-53.

121. Zand, T., et al., *Endothelial adaptations in aortic stenosis. Correlation with flow parameters.* The American journal of pathology, 1988. **133**(2): p. 407-18.

122. Miao, H., et al., *Effects of flow patterns on the localization and expression of VE-cadherin at vascular endothelial cell junctions: in vivo and in vitro investigations.* Journal of vascular research, 2005. **42**(1): p. 77-89.

123. Ibrahim, J., J.K. Miyashiro, and B.C. Berk, *Shear stress is differentially regulated among inbred rat strains.* Circulation research, 2003. **92**(9): p. 1001-9.

124. Korshunov, V.A. and B.C. Berk, *Flow-induced vascular remodeling in the mouse: a model for carotid intima-media thickening.* Arteriosclerosis, thrombosis, and vascular biology, 2003. **23**(12): p. 2185-91.

125. Nam, D., et al., *Partial carotid ligation is a model of acutely induced disturbed flow, leading to rapid endothelial dysfunction and atherosclerosis.* American journal of physiology. Heart and circulatory physiology, 2009. **297**(4): p. H1535-43.